

DOE/ID/13233--T5-Pt, 3

AN EVALUATION OF DIRECT PRESSURE SENSORS  
FOR MONITORING  
THE ALUMINUM DIE CASTING PROCESS

A Thesis

Presented in Partial Fulfillment of the Requirements for  
the Degree Master of Science in the  
Graduate School of The Ohio State University

By

Xueheng Zhang, M.S.E.

\*\*\*\*\*

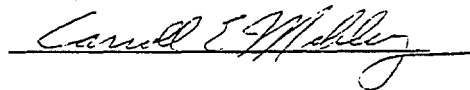
The Ohio State University  
1997

Master's Examination Committee:

Professor Carroll E. Mobley, Adviser

Professor Jerald R. Brevick

Approved by



Adviser

Department of Materials Science & Engineering

*df*  
DISTRIBUTION OF THIS DOCUMENT IS UNLIMITED

MASTER

## **DISCLAIMER**

**Portions of this document may be illegible in electronic image products. Images are produced from the best available original document.**

## ABSTRACT

This study was conducted as part of the U.S. Department of Energy (DoE) sponsored project "Die Cavity Instrumentation". One objective of that project was to evaluate thermal, pressure, and gas flow process monitoring sensors in or near the die cavity as a means of securing improved process monitoring and control and better resultant part quality. The objectives of this thesis are to (1) evaluate a direct cavity pressure sensor in a controlled production campaign at the GM Casting Advanced Development Center (CADC) at Bedford, Indiana; and (2) develop correlations between sensor responses and product quality in terms of the casting weight, volume, and density.

A direct quartz-based pressure sensor developed and marketed by Kistler Instrument Corp. was acquired for evaluation as an in-cavity liquid metal pressure sensor. This pressure sensor is designed for use up to 700 ° C and 2000 bars (29,000 psi). It has a pressure overload capacity up to 2500 bars (36,250 psi).

Based on the data acquired from a OSU die casting campaign and GM production die casting campaign, the Kistler direct pressure sensor was judged reliable and durable. Pressure records from the Kistler direct pressure sensor provide insight into the die casting process and serve as necessary complementary data to the hydraulic pressure record. The Kistler sensor pressure records allow definition of the impact pressure on cavity fill, the start of intensification, the cavity pressure rise time, the gate freezing time, and the onset of flashing. The Kistler pressure sensor operated without any sign of degradation over the one hundred and fifty-six shot campaign at GM. It is found that the casting volume, density, and weight correlate best a mean pressure between the average hydraulic pressure and the average pressure derived from the Kistler direct pressure sensor.

#### **DISCLAIMER**

*This report was prepared as an account of work sponsored by an agency of the United States Government. Neither the United States Government nor any agency thereof, nor any of their employees, makes any warranty, express or implied, or assumes any legal liability or responsibility for the accuracy, completeness, or usefulness of any information, apparatus, product, or process disclosed, or represents that its use would not infringe privately owned rights. Reference herein to any specific commercial product, process, or service by trade name, trademark, manufacturer, or otherwise does not necessarily constitute or imply its endorsement, recommendation, or favoring by the United States Government or any agency thereof. The views and opinions of authors expressed herein do not necessarily state or reflect those of the United States Government or any agency thereof.*

Dedicated to my parents

## ACKNOWLEDGMENTS

I wish to thank my adviser, Professor Carroll Mobley, for intellectual and financial support, encouragement, and enthusiasm which made this thesis possible, and for his patience in correcting both my stylistic and scientific errors.

I am grateful to Professor Jerald Brevick for his constructive role in my studies and thesis writing. I wish to thank those who helped me in my two-year studies here, especially Xiaopo Ma, Jian Zhang, Qi Shi, Angela Wollenburg, Lloyd Barnhart and Gary Dodge. I wish to thank Douglas Todora and Derek Peelle for the Archimedes' density measurements and providing me with all the casting volume, density, and weight data. I also would thank the staff at the GM CADC for their kind support.

This research was sponsored by the U.S. Department of Energy (DoE) and was monitored by The North American Die Casting Association (NADCA).

## VITA

September 7, 1965.....Born - Shanghai, China

1985.....Graduation Diploma  
Shanghai Jiao Tong University

1985-1988.....Technician  
Shanghai Research Institute of  
Tool & Die Technology

1991.....M.S.E., Graduation Diploma  
Shanghai Jiao Tong University

1990 - 1993.....Computer Software Programmer  
Shanghai DaiKei Data Processing Co., Ltd.

1995 - present.....Graduate Teaching and Research Assistant  
The Ohio State University

## FIELDS OF STUDY

Major Field: Materials Science and Engineering

Metal Forming

Mold and Die Design and Manufacturing

## TABLE OF CONTENTS

	<u>Page</u>
Abstract.....	ii
Dedication.....	iv
Acknowledgments.....	v
Vita.....	vi
List of Tables.....	ix
List of Figures.....	x
Chapters:	
1. Introduction.....	1
1.1 Process description.....	1
1.2 Technical background of the project and problem statement.....	4
1.3 Research objectives.....	7
2. Preliminary review.....	8
2.1 Introduction.....	8
2.2 Literature review.....	9
2.3 Industrial survey.....	27
3. Evaluation of Kistler direct pressure sensors in die casting campaigns.....	28
3.1 Introduction.....	28
3.2 Pressure sensor.....	29
3.3 Experiment set-up for OSU die casting campaign.....	35

3.4 Results from OSU ERC/NSM campaign and discussion.....	39
3.5 Results from GM CADC Bedford campaign and discussion.....	45
4. Examining the correlations between the Kistler direct pressure sensor outputs and casting weight, volume and density.....	69
4.1 Introduction.....	69
4.2 Archimedes' density measurement.....	70
4.3 The effects of applied pressure on the casting volume.....	75
4.4 The effects of applied pressure on the casting density.....	80
4.5 The effects of applied pressure on the casting weight.....	83
5. Conclusions and recommendations.....	92
Bibliography.....	94
Appendices	
A. NADCA survey of die casting cavity instrumentation.....	96
B. Technical Specifications of Buhler H-250SC.....	98
C. Machine set-up analysis for OSU die casting campaign.....	99
D. PQ <sup>2</sup> analysis.....	101
E. DoE/GM summary.....	102

## LIST OF TABLES

<u>Table</u>	<u>Page</u>
1.1 Process Variables for Cold Chamber Die Casting.....	5
2.1 Die casting system characterization.....	13
2.2 Tensile strength test piece characterization.....	15
3.1 Table of unit conversions.....	30
3.2 Average and standard deviation of some process variables of earlier stages before intensification starts.....	47
3.3 The average and standard deviation values of pressure parameters, intensification stroke, pressure difference and pressure rise time of sets II, III, IV, and V.....	68
4.1 Nominal composition range for Aluminum alloy 380 (weight percent).....	70
4.2 Casting weight plus overflows, and trimmed casting weight, volume, and density of the selected shots.....	74
4.3 Various pressure parameters of the selected shots.....	75
4.4 Actual casting weight, calculated casting weight, and average relative error.....	84
4.5 Weight, volume, and density of overflow and runner and biscuit of shots 20, 50, 60, 90, 91, and 120.....	88

## LIST OF FIGURES

<u>Figure</u>	<u>Page</u>
1.1 Operating sequence of the cold chamber die casting process.....	3
2.1 Thermocouple traces from various depths in a die casting die .....	9
2.2 Temperature distribution, measured temperature and calculated surface temperature and heat flux vs. time .....	11
2.3 Structure of Mochiku et al. temperature sensor.....	11
2.4 Thermocouple record for selected die casting cycle.....	12
2.5 Sectioned Papai and Mobley thermocouple probe tip.....	13
2.6 Relative porosity as a function of pressure applied during solidification.....	14
2.7 Effects of metal pressure on tensile strength and specific gravity of test piece.....	16
2.8 Structure of pressure sensor.....	17
2.9 Schematic drawing of sample castings specimen and transferred pressure gauges.....	17
2.10 Transferred pressure curves by various measuring methods.....	19
2.11 Change in solidification time for different sections of castings.....	20
2.12 Transferred pressure curves for various gate thickness with and without insulating film.....	20

2.13 Relation between gate thickness solidification time of gate and duration of the maximum transferred pressure.....	21
2.14 Transferred pressure curves for diecasting.....	22
2.15 Relation between surface roughness, maximum transferred pressure and molten metal velocity.....	23
2.16 Relation between internal defects, maximum transferred pressure and molten metal velocity .....	23
2.17 System for measuring gas pressure in die cavity.....	25
2.18 Gas pressure curve of thin wall box castings cast in 1200-ton machine.....	26
3.1 Kistler direct pressure sensor and specifications.....	31
3.2 Kistler pressure sensor 1 calibration curve.....	33
3.3 Kistler pressure sensor 2 calibration curve.....	33
3.4 Calibration loading beyond configured operating limits.....	34
3.5 Dynamic calibration curve of Kistler pressure sensors.....	34
3.6 Wall die casting for OSU die casting campaign.....	37
3.7 Locations of pressure sensors and thermocouple probes.....	38
3.8 Metal pressures from hydraulic pressure and Kistler pressure sensors.....	42
3.9 Cavity pressure record From Kistler sensor 1.....	43
3.10 Cavity pressure record from Kistler sensor 2.....	44
3.11 Plunger Pressure-Time Curve .....	46
3.12 Temperatures at the time the die closed at different locations in the die for each shot .....	48
3.13 The Final Pressures of Each Shot .....	49
3.14 Basic Types of Pressure Difference Curves.....	52

3.15 Pressure records of shot No. 75.....	53
3.16 Pressure difference record of shot No. 75.....	54
3.17 Pressure records of shot No. 41.....	54
3.18 Pressure difference record of shot No. 41.....	55
3.19 Pressure records of shot No. 97.....	56
3.20 Pressure difference record of shot No. 97.....	56
3.21 The maximum metal pressure pressures from the hydraulic pressure of selected shots.....	59
3.22 The final pressures of selected shots.....	59
3.23 The intensification stroke length of selected shots.....	60
3.24 The maximum Kistler pressure of selected shots.....	61
3.25 Pressure rise time of selected hydraulic pressure records.....	62
3.26 Pressure rise time of selected Kistler pressure records.....	63
3.27 Pressure difference 100 ms after minimum pressure difference.....	64
3.28 Pressure difference 1900 ms after minimum pressure difference.....	65
3.29 Impact pressure of selected shots .....	66
3.30 Pressure records of shot No. 156.....	67
3.31 Pressure difference records for shot No. 156.....	68
4.1 Schematic of Archimedes' measurement system.....	73
4.2 The effect of final pressure on the casting volume.....	76
4.3 The effect of the max metal pressure from hydraulic pressure on the casting volume.....	77
4.4 The effect of average Kistler pressure on the casting volume.....	77

4.5 The effect of the maximum Kistler pressure on the casting volume.....	78
4.6 The effect of mean pressure on the casting volume.....	78
4.7 The effect of final pressure on the casting density.....	80
4.8 The effect of maximum metal pressure from hydraulic pressure on the casting density.....	81
4.9 The effect of average Kistler pressure on the casting density.....	81
4.10 The effect of maximum Kistler pressure on the casting density.....	82
4.11 The effect of mean pressure on the casting density.....	82
4.12 The effect of final pressure on casting weight.....	85
4.13 The effect of maximum metal pressure from hydraulic pressure on the casting weight.....	85
4.14 The effect of average Kistler pressure on the casting weight.....	86
4.15 The effect of maximum Kistler pressure on the casting weight.....	86
4.16 The effect of mean pressure on the casting density.....	87
4.17 Density of runner and biscuit, casting, and overflows vs. reciprocal of final pressure.....	89
4.18 Density of runner and biscuit, casting versus reciprocal of final pressure for runner and biscuit and reciprocal of mean pressure.....	91

## CHAPTER 1

### INTRODUCTION

#### 1.1 PROCESS DESCRIPTION

Die casting is a cost effective near net shape manufacturing process for mass production of thin walled and complex shape products with excellent surface finish and close dimensional tolerance. In this process molten metal, primarily aluminum, zinc, and magnesium alloy, is injected at high velocities into reusable metallic molds and solidified under pressure. Die casting allows production of a wide variety of castings. The weights of castings can vary from a few grams to 20 kilograms. Complex products such as transmission cases and engine blocks can be made using this process.

The three primary variations of the die casting processes are the hot chamber process, the cold chamber process, and direct injection [1]. The difference between the hot chamber process and cold chamber process is that in hot chamber die casting the

actuator is placed in intimate contact with the molten metal while in cold chamber die casting the actuator is separated from the molten metal reservoir. Direct injection is similar to the injection molding of polymers [1]. Aluminum alloy die castings are traditionally made using the cold chamber die casting process. A cold chamber die casting machine usually consists of a melting furnace or holding furnace, ladling system, molten metal injection system, die holding system, and spraying system. A schematic diagram of the primary steps of a cold chamber die casting process is shown in Figure 1.1.

The cold chamber die casting process consists of the following basic steps [2]:

1. die closure, where the cover and ejector dies are closed and locked with the required force,
2. ladling, where the molten metal is ladled into the shot sleeve from the furnace,
3. cavity filling, where the plunger pushes the molten metal into the die cavity,
4. solidification, where the metal is held under pressure until it solidifies,
5. die opening, where the cover die moves backward, the plunger advances to insure the diecasting stays in the ejector die. Cores, if any, retract. Then, the diecasting is ejected.
6. die spray and lubrication, where the die is sprayed with coolant and lubricant. (This step is not shown in Figure 1.1)

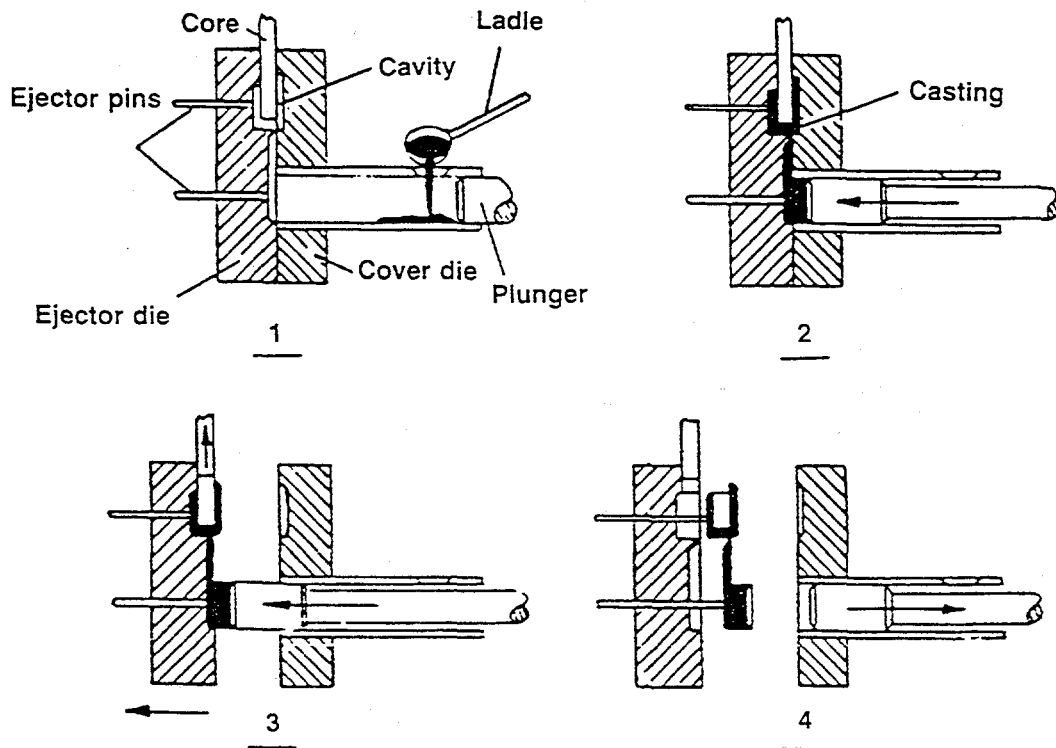


Figure 1.1 Operating sequence of the cold chamber die casting process [2]

## 1.2 TECHNICAL BACKGROUND OF THE PROJECT & PROBLEM STATEMENT

To reproducibly make die castings of acceptable quality, die design and process control are two key factors. Assuming that one begins with a properly designed die, the process variables which must be controlled are listed in Table 1.1.

Research studies by Sully [1] , and Kaye and Street [3] have shown that successful die casting is contingent upon the maintenance of several variables. However, the interdependence among these variables complicates the problem. For the present, efficiency and quality can be achieved empirically by monitoring the process variables, studying the effects of variation of each on a given part and controlling the variables for each individual job. In a first stage application of process control, the following steps are necessary in the absence of a complete scientific model [4]:

1. Monitor the process
2. Derive empirical model
3. Establish setpoints for independent variables currently controlled automatically
4. Maintain dependent variables by periodic adjustments

Melting Furnace	Alloy Composition
	Melt Temperature
	Melt Treatment
Ladling System	Ladling Time
Metal Injection System	Shot Sleeve Dimensions
	Shot Delay Time
	Shot Profile
	Cavity Fill Time
	Intensification Pressure
Dies	Tie Bar Load
	Die Temperature
Ejection System	Die Open Time
	Ejection Timing
Spraying	Spray Type
	Spray Timing
	Spraying Duration
	Spray Amount

Table 1.1 Process variables for cold chamber die casting [5]

In a second stage, the following steps would be taken after the critical variables are identified in Stage I:

1. Feedback control all critical variables,
2. Maintain constant optimum values,
3. Provide alarms to indicate inability to maintain process with limits.

To reach such a goal in a single step is impractical at present. According to Mochiku et al. [6], the poor understanding of the die casting process results from the following:

1. The physical phenomena which occur during the casting process have not been sufficiently investigated,
2. The sensors which are needed to analyze the detailed behavior of the process do not currently exist,
3. A die casting system which incorporates detailed process knowledge and related sensors has not yet been developed.

To obtain accurate data, characterizing the die casting process is critical to the development of effective control algorithms. The most practical way is to obtain the data which are used in process control directly from the die casting as it is being cast in the die cavity. Measurement of the pressure on molten metal, the temperature of the die surface contacting with molten metal, and gas vent condition is expected to provide the most sensitive records of the conditions under which the part is made.

### 1.3 RESEARCH OBJECTIVES [5]

This study is part of the U.S. Department of Energy (DoE) sponsored project "Die Cavity Instrumentation", which aims to evaluate process monitoring sensors that record the thermal, pressure, and gas flow condition in or near die cavity as a means of securing improved process sensors whose outputs better correlate with resultant part quality.

The objectives of this thesis are to:

1. Evaluate a commercially available pressure sensor in a OSU die casting campaign and a controlled production campaign at GM Casting Advanced Development Center at Bedford, Indiana.
2. Characterize the porosity of die castings produced during the beta site campaign and develop correlations between product quality, in terms of the density, and sensor responses.

## CHAPTER 2

### PRELIMINARY REVIEW

#### 2.1 INTRODUCTION

A literature review on how to measure and control process variables and to identify and correlate casting defects to these variable was undertaken as a part of the DoE project. Additionally, a industrial survey to obtain an assessment of the current industrial usage of sensors to measure the thermal and pressure fields and gas flow rates from the die cavity of US die casting companies was conducted.

## 2.2 LITERATURE REVIEW

Many die casting process parameters have been defined; however some have proven to be more crucial to the process and product than others.

Die temperature is one of the most important factors influencing the quality of die castings, their production rate, and die life. The surface temperature and the near surface thermal gradient in the die are majoring characterizing parameters [7]. Figure 2.1 shows the temperature gradient present in a die. In this case a heavy section aluminum casting was being produced with a 60 second cycle. Other detailed information was not provided. Obviously no evidence of die spray can be found from these traces.

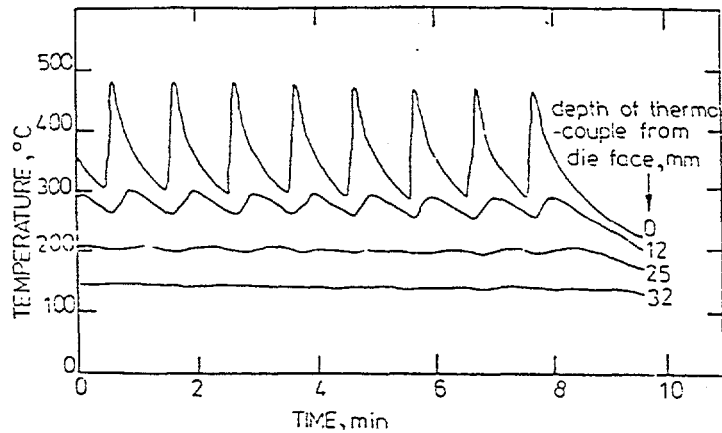


Figure 2.1 Thermocouple traces from various depths in a die casting die [8].

According to Booth et al [8] the temperature gradient in the die may be divided into two zones, (a) where the cyclic fluctuation are present; and (b) where these variations are lessened and a steady gradient exists. The temperature fluctuations are almost zero at 32 mm from the cavity surface.

Mochiku et al. [6] proposed a new concept, "intelligent die casting" in which, seven kinds of sensors are simultaneously used to gather data. The sensors used were pressure, temperature, gap, deformation, toggle pin, tie bar, and 6-axis force sensors. Although such a complete system is not generally used, the sensors essential to the system have been produced. They produced and investigated a die surface temperature sensor to measure the temperature on the interior surface of the die and heat flux through the die surface. Temperature T1 and T2 are measured at two points x1 and x2, which are located along the same surface normal to the die surface, but at different depths from the surface. The surface temperature ( $T_s'$ ) and heat flux ( $\phi$ ) are calculated from these temperature measurements. The resulting measured and calculated values appear as shown in Fig 2.2 (b). The structure of the sensor is shown in Figure 2.3. Two chromel-alumel thermocouples are welded on to a detecting block at the bottom of holes which are located at distance of 0.4 mm and 0.8 mm from the sensing surface. With the die surface temperature sensor, they detected the arrival of molten metal in a cavity and a overflow; estimated the soundness of molten metal; determined suitable amount of die lubricant; and established suitable operating temperature of a die. The die cavity has a M-shape, serpentine path of 630 mm in length [6].

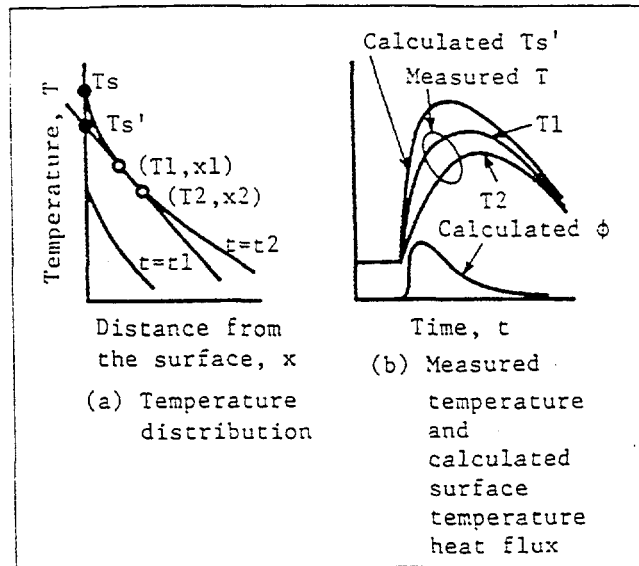


Figure 2.2 Temperature distribution, measured temperature and calculated surface temperature and heat flux vs. time [6].

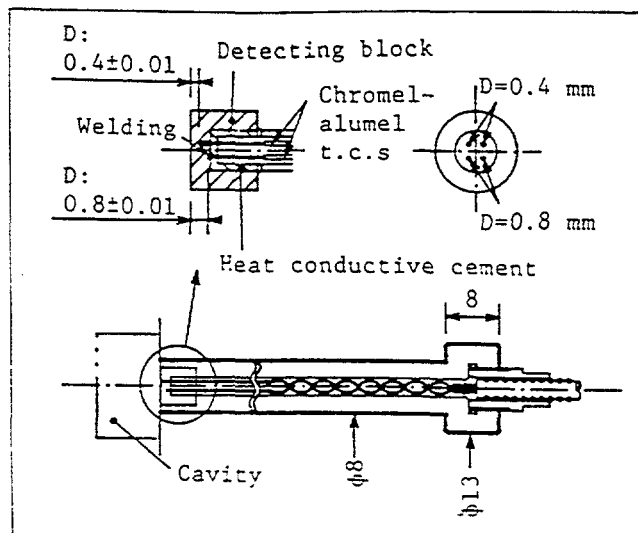


Fig 2.3 Structure of Mochiku et al. temperature sensor [6]

Papai and Mobley [7] developed a procedure to measure the thermal field (including die-cavity interface temperatures) in H-13 dies during the die casting of 380 aluminum alloy and applied a numerical method to the die thermal field data to determine the heat flux at the die-casting interface. They also investigated the effects of liquid alloy temperature, location on the casting, applied intensification pressure level, die surface roughness, and lubricant spraying duration on the heat transfer to the die. A bowl shaped casting with wall thickness varying from one section to another was selected. The thermocouples (chromel-alumel) were mounted in removable cores at depths of zero, 0.25, 1.52 and 12.7 mm relative to the casting-die interface, similar to the thermocouples used in this research. A thermocouple record for a selected die casting cycle is shown in Figure 2.4. Table 2.1 gives the information on this die casting system characterization. A photograph of the sectioned thermocouple probe tip is shown in Figure 2.5.

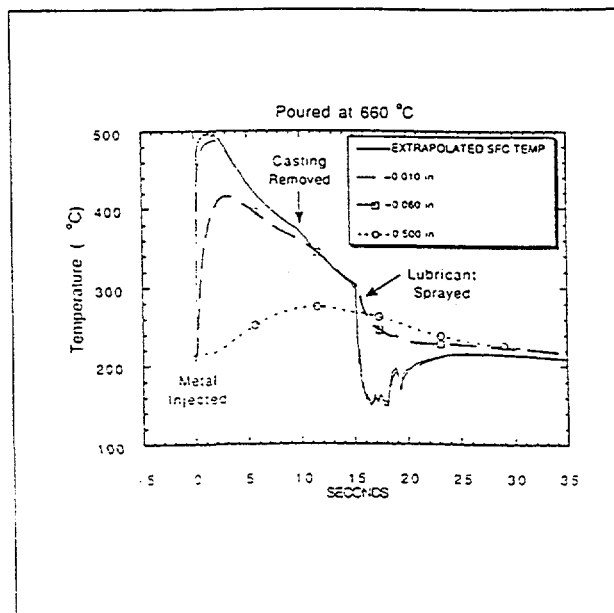


Figure 2.4 Thermocouple record for selected die casting cycle [7].

<b>Casting:</b>	<b>380 Aluminum Alloy Bowl</b>
Bowl Casting Volume:	13.9 cubic in.
Total Casting Volume:	19.5 cubic in.
Total Casting Weight:	1.75 lb
Thermocouple Locations (relative to die surface):	0.000, 0.25, 1.52, 12.7 mm (0.0, 0.010, 0.060, 0.500 in.)
Plunger Diameter:	2.09 in. (5.3 cm)
Sleeve Length:	19.75 in. (50.165 cm)
Percentage Fill:	29%
Plunger Velocity:	Two Stage; 10 in./sec, 75 in./sec.
Gate Area:	0.07 x 2.0 in. = 0.14 square in.
Gate Velocity:	154 ft/sec (47 m/sec)
Alloy Pouring Temperature:	650 and 760°C (1200 and 1400°F)
Applied Pressure:	5,600 and 15,000 psi
Locking Force:	600 tons
Lubricant:	1/40 dilution graphitic agent in water
Lubricant Spray Duration:	Light = 2 sec.; Heavy = 4 sec.
Die Closed Time:	10 sec.
Die Open Time:	15 to 25 sec.
Total Cycle Time:	25 to 30 sec.
Thermal Properties of the H-13 Steel Die (9):	
Thermal Conductivity, k =	$0.0587 + 8.6 \times 10^{-4}T$ (cal/cm C sec)
Density, $\rho$ =	$7.8 - 2.5 \times 10^{-4}T$ (g/cm <sup>3</sup> )
Specific Heat, c =	$0.110 - 1.12 \times 10^{-4}T + 7.5 \times 10^{-6}T^2$ (cal/g C)

Table 2.1 Die casting system characterization [7]

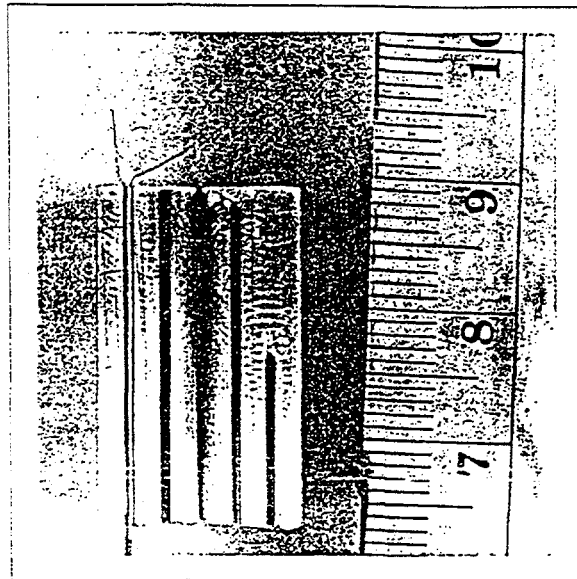


Figure 2.5 Sectioned Papai and Mobley thermocouple probe tip [7]

Cavity pressure is a critical process variable to the quality of the product. Most investigations have shown that increasing the level of cavity pressure results in improved internal casting quality. The porosity associated with solidification shrinkage and insoluble gases present in the solidifying alloy can be reduced with increasing pressure. A relationship between the final pressure in injection cylinder and porosity of a small aluminum cylinder head is shown in Figure 2.6. The equation of the trendline of percent porosity, %P, vs. final pressure,  $P_{\text{final}}$ , is  $\%P = 16.59 P_{\text{final}}^{-0.7845}$  ( $R^2 = 0.9943$ ) if it is assumed a power trendline or  $\%P = 0.0277 P_{\text{final}}^2 - 0.7961 P_{\text{final}} - 7.8714$  ( $R^2 = 0.9995$ ) if it is assumed a polynomial trendline.

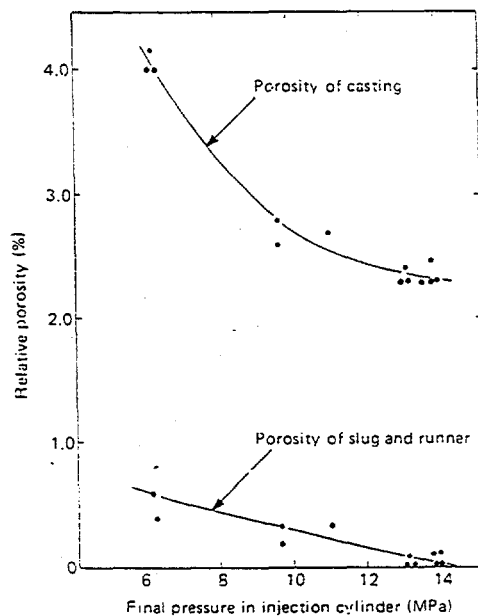


Figure 2.6 Relative porosity as a function of pressure applied during solidification [3]

Babington and Klepinger [9] found that internal soundness improved with increasing the level of cavity pressure up to 15,000 psi and remained constant. Philipot et al. [10] evaluated the effect of gate velocity during fast shot and cavity pressure 0.6 sec after shot rod impact. Their results reveal that the theoretical cavity pressure, measured 0.6 sec after impact, and the average gate velocity both have significant effects on internal casting quality. Lower gate velocities and higher cavity pressures yielded lower porosity castings. Tokui et al., [11] conducted research on the vertical pressure die casting process and found that if pressures above 30Mpa (4350 psi) are applied to the molten metal, castings of higher tensile strength and density could be obtained. The casting conditions and the size of the round bar test pieces are shown in Table 2.2. Figure 2.7 shows the results of the research.

	VERTICAL PRESSURE DIE CASTING PROCESS	CONVENTIONAL DIE CASTING PROCESS
MATERIAL	A380	A380
CASTING TEMPERATURE (°C)	740	680
CASTING PRESSURE (MPa)	50	80
DIAMETER OF THE TEST PIECE (mm)	8,10,14	6.5,10,14
SURFACE OF THE TEST PIECE	AS CAST	AS CAST
HEAT TREATMENT	NO	NO

Table 2.2 Tensile strength test piece characterization [11]

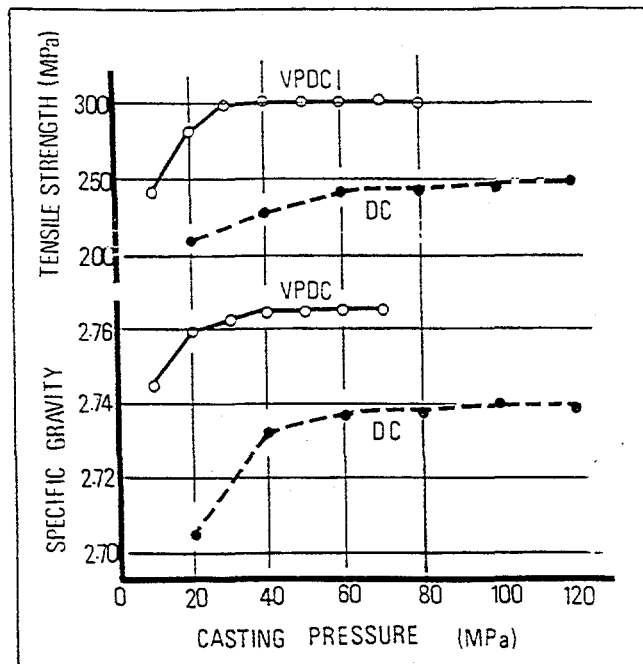


Figure 2.7 Effects of metal pressure on tensile strength and specific gravity of test piece[11]

Mochiku et al. [6] developed and used a pressure sensor to measure the pressure acting on the die during the casting process and the ejecting force during the ejection process. The pressure and force which act on top surface of the sensor are detected by four strain gages which are glued on the detecting block. The structure of the sensor is shown in Figure 2.8. As reported, the pressure sensor was able to measure the pressure during injection and solidification; detect soldering and sticking in ejection; detect abnormality in the total system and near a gate; establish suitable operating pressure and injection speed.

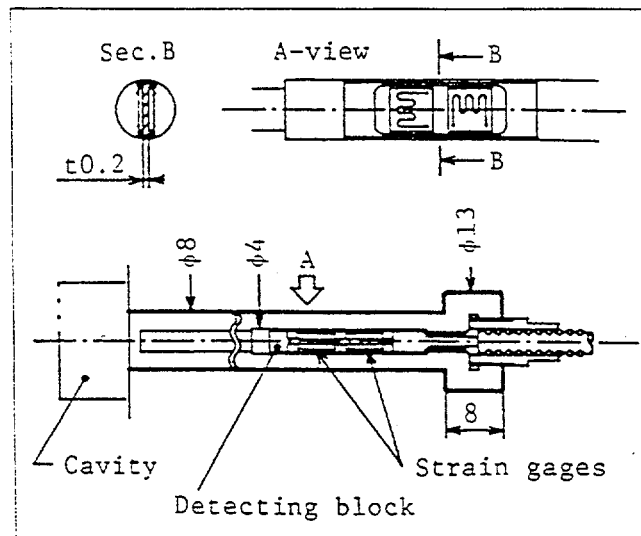


Figure 2.8 Structure of pressure sensor [6]

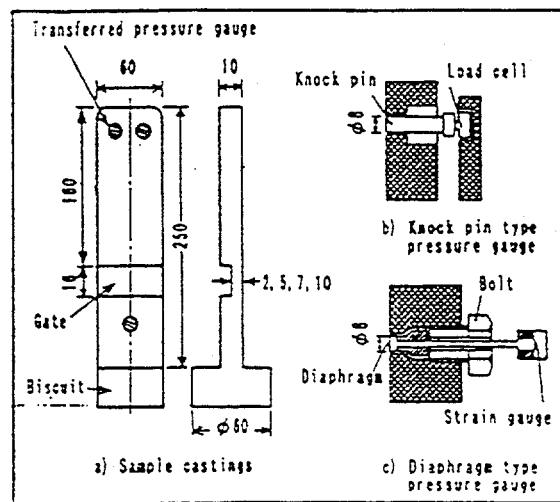


Figure 2.9 Schematic drawing of sample castings specimen and transferred pressure gauges [12]

Sugiyama et al. [12] developed and evaluated another method of measuring transferred pressure on metal in a die cavity and related the effects of transferred pressure to the quality of aluminum diecastings. The schematic drawing of the molten metal pressure gauges is shown in Figure 2.9.

The indirect metal pressure sensor used by Sugiyama et al. could measure pressures to 100 Mpa (14500 psi). The direct molten metal pressure sensor could measure the maximum pressure to 105 Mpa (15225 psi) and have a heat resistance temperature of 773 K. The cast alloy was 380 aluminum alloy and the molten metal was injected at about 853 K. Figure 2.10 shows the transferred pressure curves measured by a diaphragm-type pressure gauge and two knock-pin-type gauges (with and without stainless steel film). Sugiyama et al. [12] found that when the knock-pin-type pressure gauge is used, the measured pressure value could be affected by the fins in the gap between the die and the gauge. By applying a 0.05 mm thick stainless steel film, the same value as that measured by diaphragm-type pressure gauge can be obtained. The pressure at the thickness center of a casting cannot be measured accurately by the measurement on the surface, owing to the pressure drop caused by the solidification layer near the surface.

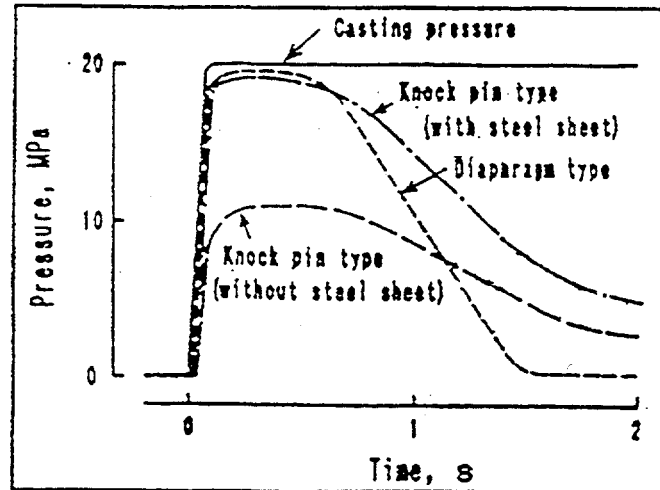


Figure 2.10 Transferred pressure curves by various measuring methods [12]

By applying a film of insulating material, Sugiyama et al. [12] measured the transferred pressure at the center of the section. Figure 2.11 shows the solidification time of the section of the sample castings of different thickness. Figure 2.12 shows the transferred pressure curves for 10 mm thickness sample castings with and without the insulating film. The gate thickness was 2, 5, 7, and 10 mm. They reported that the duration of pressure transfer was governed mainly by solidification at the gate and took only about 20% of the solidification time at the gate.

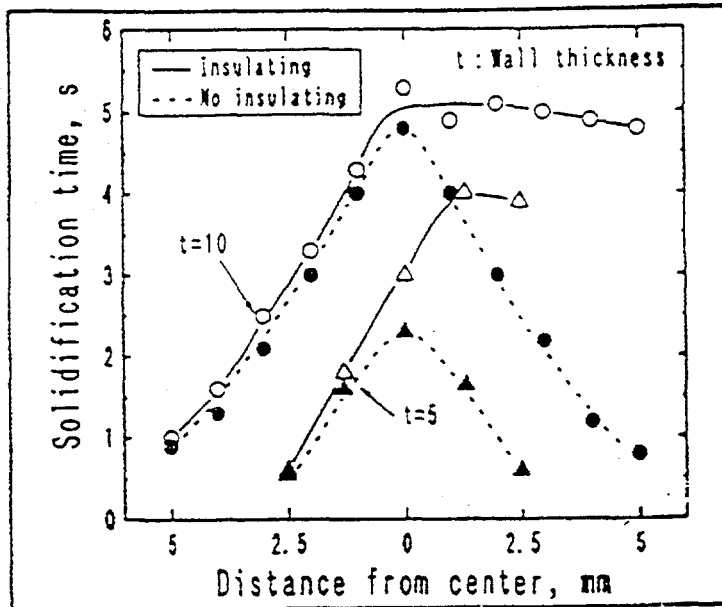


Figure 2.11 Change in solidification time for different sections of castings [12]

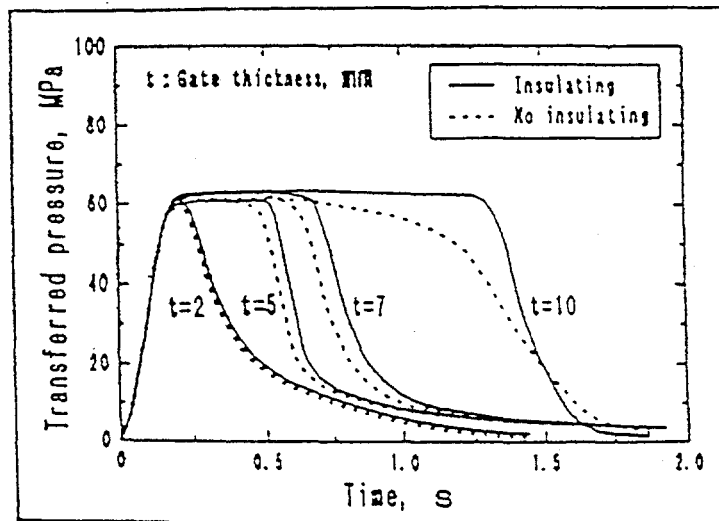


Figure 2.12 Transferred pressure curves for various gate thickness with and without insulating film [12].

The relation between gate thickness and the duration of the maximum transferred pressure measured using insulating film is shown in Figure 2.13. The duration of the maximum transferred pressure at a location, just in front of the gate was constant at about 1.4 sec. However, at the point a, beyond the gate, the duration of the maximum transferred pressure became longer with increasing gate thickness.

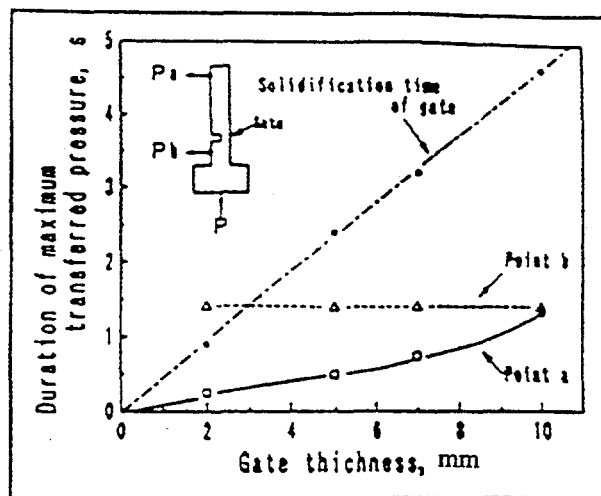


Figure 2.13 Relation between gate thickness solidification time of gate and duration of the maximum transferred pressure [12].

Figure 2.14 gives an example of the transferred pressure curves obtained by measuring pressure in the runner and at two points within the cavity. The maximum transferred pressure within the cavity was slightly lower than in the runner and much lower in the end of the cavity. The duration of the maximum transferred pressure was 0.4 sec in the runner, 0.25 sec in the cavity and slightly shorter at the end of the cavity. The relationships between molten metal velocity, maximum transferred pressure and surface roughness of castings and between molten metal velocity, maximum transferred pressure and internal defects was reported as shown in Figure 2.15 and Figure 2.16. It was reported that surface roughness of the diecastings decreased with increasing transferred pressure and molten metal velocity and internal defects, like blowholes, diminished with increasing transferred pressure and disappeared at pressures of 75 Mpa and larger.

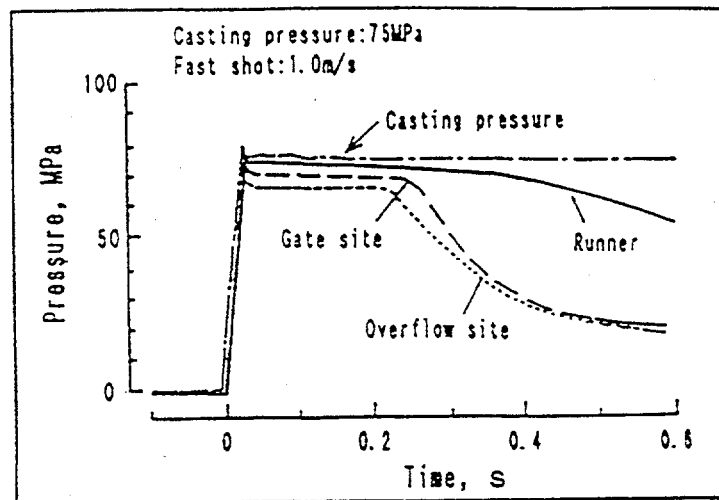


Figure 2.14 Transferred pressure curves for diecasting [12]  
(1 Mpa = 145 psi)

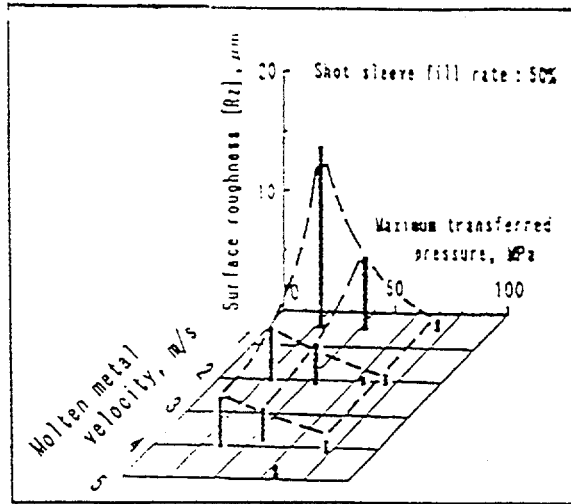


Figure 2.15 Relation between surface roughness, maximum transferred pressure and molten metal velocity [12]

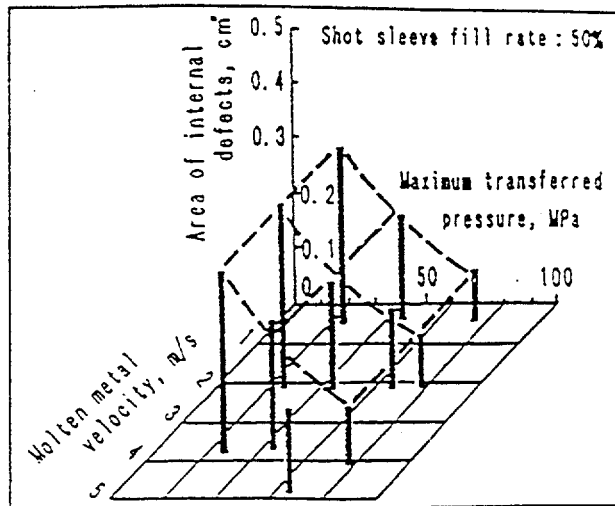


Figure 2.16 Relation between internal defects, maximum transferred pressure and molten metal velocity [12].

In the last decade, quality requirements have moved beyond configuration and dimensional control to internal defects control. Porosity is usually considered deleterious because it reduces the load-bearing cross-sectional area, causes stress concentration, may give rise to blisters on the surface and leakage. The porosity originates from two sources [13] : solidification shrinkage and gas.

The gas porosity originates from

1. Solubility differences during solidification (i.e., gas species which are dissolved in the solidifying alloy)
2. Reactions which form gases in the system (i.e., lubricant-metal reactions)
3. Physically entrained gases which become entrapped in the solidifying system

The vent is an important part of die. It acts as a gate to release air or gas in the die cavity. Sometimes the vent may be blocked. If the air is not able to go out, the air pressure will rise during injection. To get the information on the situations of air pressure in die cavity, Yamamoto et al., [14] developed a device for measuring gas pressure at each position in a die cavity during injection of molten metal. As shown in Figure 2.17, a 3-mm dia. hole was bored through the die to insert a gas pressure conduit pipe. A gas pressure gage with a measuring range of  $1.0 \text{ kg/cm}^2$  was attached on one end of the pipe. A porous material filled the hole at the other end. The time-dependent changes in pressure in a die cavity were automatically recorded on an electromagnetic oscillograph just after the injection of the molten metal.

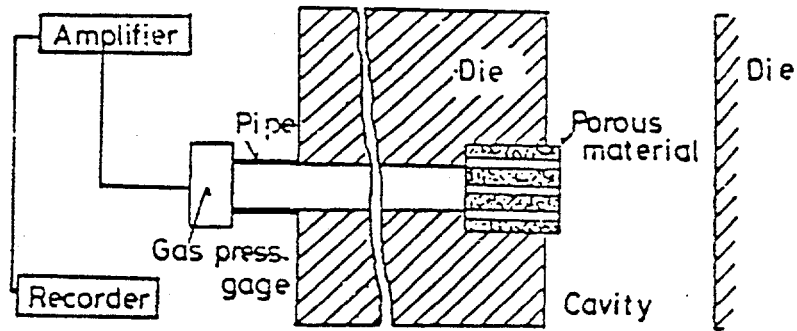


Figure 2.17 System for measuring gas pressure in die cavity [14].

Gas pressure in the die cavity of a boxed-shape casting was measured at positions 1-3 along the molten metal flow. Typical gas pressure vs. time curves in the die cavity are shown in Figure 2.18. The gas pressure in the cavity gradually becomes higher with the passage of time from injection. The changeover of the shot velocity from slow shot to fast shot abruptly increases the gas pressure. They reported that the increase in gas pressure decreases the velocity of the molten metal at the final filling position. The die casting defects frequently appear near the gate and at the final filling positions. They studied the correlations of casting defects with molten metal velocity and gas pressure in the cavity. They found that it is necessary to decrease the pressure and increase the molten metal velocity at the final filling position to prevent casting defects.

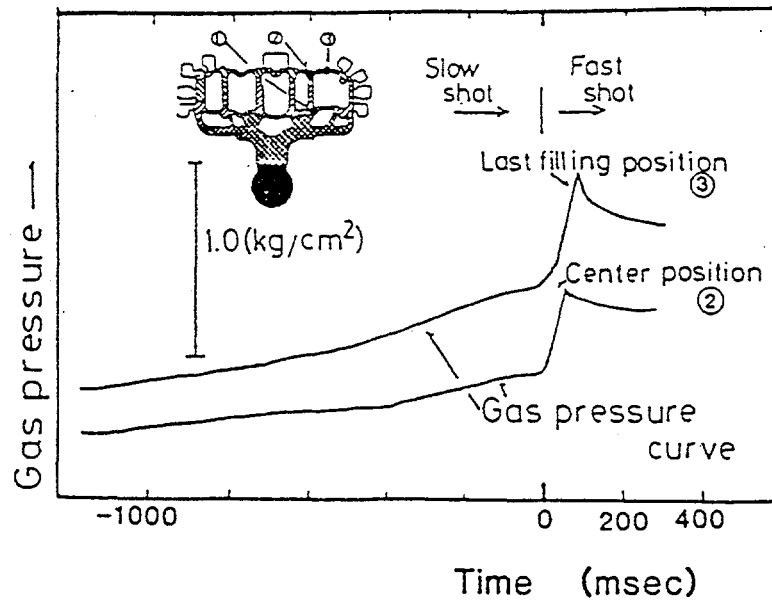


Figure 2.18 Gas pressure curve of thin wall box castings cast in 1200-ton machine [14].

Several kinds of sensors necessary for the realization of die casting process have been developed and investigated. Among these sensors, the surface temperature sensor and the shot profile pressure sensor are the most significant. Their performance during the die casting process and usefulness have been investigated through experiments. These researches indicate that to precisely monitor the die casting process is fundamental and critical for understanding of die casing process. To be accepted for industrial application, these sensors still need evaluation and development.

## 2.3 INDUSTRIAL SURVEY [5]

Shortly after initiation of this DoE-sponsored project, a survey questionnaire was prepared and sent to NADCA corporate members and distributed to company representatives attending NADCA Chapter meetings to obtain the situation of the current usage of thermal, pressure and gas flow rate sensors in die casting industry. A sample questionnaire is included as APPENDIX A. Of the 63 completed survey questionnaires, 60 were completed by U.S. die casting companies, 1 by a non-North American die casting company, and 2 by U.S. die casting equipment companies. The responding die casting companies operate 937 cold chamber die casting machines and 343 hot chamber die casting machines. The 1249 die casting machines of the U.S. die casting companies that responded represent 15.6% of the available U.S. die casting machines, based on the estimated 8000 die casting in 1994. 91% of the companies indicated that they possess the equipment to monitor the position and velocity of the plunger as a function of time during the filling process. 50% of the companies indicated that they used temperature and pressure measuring sensors near the die cavity as part of the process monitoring or control practices. Only 15% indicated that they use or have systems to monitor the gas vent condition. Only 12% indicated that they use or have systems for measuring the amount of gas removed from the die cavity. The OSU investigators surmised that the companies indicating that they monitored the amount of gas removed from the die cavity used die cavity vacuum assisted practices.

## CHAPTER 3

### EVALUATION OF KISTLER DIRECT PRESSURE SENSORS IN DIE CASTING CAMPAIGNS

#### 3.1 INTRODUCTION

The primary objective of the U.S. DoE sponsored project "Die Cavity Instrumentation" is to evaluate and develop in-cavity thermal, pressure, and gas flow sensors to monitor filling, solidification, and gas entrapment in the die cavity(s) of cold chamber die casting process and to relate the measurements of these variables to the quality of the resultant die castings. The sensors should allow the measurement of (a) the die temperature field near the die cavity surface, (b) the pressure of the liquid in the die cavity, and (c) the amount of gas exiting the die cavity during filling. These measurements are to be correlated with the plunger position-time and hydraulic pressure-time records, and related to the porosity of the resultant castings [5]. A literature review and a survey of industrial practices revealed that sensors for measuring the alloy pressure in die casting cavities are commercially available.

### 3.2 PRESSURE SENSOR

There are two principle types of pressure sensors for the measurement of the liquid alloy pressure. They are:

1. indirect pressure sensors, which use the pin's displacement to transfer the cavity pressure
2. direct pressure sensors, which use the diaphragm to transfer the cavity pressure

The indirect pressure sensors have been used by the die casting industry for many years. The major problem associated with their usage is the reliability of the measurements. Since the cavity pressure is transferred to the load cell or strain gauge of the sensor via the pin's displacement, the friction between the pin and the die or small fins in the gap between the die and the pin affects the response and the measured pressure value. The deviation from the real value is difficult to estimate due to the inconsistencies from shot to shot.

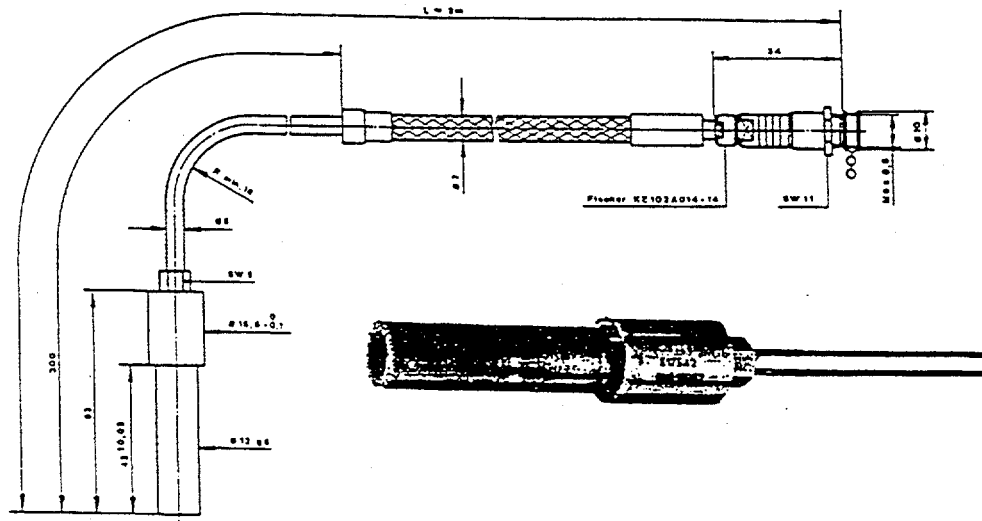
A direct quartz-based pressure sensor developed by Kistler Instrument Corp. was acquired for evaluation as an in-cavity liquid metal pressure sensor [5]. Figure 3.1 illustrates the geometry and specifications of the sensor. This pressure sensor is designed for use up to 700 ° C and 2000 bars (29,000 psi). It has a pressure overload capacity up to 2500 bars (36,250 psi). The body of the pressure sensor is 6.3 cm long and 1.2 cm diameter.

To generate an electrical output from a pressure input, pressure must first be converted into a proportional displacement or strain. This strain is then transmitted to an electrical element which generates the required signal. The Kistler pressure sensors consist of three basic parts: the sensor housing, the quartz sensing element and the diaphragm for transferring the pressure to the element. The Kistler piezoelectric pressure sensors are quartz. While quartz-based pressure sensors are ideally suited for measuring dynamic events, they cannot perform truly static measurements. Although the electrical charge delivered under a static load can be registered, it cannot be stored for an indefinite period of time. Quartz-based piezoelectric system can routinely measure large static pressure for minutes and perhaps even hours. Low level static pressures can be measured “statically” for much shorter intervals. For this reason Kistler piezoelectric pressure sensors are often described as being “quasistatic”. However, quantitative information is not provided on this issue. Temperature variations may also affect a sensor’s output.

Unit conversions which are helpful for comparison of data from various sources are listed in Table 3.1

	English to S.I.	S.I. to English
Length	1 inch = 25.4 mm	1 mm = 0.0394 inch
Weight	1 lb = 0.4536 kg	1 kg = 2.205 lb
Pressure	1 psi = $6.9 \times 10^{-3}$ Mpa	1 Mpa = 145 psi
Pressure	1 bar = 0.101 Mpa	1 Mpa = 9.864 bar
Density	1 lb/inch <sup>3</sup> = 27.679822 g/cc	1 g/cc = 0.036127486 lb/inch <sup>3</sup>

Table 3.1 Table of unit conversions



#### Technical Data

Range	bar	0 ... 2000
Overload	bar	2500
Uniform sensitivity (at 250 °C)	pC / bar	-6.7
Linearity, all ranges	% FSO	±2
Natural frequency	kHz	~30
Acceleration sensitivity	bar / g	<0.07
Operating temperature range		
Sensor, cable	°C	0 ... 300 °
Connector	°C	0 ... 200 °
Temperature coefficient of sensitivity	% / °C	±0.01
Insulation resistance		
at 20 °C	Ω	10 <sup>12</sup>
at 300 °C	Ω	10 <sup>11</sup>
Weight (Type 6152AA0.4)	g	250

Figure 3.1 Kistler direct pressure sensor and specifications [5]

The Kistler pressure sensors were calibrated before their application in the OSU die casting campaign. Two pressure sensors were used in the OSU campaign, which is a part of this U.S. DoE sponsored project. A given load was applied by means of a press and the measurements were recorded. The plots of applied and measured pressure for each sensor are shown in Figure 3.2 and Figure 3.3, respectively. The duration of each load was not recorded and the calibration was conducted at room temperature. The maximum deviation of the measured pressure from the applied pressure over the range of 0 through 1000 bars was 30 and 50 bars for sensors 1 and 2, respectively [15]. The maximum deviation from the actual can be expected to be 70 to 100 bars at the maximum cavity temperatures of 400 to 450 ° C and at cavity pressure of 1000 bars due to the 0.01%/° C temperature coefficient of sensitivity [15]. Figure 3.4 illustrates the applied and measured pressures when the applied pressure exceeds the operating range (0-1000 bars). Figure 3.5 illustrates the response of the two sensors during dynamic loading and unloading. In this figure the Kistler pressure sensors recorded a constant pressure 9.6 bars for over 2 seconds. For higher pressure, the period during which the pressure is constant is even longer. Two seconds are adequate for recording most events associated with the die casting process. The pressure is dynamic throughout most of the die casting process.

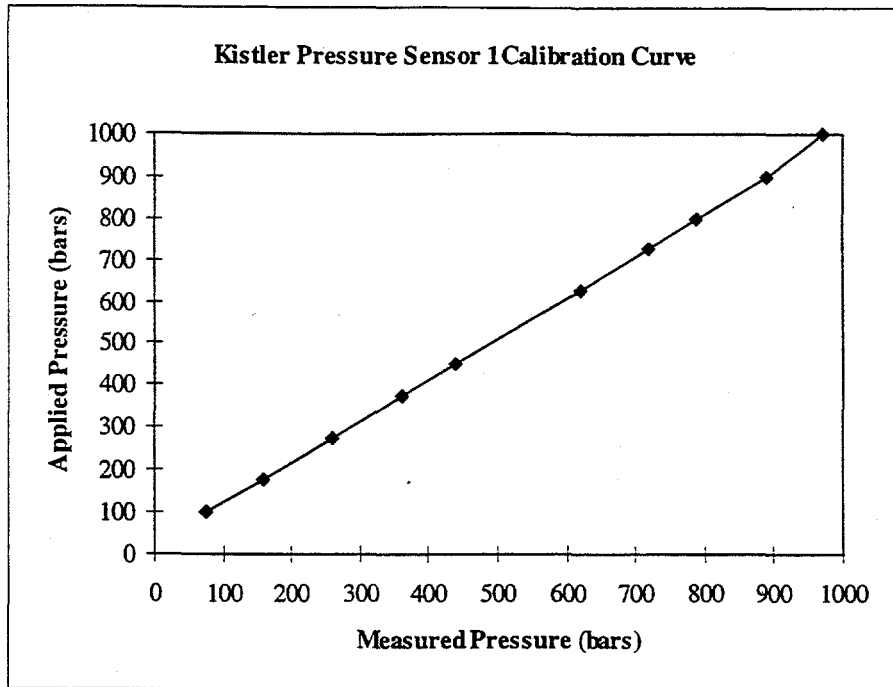


Figure 3.2 Kistler pressure sensor 1 calibration curve [15] (1 bar = 0.101 Mpa)

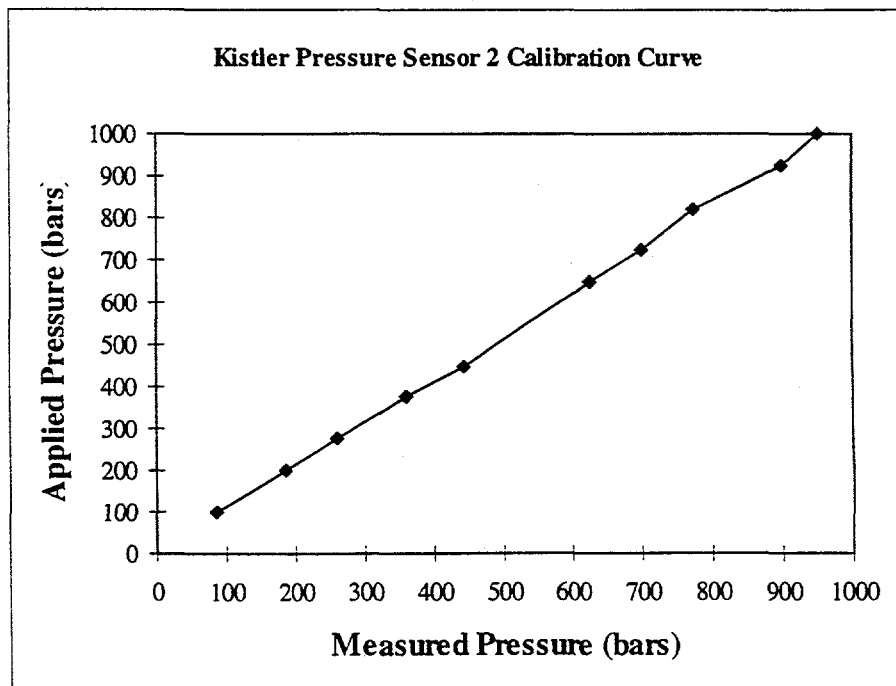


Figure 3.3 Kistler pressure sensor 2 calibration curve [15] (1 bar = 0.101 Mpa)

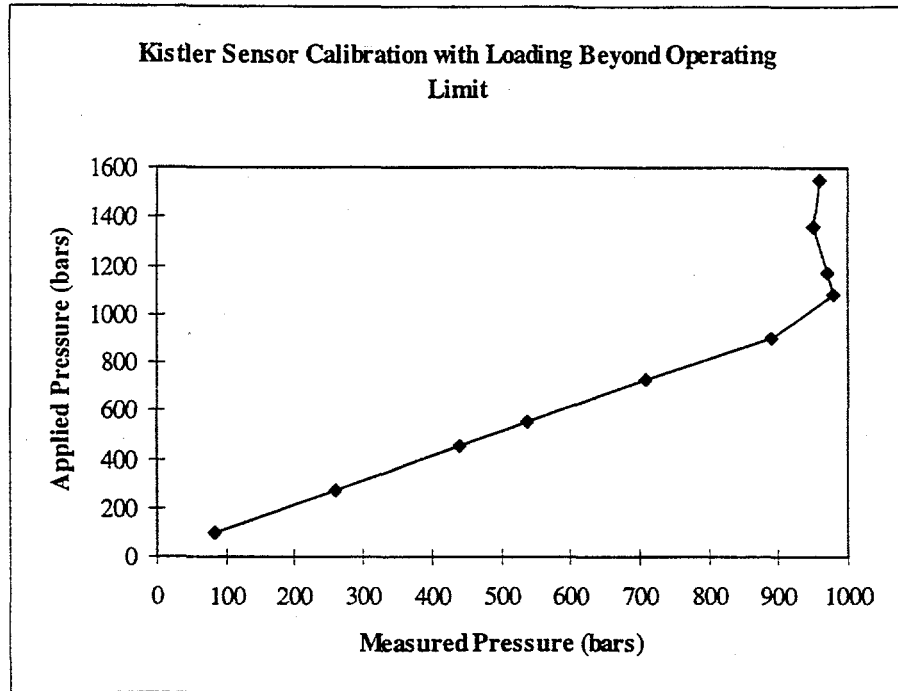


Figure 3.4 Calibration loading beyond configured operating limits [21]  
(1 bar = 0.101 Mpa)

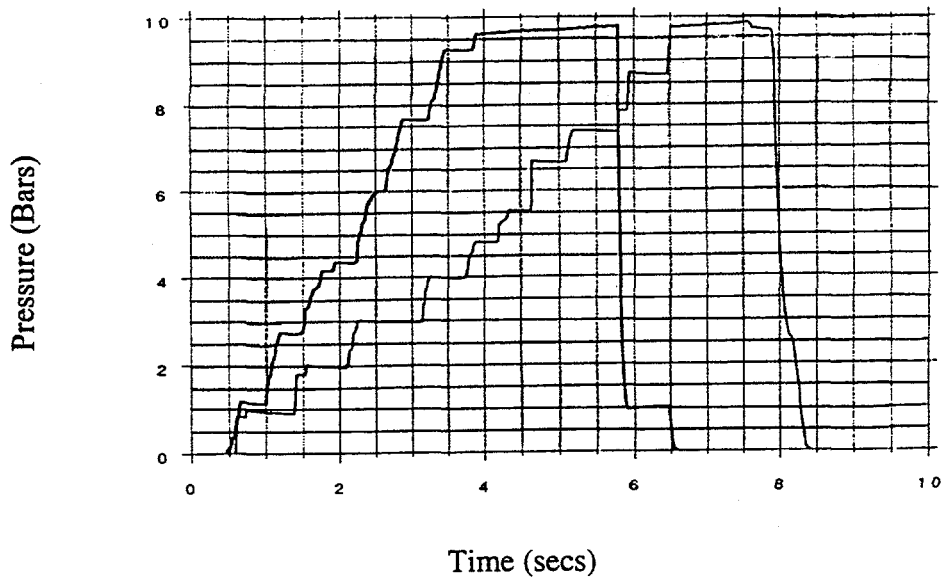


Figure 3.5 Dynamic calibration curve of Kistler pressure sensors [15]  
(The darker line is sensor 1, 1 bar = 0.101 Mpa)

### 3.3 EXPERIMENT SET-UP FOR OSU DIE CASTING CAMPAIGN [15]

The die casting machine used for the OSU campaign was a Buhler H-250SC system located in the Manufacturing Laboratory of the Engineering Research Center for Net Shape Manufacturing (ERC/NSM) at The Ohio State University. The technical specifications of Buhler H-250SC are listed in APPENDIX B. The Buhler SC machine has an improved shot control system and the ability to collect plunger position-time data used to interpret the die cavity filling and solidification phenomena. The temperature and pressure versus time records to be taken from the die cavity sensors were synchronized with the plunger position-time record and the cylinder hydraulic pressure-time record taken directly from the Buhler die casting machine. The selection of a die casting geometry and the associated die is an important factor in the evaluation of the process variables and the sensors measuring them. The die casting die was provided by OSU ERC/NSM and had been used in previous research. Its dimensions and configurations allowed it to be modified to install these sensors. A drawing of the diecasting, called the "Wall Die Casting", is shown in Figure 3.6. The advantages of this selection for this study are:

1. the presence of a relatively flat, uniform thickness gate area, which is preferred for the location of opposing temperature probes for an accurate measurement of the gate freezing time,
2. the availability of flat, uniform thickness regions in the casting for the location of pressure sensors and thermal probes,

3. the convenient location of vents which allow the placement of vent flow sensors,
4. the presence of walls which allow for assessing the effect of the process variables on the quality of the casting in the blind (unvented) wall area versus the ventable areas,
5. the diecasting size and shape which allow for easy radiographic determination of porosity distribution and Archimedes' density measurements.

For the campaign at OSU ERC/NSM, four temperature probes (two on opposing sides of the gate, and two on opposing sides of the pressure sensors) and two pressure probes were used at the locations indicated in Figure 3.7. The thickness of the gate was 0.08 inch and the gate area was 0.32 inch<sup>2</sup>. The thickness of wall was 0.20 inch. The operation variables decided for the chosen alloy, die and machine is provided in APPENDIX C. 11.05 inch<sup>3</sup> of Al alloy 390 melt was injected into the die cavity at a gate velocity of 1400 inch/sec and at an injection pressure of 70.64 psi to achieve a cavity fill time 12.1 ms. A locking force of 63,505 lbs was required to counter the intensification pressure of 1413 psi. A PQ<sup>2</sup> analysis was performed and a flow rate 504 inch<sup>3</sup>/sec at the required injection pressure was decided for a plunger diameter of 19.37 inches as shown in APPENDIX D. The output of each sensor was collected using computer based data acquisition system. The frequency of data collection was rather high because most of the die casting events, such as cavity filling, pressure intensification, and vent exhausting, occur in time frames of tens of milliseconds.

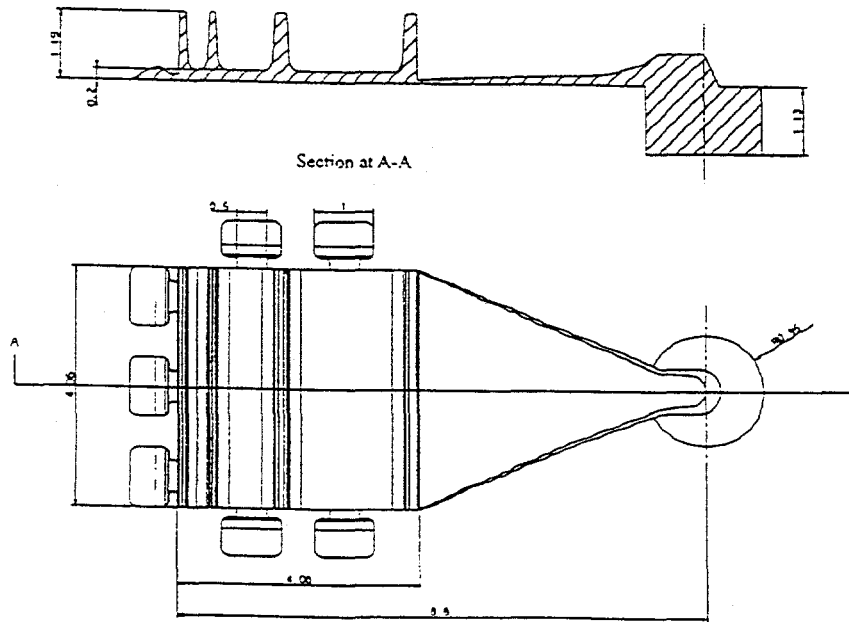
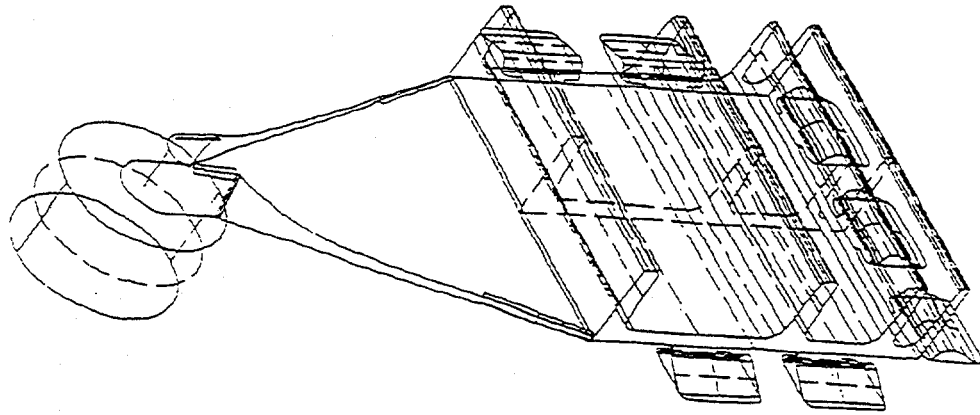


Figure 3.6 Wall die casting for OSU die casting campaign [15]

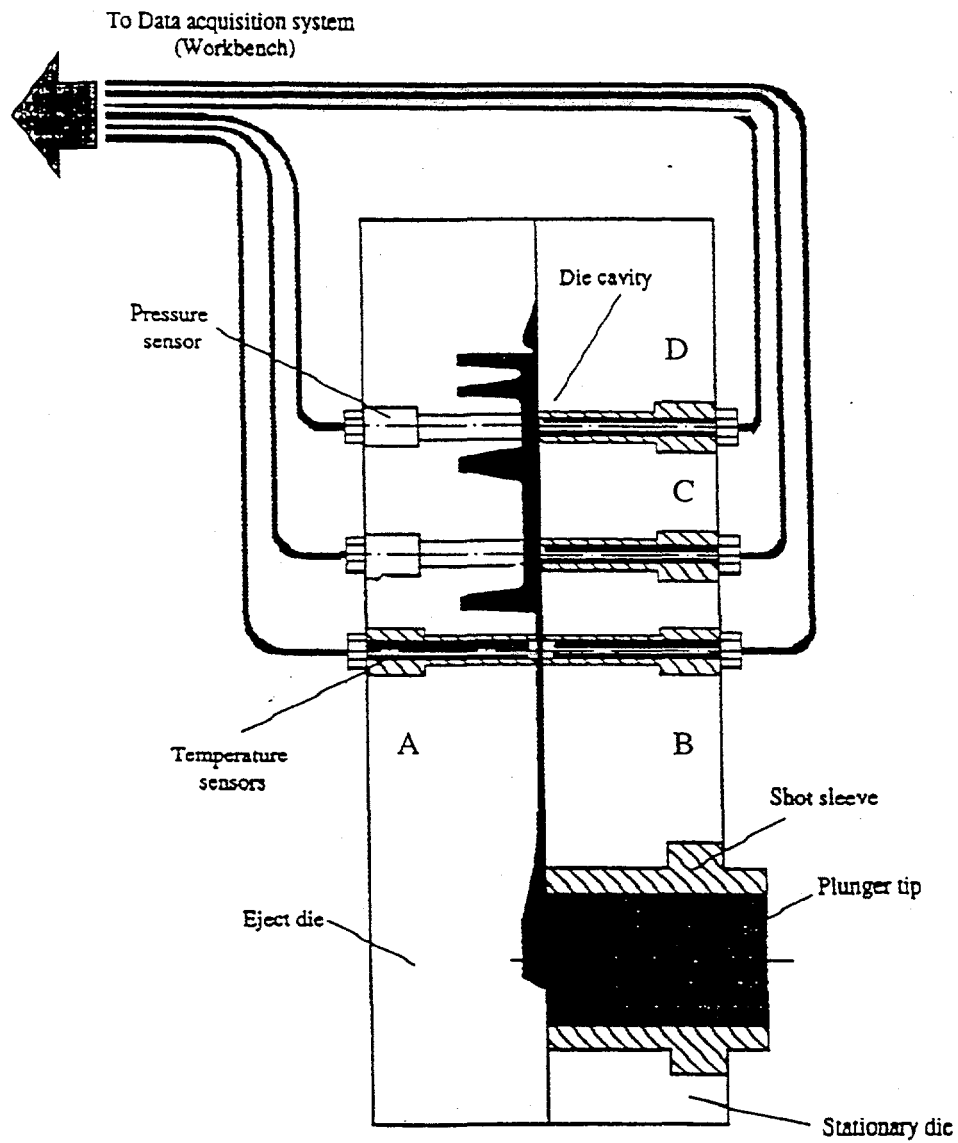


Figure 3.7 Locations of pressure sensors and thermocouple probes [5]

### 3.4 RESULTS FROM OSU ERC/NSM CAMPAIGN AND DISCUSSION

A die casting campaign was conducted on the Buhler H-250SC die casting machine using the wall die with the pressure and thermal probes installed. The machine was programmed according to the results of the machine set-up analysis. Because of shot sleeve to plunger tip friction, no intensification pressure was applied and the injection pressure was set at 200 bars, not the calculated value. Since the machine was run in the manual mode, the cycle time is not consistent from shot to shot, a quasi steady state condition in the dies was never reached. The data shown below are for the same shot.

The time that the melt entered into the cavity from the gate can be identified when the thermocouples at the gate increased in temperature. The freezing time of the gate can be estimated by the time that the temperature reached a peak and started to decay. This reason is that there was no latent heat left at that time to be transferred into the die. The observed gate freezing time is 0.4 second. The calculated freezing time of 0.45 second was obtained using a one-dimensional-finite-element-analysis program BINORM. The maximum temperature, associated with the local time to completed solidification. The freezing time was about 0.8 second at location C and 1.4 seconds at location D. It should be noticed that the location D is farther from the gate than location C. The calculated freezing time of 1.5 seconds was obtained using BINORM analysis.

Figure 3.8 compares the metal pressure calculated from the hydraulic pressure to the metal pressure measured by two Kistler direct pressure sensors. Both the Kistler sensor and machine hydraulic record indicated an impact pressure spike during the initial stage of metal injection. Then the metal pressure calculated from hydraulic pressure decayed with vibration to the programmed injection pressure of 200 bars (2940 psi) and remained relatively constant, while the metal pressures measured by pressure sensors continued to decrease with vibration until they reached zero. The freezing time at the locations of these pressure probes can be decided from the point where the pressure measured is zero. The pressures recorded by the pressure probes went to zero in 1.4 seconds and 1.1 seconds as illustrated in Figure 3.9 and Figure 3.10 respectively. The time to complete solidification determined from the pressure probes is fairly consistent with the time determined from the thermal probe and the calculated solidification time using BINORM. The little difference maybe due to the different response times of thermal probes and pressure probes and the limitation of the one dimensional finite element analysis program BINORM.

Generally, the agreement between the metal pressure based on the hydraulic record and the pressure sensors was relatively close because the size of the casting is small. Pressure records from pressure probes and hydraulic pressure reached their peak at same time. The large difference between the peak pressure measured by the in-cavity sensors and the hydraulic pressure during metal injection (0-50 millisecond) was attributed to the plunger tip sticking situation clearly. This demonstrated one of the

benefits of the Kistler in-cavity pressure sensors. Without them, the reason for the large hydraulic pressure spike during injection (which caused significant flashing problems) would have been much more difficult to discover.

The pressures measured from pressure probes were about 200 bars when the gate froze at about 0.4 second according to the thermal record. After that the pressures from pressure probes continuously decreased due to the shrinkage from solidification. The vibration may be due to the control problem with the machine injection system. The frequency of the vibration is about 20 Hz in Figure 3.9 and Figure 3.10.

Pressure vs. Time  
Shot No. 13  
(07-23-96)

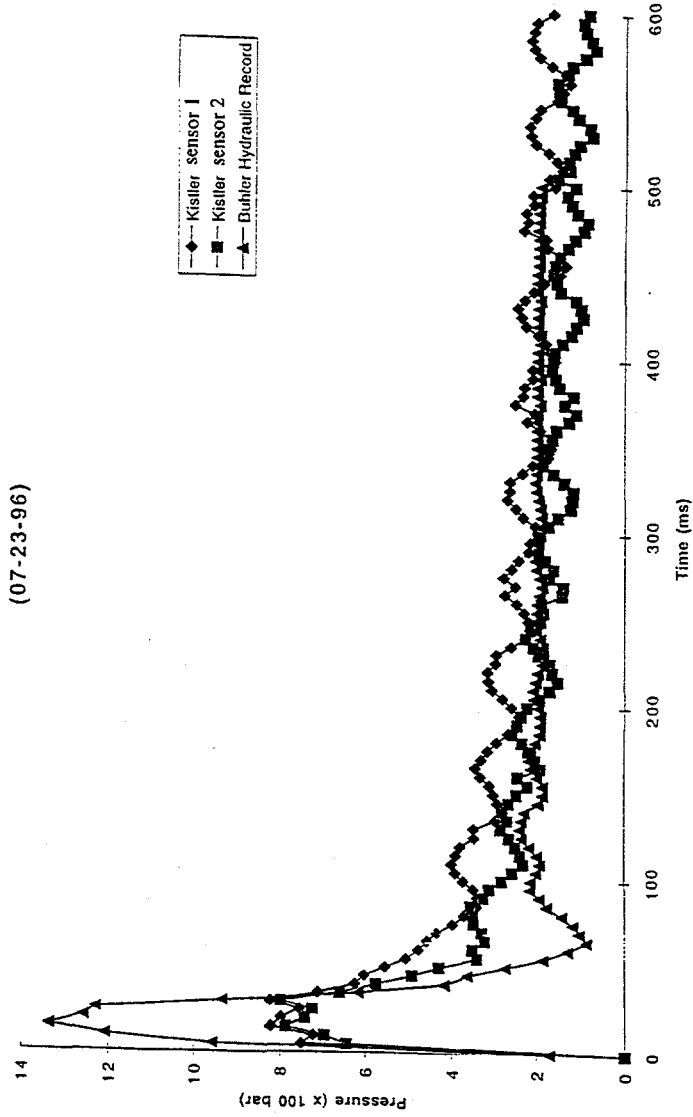


Figure 3.8 Metal pressures from hydraulic pressure and Kistler pressure sensors (1 bar = 0.101 Mpa)

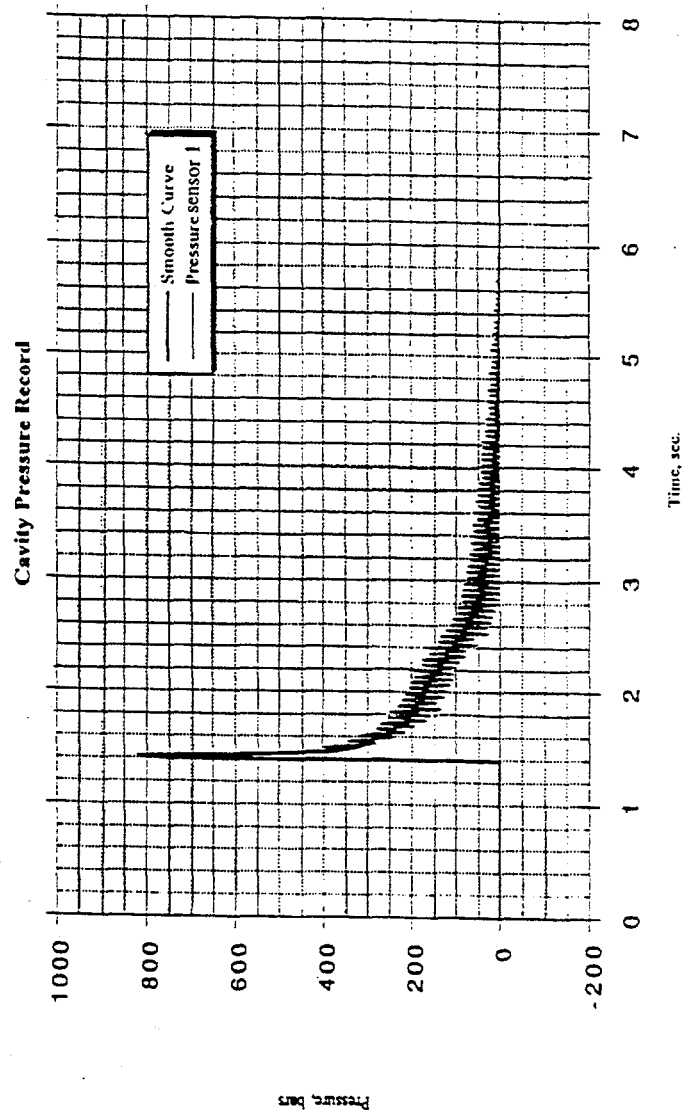


Figure 3.9 Cavity pressure record from Kistler pressure sensor 1 (1 bar = 0.101 Mpa)

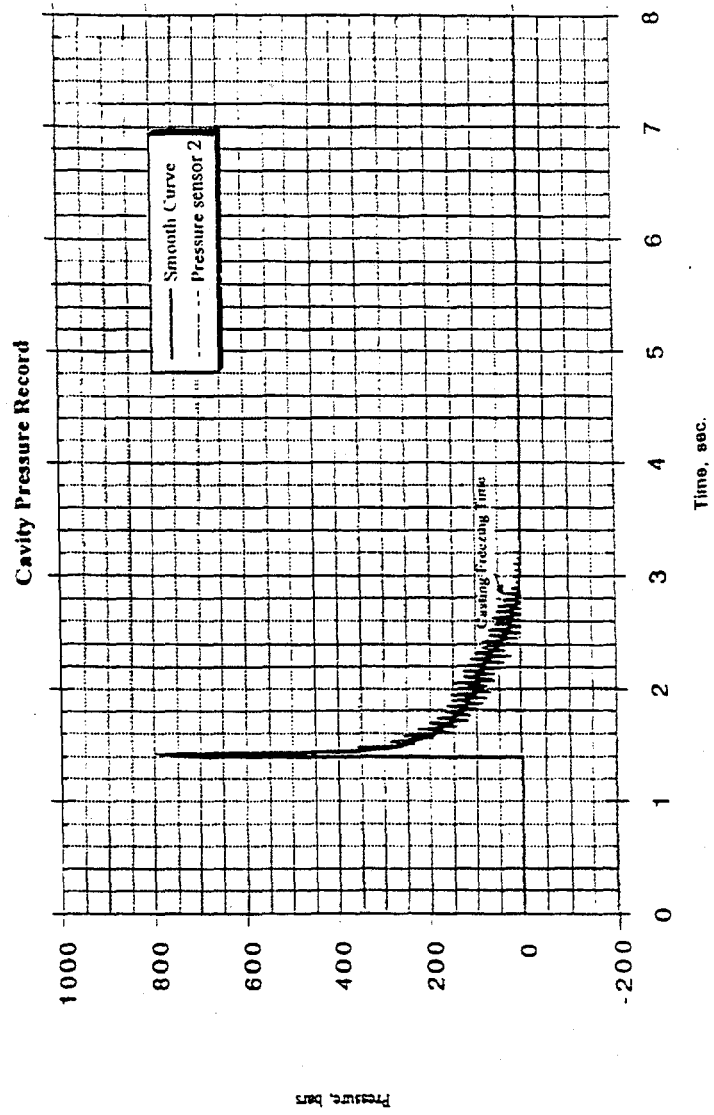


Figure 3.10 Cavity pressure record from Kistler pressure sensor 2 (1 bar = 0.101 Mpa)

### 3.5 RESULTS FROM GM CADC BEDFORD CAMPAIGN AND DISCUSSION

A die casting campaign was conducted at GM Casting Advanced Development Center (CADC) at Bedford, Indiana using a 3000 tons (U.S.) Prince die casting system to die cast a rear axle transmission case. The trimmed transmission case weight ranges from 11.8 to 12.7 kg. The die included a Kistler direct cavity pressure sensor on a sliding core located about 25.4 cm from the nearest ingate. More than fourteen individual thermocouples were installed at various locations throughout the die. All of the thermocouples were 1/2 inches or more from the die-cavity interface. Shot profiles were acquired using the Pro-Manager program on the Prince Machine. The purpose of this beta site campaign was to evaluate the Kistler pressure sensor as a complementary and/or improved sensor to the shot profile record for better understanding die casting process and predicting product quality measurements, such as part weight, volume, and density.

The shot profile contains velocity, head pressure, and rod pressure versus position and time records. Position based sampling is used while the shot is moving. Time based sampling is used once the shot has slowed to an operator determined value which is referred to as the 'End of Shot Velocity'. Figure 3.11 illustrates a typical pressure record in die casting process shot profile. In the intensification stage, increasing pressure is exerted to force more melt into the die cavity to feed shrinkage and gas porosity. In the dwell stage, the metal is held under a pressure (intensification pressure) until the metal solidifies.

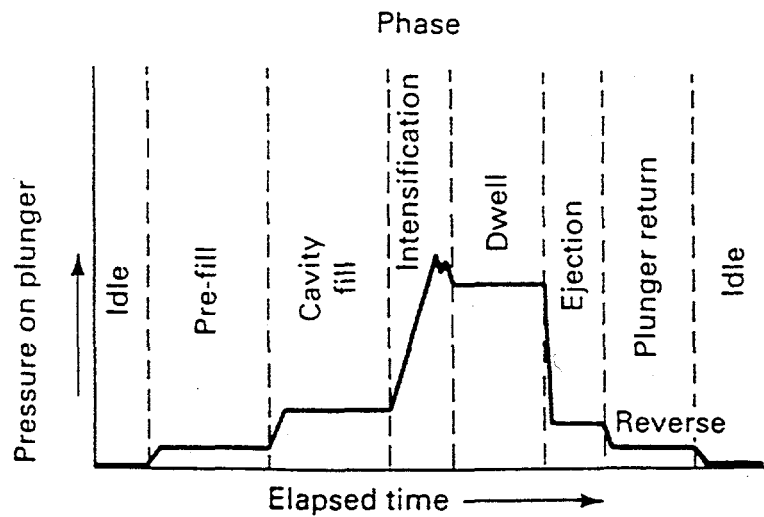


Figure 3.11 Plunger Pressure-Time Curve [1]

Only part of the pressure record, from the end of cavity fill, intensification, to dwell, will be analyzed. In the GM CADC campaign, 156 rear axle transmission cases were produced. The values of the process variables of earlier stages before intensification stage starts are relatively stable in 156 shots. Cavity fill pressures for all shots were set to about 4000 psi. The average,  $\bar{X}$ , and standard deviation,  $\sigma$ , of these process variables are listed in Table 3.1. The meanings of all the abbreviated names of process variables used in this thesis are[21]:

$P_{\text{final, H}}$  = final pressure (hydraulic), the average head pressure over a user settable window after end of shot, where the position based shot profiles end

Slow Vel = slow velocity

Inter Vel = intermediate velocity

Fast Vel = fast velocity

Act Ft Pos = actual fast velocity start position

Vel Rise = velocity rise time, the amount of time for the velocity to  
change from the user defined start and end velocity

Pres Rise = intensification pressure rise time, the amount of time for the head  
pressure to rise to an operator set value

Fil time srt = fill time start position

Fill time = the time for the shot plunger to move from the fill time start position to  
the end of shot position

B\_L = biscuit length

Inten Strk = intensification stroke length

End Pos = end of shot position, where the shot has slowed to an operator  
determined value and the time based sampling starts

End Vel = end of shot velocity, the velocity when the time based sampling starts

T\_Sleeve = the alloy temperature in shot sleeve

T\_Ladle = the alloy temperature in ladle

	Slow Vel (inch/sec)	Inter Vel (inch/sec)	Fast Vel (inch/sec)	Act Ft Pos (inch)	Vel Rise (ms)	Fil time srt (inch)
$\bar{X}$	10.0	24.9	98.1	27.41	15	26.76
$\sigma$	0.2	0.1	0.9	0.07	3	0.19
	Fill time (ms)	End Pos (inch)	End Vel (inch/sec)	T_Sleeve (°F)	T_Ladle (°F)	
$\bar{X}$	154	39.46	61.1	1214.3	1251.7	
$\sigma$	7	0.19	4.2	5.6	5.1	

Table 3.2 Average and standard deviation of some process variables  
of earlier stages before intensification starts

The 156 shots were divided into six sets based on the hydraulic pressure levels used and the status of the die casting system. During the first set, consisting of shots No. 1 through No. 20, the die and shot sleeve system were heating up due to system start up, after which die casting system (die and shot sleeve) reached a thermal quasi-steady state. Figure 3.12 shows the temperatures from various thermocouples in the die at the time the die closed for each shot.

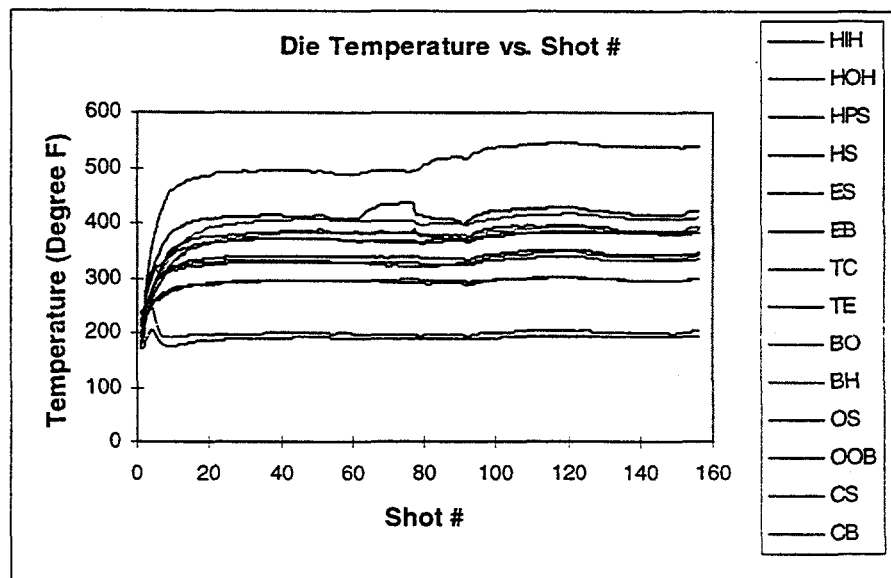


Figure 3.12 Temperatures at the time the die closed at different locations in the die for each shot

The die temperature at various locations remained relatively constant throughout the production campaign indicating that the system was in thermal quasi steady state. The temperature changes in two locations, which can be seen from the two highest temperature-time records from thermocouples TC and TE in Figure 3.12, may be attributed to variation in the local die spray to that region.

In the first set, the hydraulic intensification pressures of shot No. 2, 3, 4 and 5 were 1300 psi (hydraulic) while the others were about 2500 psi (hydraulic). In the second set (shots No. 21 through 50), the die was at thermal quasi steady state and the hydraulic intensification pressures were about 2500 psi (hydraulic). In the third set (shots No. 51 through 90), the hydraulic intensification pressures were about 1300 psi (hydraulic). In the fourth set (shots No. 91 through 121), the intensification pressures were about 3900 psi (hydraulic). To check the reproducibility of the die casting system and experiment, the intensification pressures were again about 2500 psi (hydraulic) for the fifth set (shots No.122 through 151). The hydraulic pressure was increased in the sixth set (shots No. 152 through 156) to investigate the onset of flashing. The final pressure (hydraulic) of each shot is plotted in Figure 3.13.

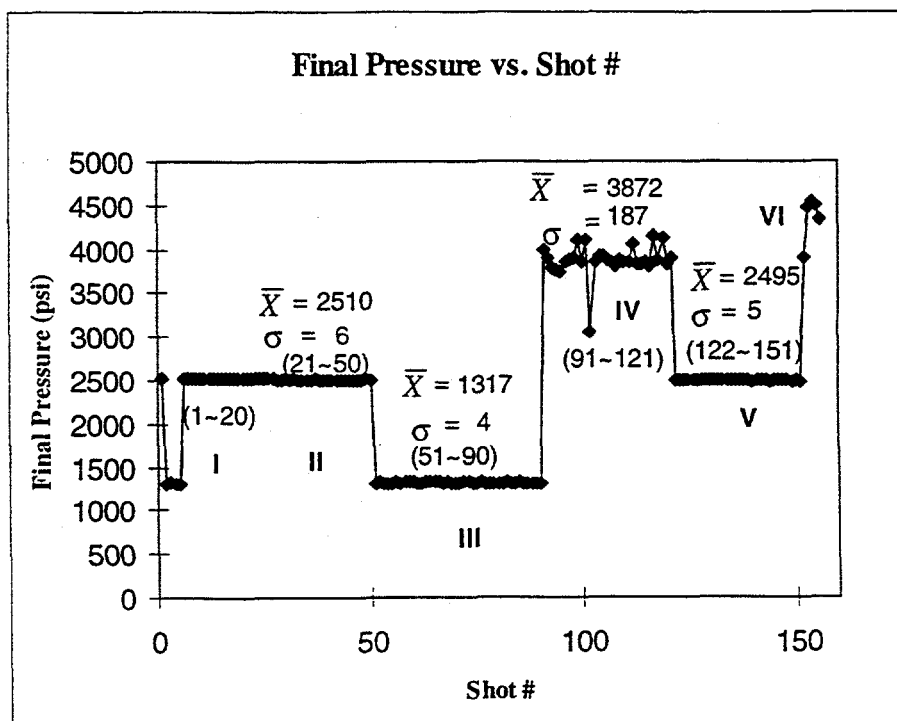


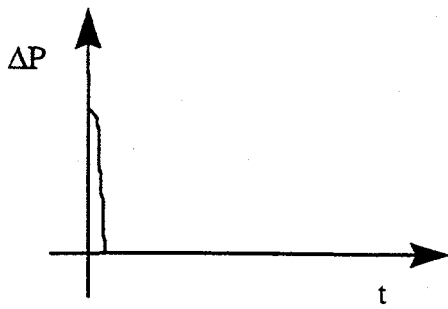
Figure 3.13 The final pressures (hydraulic) of each shot

As shown in Figure 3.13 the average final pressure was 2510, 1317, 3872 and 2495 psi for sets II, III, IV, and V, respectively. Standard deviations were 4 to 6 psi for sets II, III, IV, and 187 psi for set V.

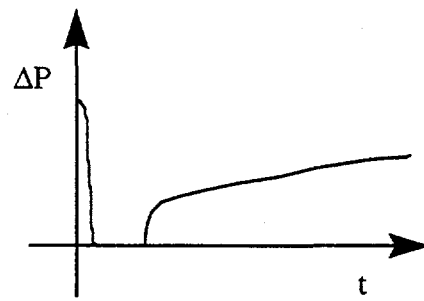
To evaluate the behavior the Kistler pressure probe, six shot profiles were selected from each of sets of II, III, IV and V. The first seven shots (shots No.1 through 7) and the last five shots (shots No.152 through 156) were also selected. The criteria for the selection in four sets (from set II through set V) is based on the values of intensification stroke, two with smallest values, two with medium values and two with the largest values. The hydraulic pressure of the shot profiles for these shots was converted to metal pressure by multiplying by the ratio of cross section areas of the plunger tip and the rod. The ratio used was 3.64. The pressure unit used was pounds per square inch (psi), and the pressure measured from Kistler pressure sensor (Kistler pressure) was converted from volts to pounds per square inch (psi). Both the hydraulic and Kistler pressure-time records were re-plotted using a Microsoft Excel spreadsheet. The plots of the pressure difference between the metal pressure converted from hydraulic pressure record and the pressure measured using Kistler pressure sensor were also made using the data of above re-plotted pressure-time records (pressure difference = the metal pressure converted from hydraulic pressure minus the Kistler pressure).

Conceptually, several possible pressure difference curves could occur. Figure 3.14 illustrates these situations and the following are the associated explanations.

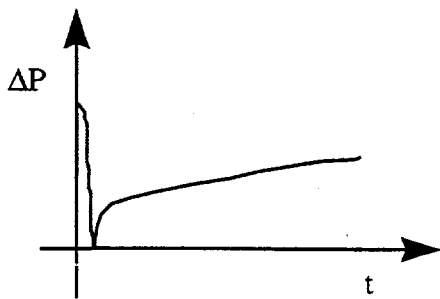
1. For case A, the Kistler pressure reaches the cavity filling pressure and remains zero when the Kistler pressure equals the metal pressure from hydraulic pressure
2. For case B, the pressure difference increases when the intensification starts, since the metal pressure from hydraulic pressure is larger than the Kistler pressure
3. For case C, the intensification starts as soon as the Kistler pressure reaches the cavity filling pressure.
4. For case D, before the Kistler pressure reaches the cavity filling pressure the intensification starts and the metal pressure from the hydraulic pressure is larger than the Kistler pressure.
5. For case E, in some region of the pressure difference curve the pressure difference is negative, where Kistler pressure is larger than the metal pressure from hydraulic pressure. This can be explained by impact occurring in the die cavity. During the cavity filling, the moving parts of the system contain considerable kinetic energy. The hydraulic fluid, hydraulic cylinder piston, plunger, plunger rod and molten metal all have mass and are moving at high speeds. When the cavity fills, these masses must stop moving. The energy is dissipated by causing higher pressure in the die cavity and creating a pressure spike or flashing [17].
6. For case F, due to larger intensification pressure, the pressure difference is larger than that with smaller intensification pressure.



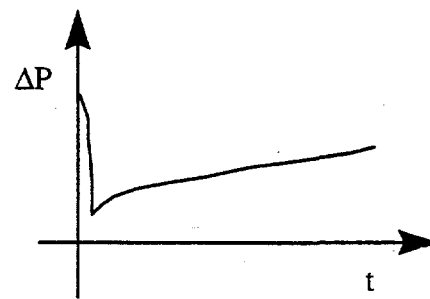
Case A: No impact



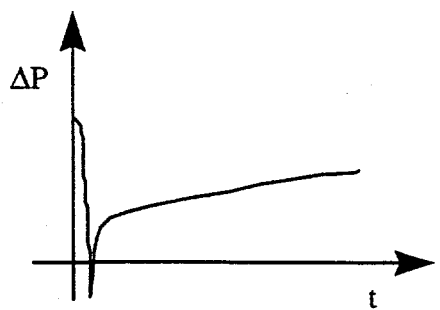
Case B: No impact, delayed intensification



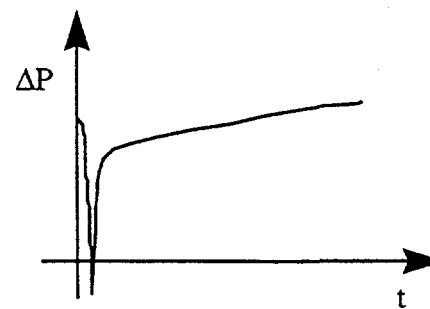
Case C: Intensification, no impact



Case D: No impact, earlier intensification



Case E: Impact, intensification



Case F: Impact, higher intensification pressure

Figure 3.14 Basic types of pressure difference curves

Figures 3.15 through 3.20 show the pressure and pressure difference records of three different experimental intensification pressures. Flashing of the die was not observed in these three shots.

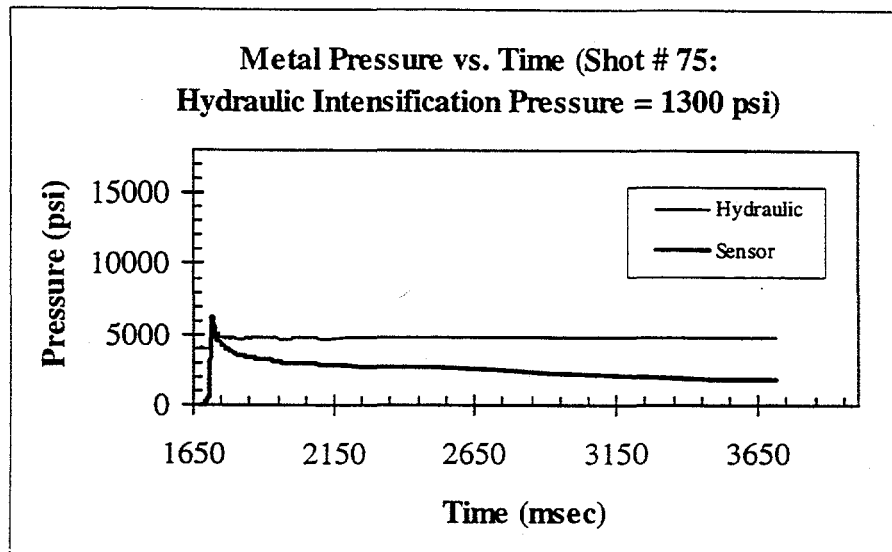


Figure 3.15 Pressure records of shot No. 75

In Figure 3.15, spikes induced from impact that occur on both pressure curves are noticeable. This fact is further confirmed by the corresponding pressure difference record as shown in Figure 3.16, where the value of the minimum pressure difference is negative.

In pressure record of shot No. 41, Figure 3.17, a small spike can be noticed on the Kistler pressure curve. The fact that impact occurred in the die cavity is also confirmed by its corresponding pressure difference record (Figure 3.18), even if no spike can be seen on pressure curve from hydraulic pressure.

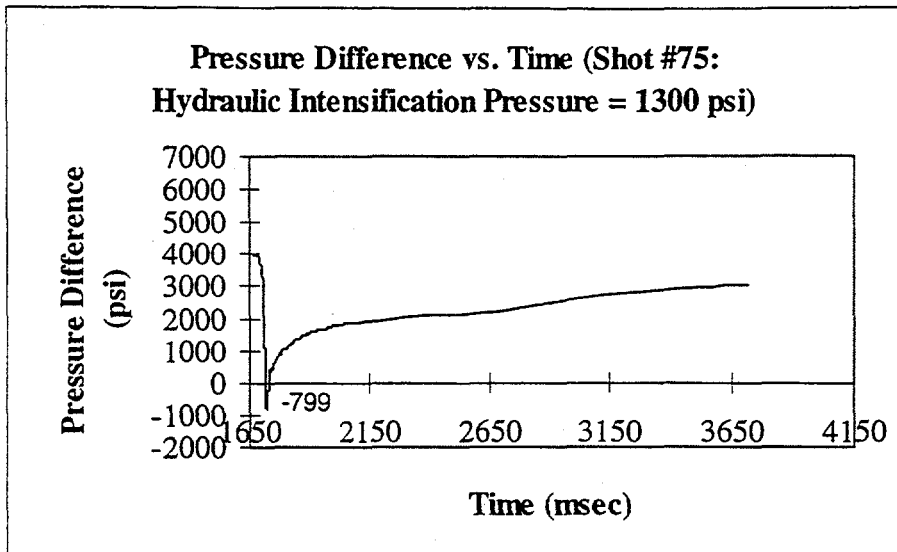


Figure 3.16 Pressure difference record of shot No. 75

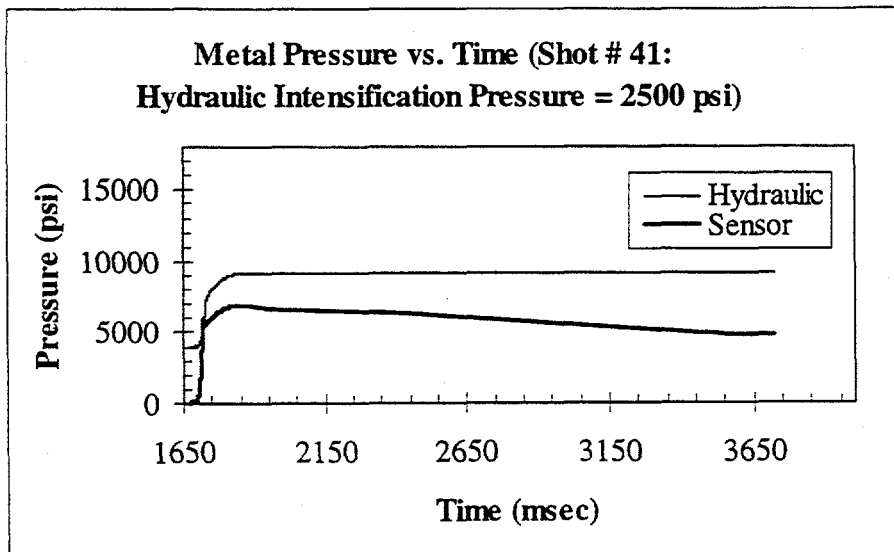


Figure 3.17 Pressure records of shot No. 41

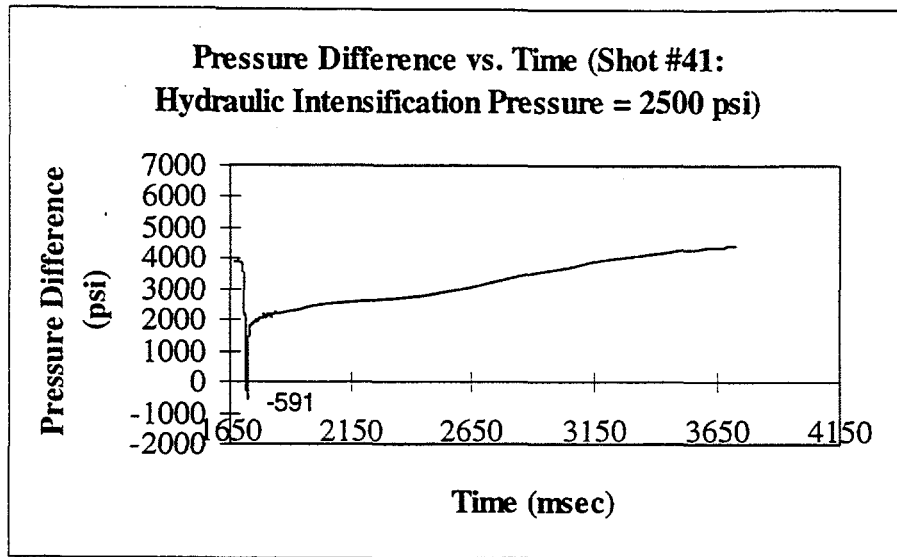


Figure 3.18 Pressure difference record of shot No. 41

Because of the higher intensification pressure, the pressure difference after the impact with higher intensification pressure is larger than that with lower intensification pressure. This is also confirmed by comparing the pressure difference curves of shot # 41 and shot # 75.

For shot # 97 in Figure 3.19, spikes induced from impact that occur on both pressure curves are noticeable. This fact is further confirmed by the corresponding pressure difference record as shown in Figure 3.20, where the value of the minimum pressure difference is negative. In Figure 3.20 the metal pressure from hydraulic pressure record takes longer time to reach the desired intensification pressure than shot # 41 and shot # 75. The Kistler pressure also takes longer time to reach the peak value. The pressure difference of shot # 97 just after impact is smaller than that of shot # 41. This

can be explained by the fact that the pressure rise time of the hydraulic pressure of shot # 97 are larger than that of shot # 41.

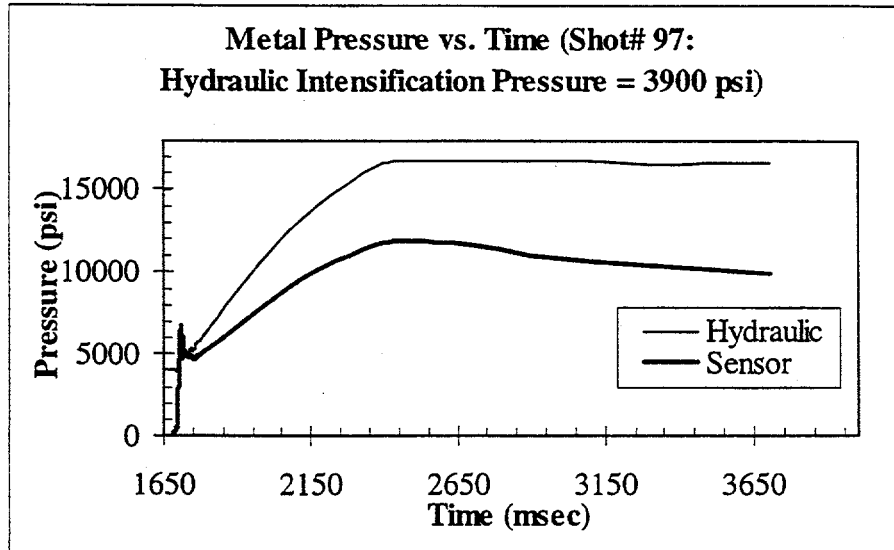


Figure 3.19 Pressure records of shot No. 97

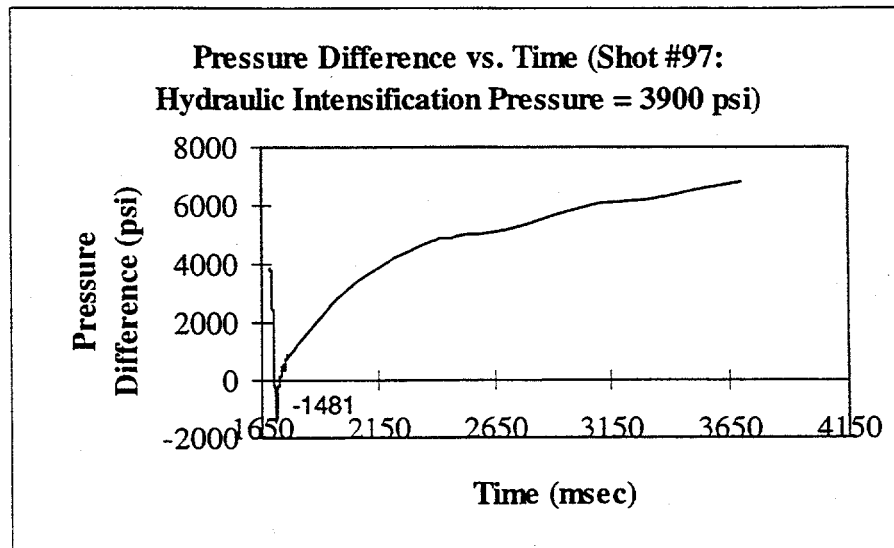


Figure 3.20 Pressure difference record of shot No. 97

Several parameters such as the pressure rise time of the hydraulic pressure, PRt H, pressure rise time of the Kistler pressure, PRt K, maximum metal pressure from the hydraulic pressure,  $P_{H, \max}$ , maximum Kistler pressure,  $P_{K, \max}$ , impact pressure or minimum pressure difference,  $P_{\text{impact}}$ , pressure difference 100 ms after impact,  $\Delta P_{100\text{ms}}$  and pressure difference 1900 ms after impact,  $\Delta P_{1900\text{ms}}$  were taken from pressure records to analyze the performance of the Kistler direct cavity pressure probe with respect to the hydraulic pressure records. The following are the list of various pressure parameters and related variables used in this thesis:

$P_{K, 2000\text{ms}}$  = pressure value measured from Kistler pressure sensor at 2000 ms after end of shot or time based sampling starts

$P_{H, \max}$  = the maximum metal pressure converted from hydraulic pressure

$t_{H, \max}$  = the time of the  $P_{H, \max}$  when it was measured

$P_{K, \max}$  = the maximum pressure measured from Kistler pressure sensor

$t_{K, \max}$  = the time of the  $P_{K, \max}$  when it was measured

$P_{H, \text{impact}}$  = the metal pressure converted from hydraulic pressure when the impact occurred

$P_{K, \text{impact}}$  = the pressure measured from Kistler pressure sensor when the impact occurred

$P_{\text{impact}} = P_{H, \text{impact}} - P_{K, \text{impact}}$

$t_{\text{impact}}$  = the time when the impact occurred

$\Delta P_{100\text{ms}}$  = pressure difference at 100 ms after minimum pressure difference

$\Delta P_{1900ms}$  = pressure difference at 1900 ms after minimum pressure difference

PRt H = pressure rise time of the hydraulic pressure is the time to take to go from 10% of the pressure range (from cavity filling pressure to maximum hydraulic pressure) to 90% of the pressure range

PRt K = pressure rise time of the pressure measured from Kistler pressure sensor, or Kistler pressure, is the time to take to go from 10% of the pressure range (from zero to maximum Kistler pressure) to 90% of the pressure range

All the data collected are in APPENDIX E.

The maximum metal pressures from the hydraulic pressure records of selected shots are plotted in Figure 3.21. As shown in the figure the average maximum metal pressure from the hydraulic pressure was 9223, 5626, 16758 and 9425 psi for sets II, III IV and V, respectively. The standard deviations are 76 psi and 59 psi for 1300 psi (hydraulic) set and 3900 psi (hydraulic) set, respectively. For the two 2500 psi (hydraulic) sets, the standard deviation values of the set II and set V are 35 psi and 281 psi respectively. The fact that the standard deviation of set V is so high and the discontinuity occurs in set V can not be explained by the final pressure in Figure 3.22.

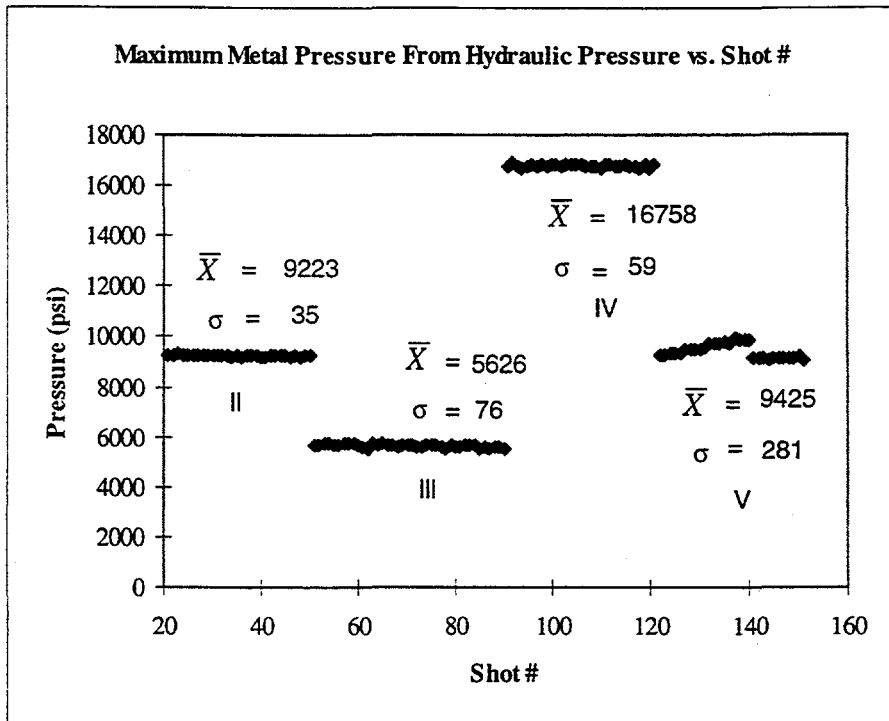


Figure 3.21 The maximum metal pressure pressures from the hydraulic pressure of selected shots

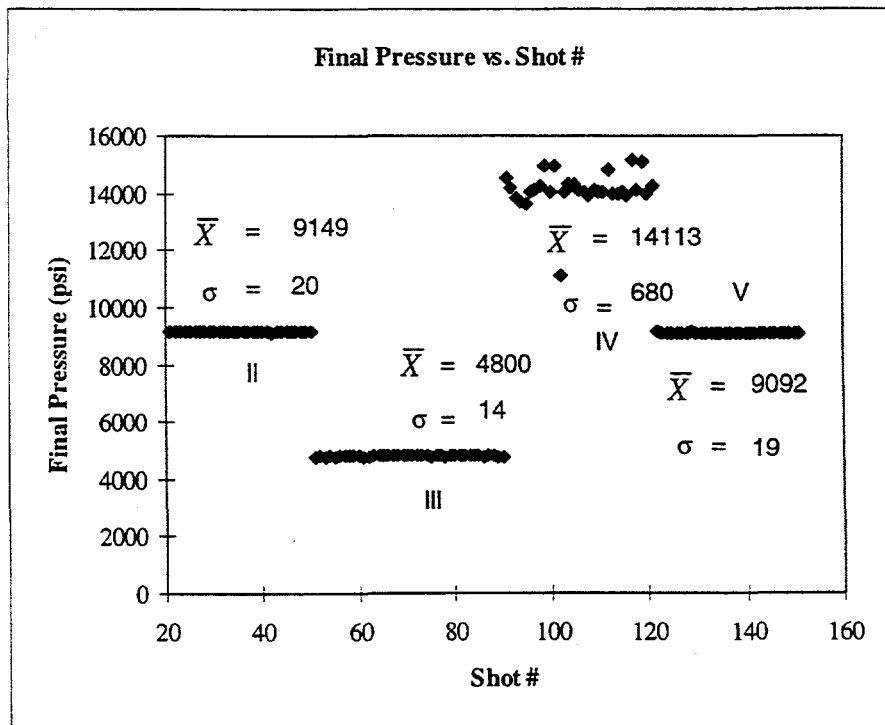


Figure 3.22 The final pressures of selected shots

For the two 2500 psi (hydraulic) sets in Figure 3.23, the average intensification stroke lengths are 0.37 and 0.4 inch for sets II and V, respectively. The standard deviation values of the set II and set V for the intensification stroke length are 0.03 and 0.09 inch, respectively. The higher average and larger standard deviation of set V in intensification stroke length versus shot # in Figure 3.23 explain the higher average value and bigger standard deviation of set V as compared to the set II. However, the discontinuity can not be explained by both figures.

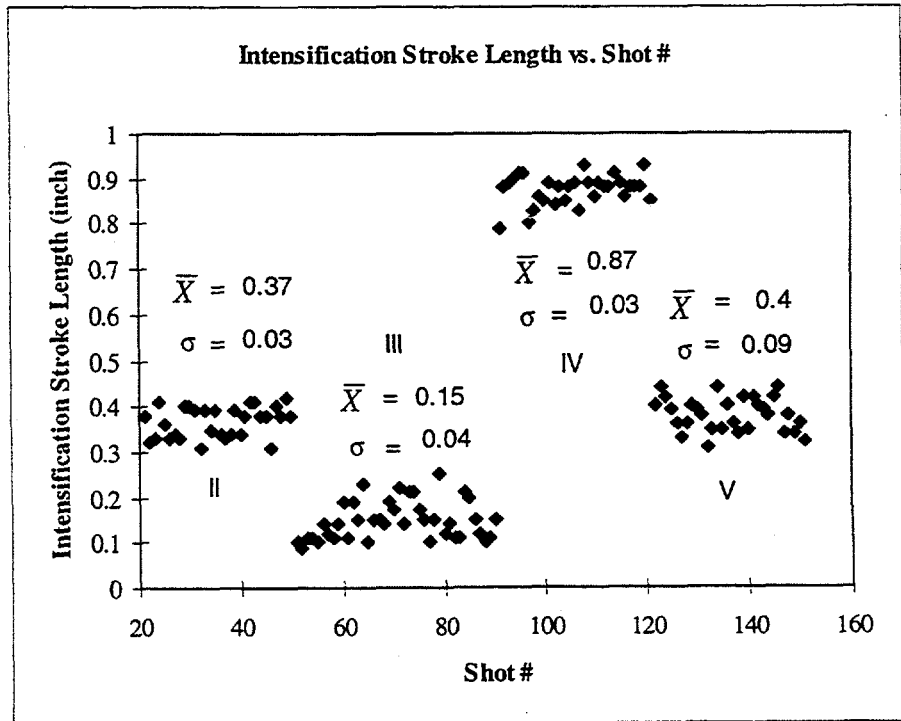


Figure 3.23 The intensification stroke length of selected shots

The maximum Kistler pressure versus shot # confirms the existence of the discontinuity in set V in Figure 3.21. For the two 2500 psi (hydraulic) sets in Figure 3.24, the standard deviation values are 178 and 473 psi and the average maximum Kistler pressure are 7037 and 7354 psi for sets II and V, respectively.

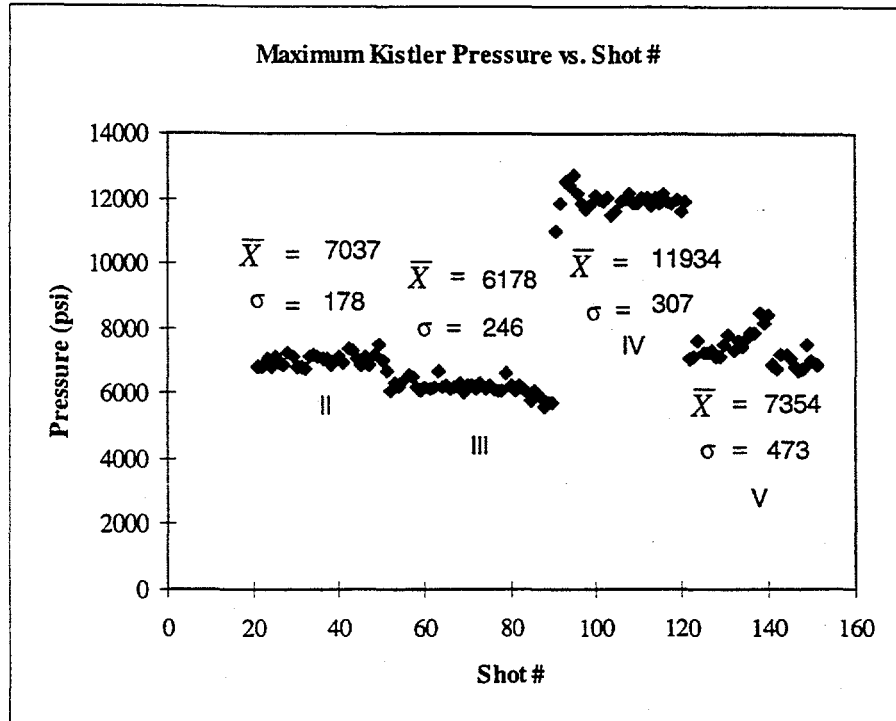


Figure 3.24 The maximum Kistler pressure of selected shots

Figures 3.25 and 3.26 show the Kistler pressure and hydraulic pressure records are nearly identical for the pressure rise time. The time resolution and accuracy of the Kistler pressure record is equal in capability to the hydraulic pressure record. In both figures, the average value of pressure rise time for the 3900 psi (hydraulic) set is larger than those of the 2500 psi (hydraulic) sets and the average values of pressure rise time for the 2500 psi

(hydraulic) sets is larger than that of the 1300 psi (hydraulic) set. The average value of pressure difference 100 ms after minimum value (Figure 3.27) for the 2500 psi (hydraulic) set is larger than the 3900 psi (hydraulic) set due to the longer pressure rise time of the 3900 psi (hydraulic) set. Since the intensification pressures of 1300 psi (hydraulic) set are smaller than the 2500 psi (hydraulic) sets, the average value of pressure difference for the 1300 psi (hydraulic) set is still smaller than that of 3900 psi (hydraulic) set. Except the highest point, it is found that in each set in Figure 3.25 and Figure 3.26 the data points with longer pressure rise time usually accompany big impact spikes on the hydraulic and the Kistler pressure-time records. The larger the hydraulic pressure rise time, the larger the Kistler pressure rise time.

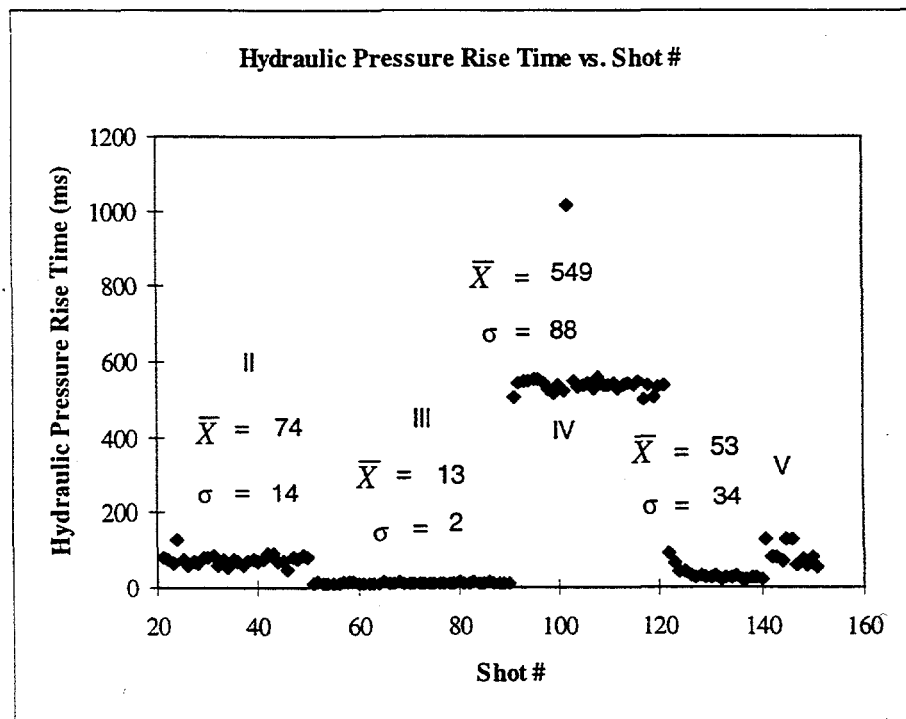


Figure 3.25 Pressure rise time of selected hydraulic pressure records

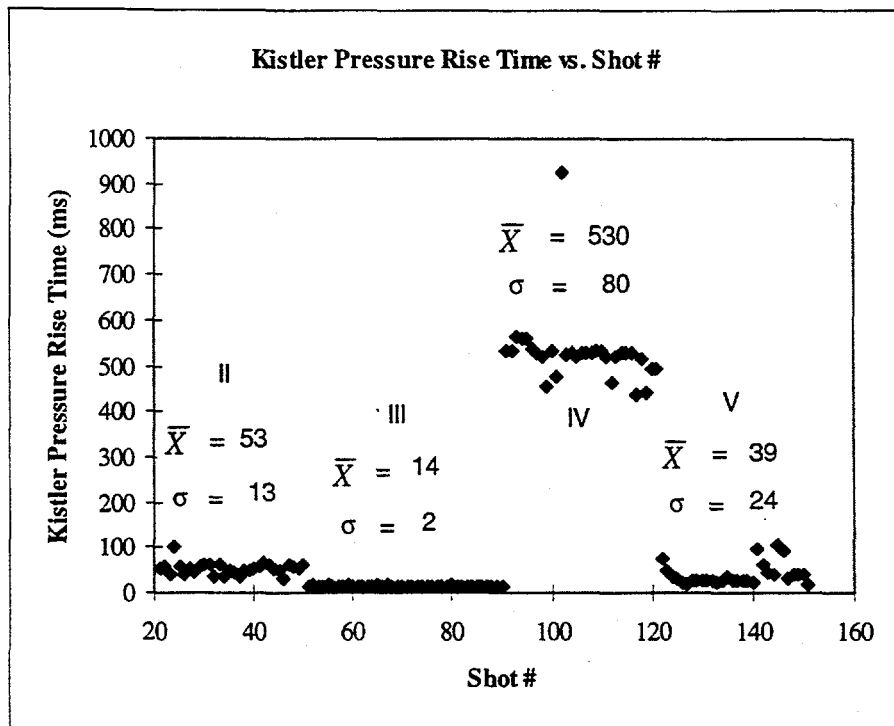


Figure 3.26 Pressure rise time of selected Kistler pressure records

From Figure 3.27, it can also be noticed that the data points of second 2500 psi set has more scatter than the first 2500 psi set; the 3900 psi set has even more scatter than late 2500 psi set. Figure 3.28 illustrates the pressure difference 1900 ms after minimum pressure difference. As shown in figure the average impact pressure was 4374, 2968, 6528 and 4627 psi for sets II, III, IV, and V respectively. The standard deviations are 195 and 526 psi for the 1300 psi (hydraulic) set and the 3900 psi (hydraulic) set, respectively. For the two 2500 psi (hydraulic) sets, the standard deviation values of the set II and set V are 293 and 292 psi respectively. There exist a very good correlation between the Kistler pressure and hydraulic pressure in Figure 3.25 since if the Kistler pressure increases with

increasing intensification pressure, the pressure difference also increases with increasing intensification pressure. It also noticed in Figure 3.28 that the higher the pressure the larger the scatter.

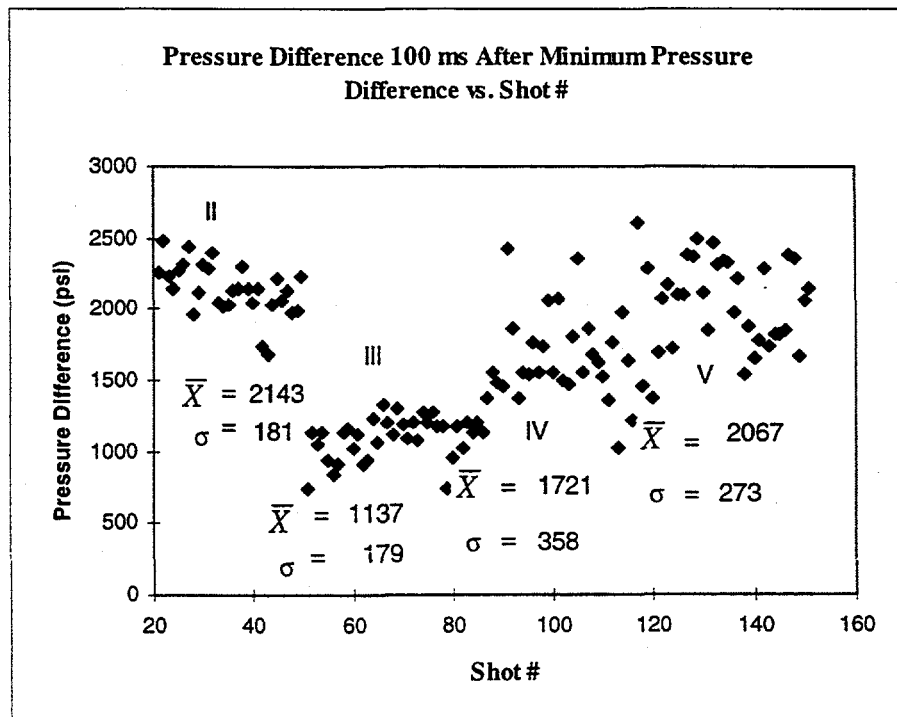


Figure 3.27 Pressure difference 100 ms after minimum pressure difference

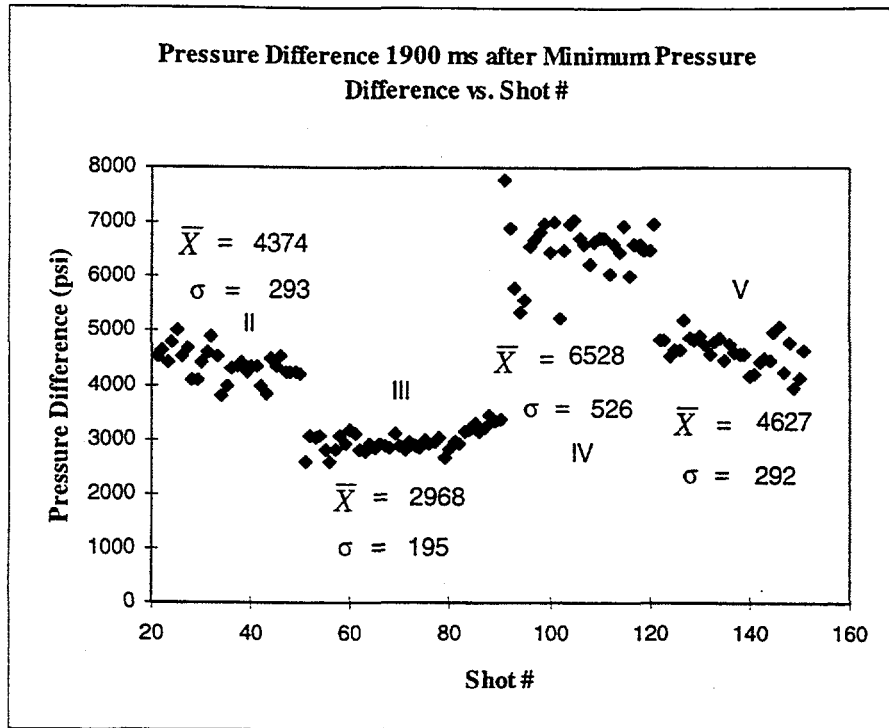


Figure 3.28 Pressure difference 1900 ms after minimum pressure difference

Figure 3.29 illustrates impact pressure of selected shots. As shown in the figure, the average impact pressure was -520, -771, -1012 and -651 psi for sets II, III IV and V respectively. The standard deviations are 152 psi and 439 psi for 1300 psi (hydraulic) set and 3900 psi (hydraulic) set respectively. For the two 2500 psi (hydraulic) sets, the standard deviation values of the set II and set V are 265 psi and 402 psi respectively. From this figure, it can be inferred that the average impact pressure of set IV is higher than set III and the average impact pressure of set III is higher than set II and set V; the scatter increases with increasing number of shots; and the impact pressure of shots 22, 123, 128, 132 is zero. The first conclusion means that even if the intensification pressure is lower it may cause bigger impact as compared to the sets II and V. Negative value

indicates that the die is closed with the required clamping force to resist the impact in the die cavity and no flashing occurs. For shots 22, 123, 128, 132, if no flashing occurred, maybe the intensification started earlier or something blocked the movement of the plunger or something remained on the parting line of the die preventing the die from closing tightly or the moving part such as slides retracted.

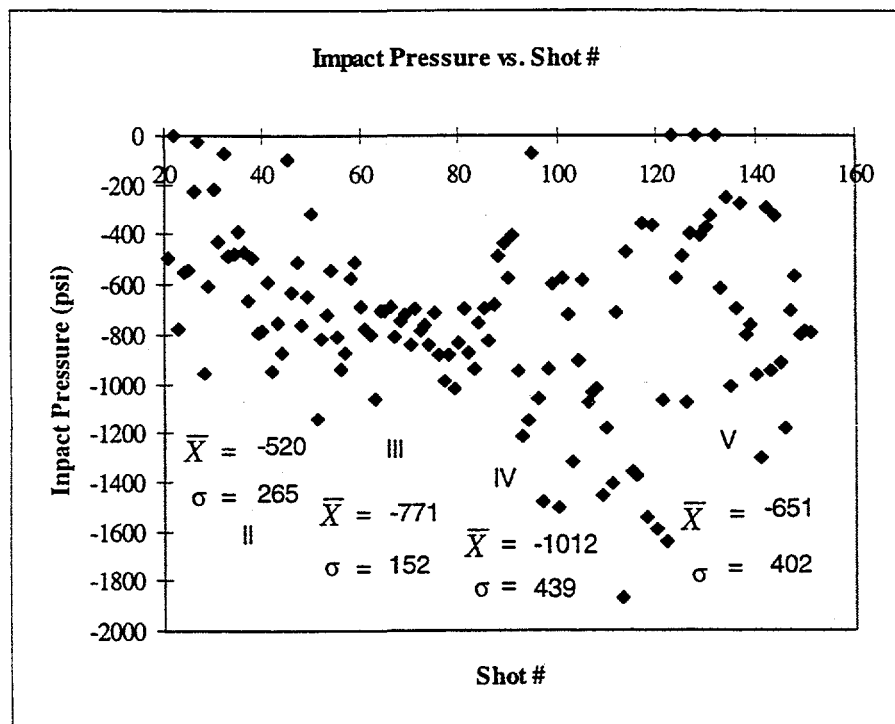


Figure 3.29 Impact pressure of selected shots

The other three shots that have no impact pressure are shots 1, 155 and 156. In shot 1, it is conjectured that the die was still cold and the gap between the die parts was not closed by thermal expansion. The last two belong to the flashing test set with die flashing and the metal pressure from the hydraulic pressure and Kistler pressure are quite

low. These facts indicate that the clamping force was not large enough to suppress die opening. As soon as the die opens, flashing occurs and the pressure in the die cavity drops. Even if the hydraulic pressure had not reached the desired final pressure, the pressure difference is large. Figure 3.30 and Figure 3.31 show the pressure and pressure difference records of the shot 156. The minimum pressure difference is positive because of the flashing; and the pressure difference is high because of low cavity pressure.

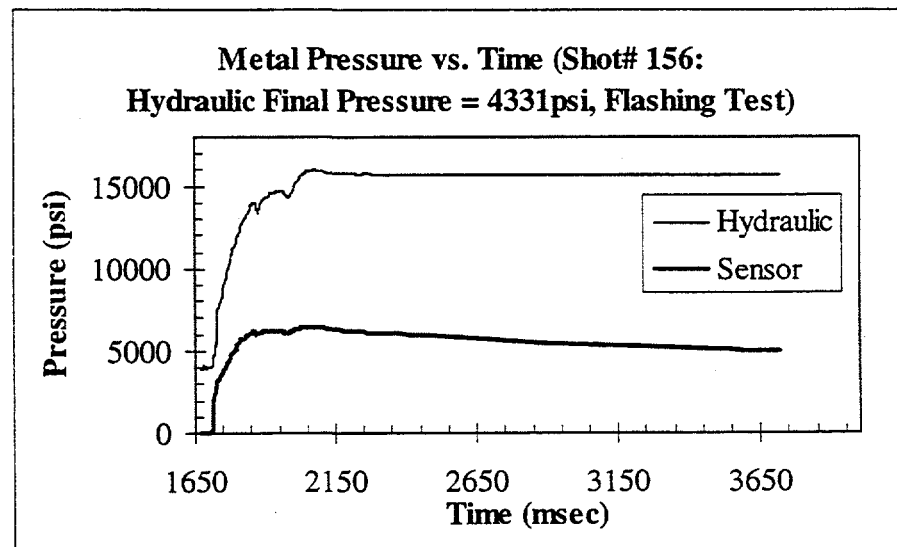


Figure 3.30 Pressure records of shot No. 156

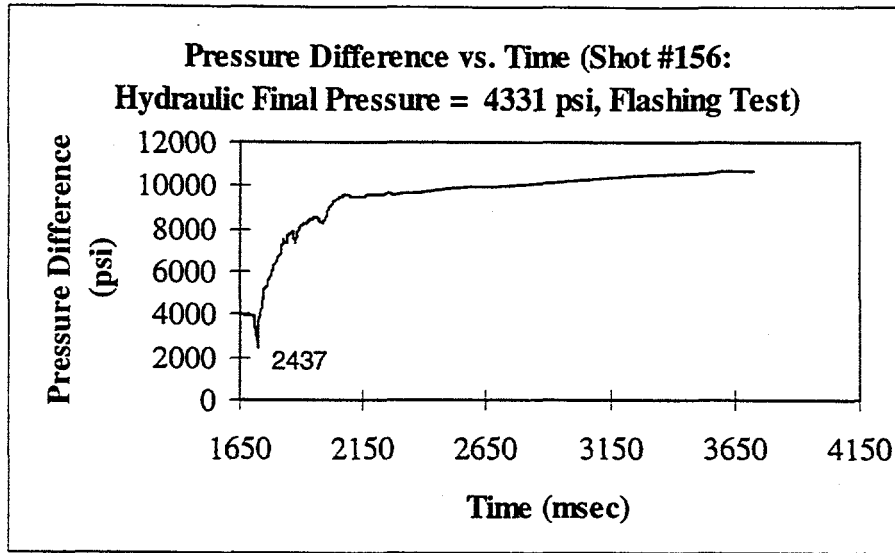


Figure 3.31 Pressure difference records for shot No. 156

The average values and standard deviation values of sets II, III, IV, V in figures from Figure 3.21 through Figure 3.28, and Figure 3.31 are listed in Table 3.1.

	set II		set III		set IV		set V	
	Average	Stdev	Average	Stdev	Average	Stdev	Average	Stdev
$P_{final}$	9149	20	4800	14	14113	680	9092	19
$P_{H,max}$	9223	35	5626	76	16758	59	9425	281
$P_{K,max}$	7037	178	6178	246	11934	307	7354	473
$P_{impact}$	-520	265	-771	152	-1012	439	-651	402
$\Delta P_{100ms}$	2150	186	1148	208	1631	237	2005	186
$\Delta P_{1900ms}$	4374	293	2968	195	6528	526	4627	292
PRt, H	74	14	13	2	549	88	53	34
PRt, K	53	13	14	2	530	80	39	24
$\delta$	0.37	0.03	0.15	0.04	0.87	0.03	0.40	0.09

Table 3.3 The average and standard deviation values of pressure parameters, intensification stroke, pressure difference and pressure rise time of sets II, III, IV, and V

In this table the pressure unit used is pound per square inch (psi), the time unit used is millisecond, and the distance unit is inch.

## CHAPTER 4

### EXAMINING THE CORRELATIONS BETWEEN THE KISTLER DIRECT PRESSURE SENSOR OUTPUTS AND CASTING VOLUME, DENSITY, AND WEIGHT

#### 4.1 INTRODUCTION

Density is an index of the casting quality. The effects of pressure applied during intensification on the density of casting were evaluated on seventeen trimmed transmission cases from the GM die casting campaign (shots 20, 50, 60, 90, 91, 120, 121, 123, 126, 131, 136, 151, 152, 153, 154, 155, and 156), biscuit and runner of shots 20, 50, 60, 90, 91, 120, and overflows of shots 50, 60, 90, 91, 120. All these shots were made after the thermal quasi steady state was reached. Shots 60 and 90 were cast with 1300 psi (hydraulic). Shots 91, 120, and 121 were cast with 3900 psi (hydraulic). Shots 20 and 50 were cast with 2500 psi (hydraulic) and belong to set II. Shots 123, 126, 131, 136 and 151 were cast with 2500 psi (hydraulic) and belong to set V. Shots 152 through 156

belong to the flashing test. Shots 155 and 156 are the two shots that had flashing. As shown in Chapter 2 Figure 2.6 from Kay and Street [3] and Figure 2.7 from Tokui [11], the porosity decreases, or the density increases, with increasing applied pressure. A model for predicting the porosity in the die castings was developed and presented in NADCA Transactions [17]. This model also indicates that the increasing applied pressure should produce decreasing porosity parts. In the measurements of the casting weight, volume and density of the trimmed transmission cases from GM CADC Bedford, it was found that the casting weight increased from 26.3789 to 28.5599 lbs; the casting volume increased from 266.33 to 285.02 inch<sup>3</sup>; the casting density increased from 0.09923 to 0.10022 lbs/inch<sup>3</sup> if the intensification pressure was increased from 1300 psi (hydraulic) to 4598 psi (hydraulic).

#### 4.2 ARCHIMEDES' DENSITY MEASUREMENT

The casting material of these transmission cases is die cast Aluminum Alloy 380. The nominal composition range for this alloy is given in Table 4.1.

Table 4.1 Nominal Composition Range for Aluminum Alloy 380 (weight percent)

<u>Silicon</u>	<u>Copper</u>	<u>Iron</u>	<u>Zinc</u>	<u>Magnesium</u>	<u>Manganese</u>	<u>Tin</u>	<u>Nickel</u>	<u>Aluminum</u>
7.5-9.5	3.0-4.0	2.0	3.0	0.10	0.50	0.35	0.50	balance

Using Archimedes' density measurement method, the castings were weighed in air and then weighed in water. The density and porosity can be calculated from these data. The following formula was used to determine the density of the casting:

$$\rho_c = \frac{W_A}{V_c} \quad (1)$$

$$V_c = \frac{W_A - W_w}{\rho_w - \rho_A} \quad (2)$$

$\rho_c$  = Casting density

$W_A$  = Casting weight in air

$V_c$  = Casting volume

$W_w$  = Casting weight in water

$\rho_w$  = Density of water

$\rho_A$  = Density of air

The following formula was used to determine the porosity:

$$f_p = \frac{\rho_t - \rho_c}{\rho_t} \times 100 \quad (3)$$

$f_p$  = Percent porosity (%)

$\rho_t$  = Theoretical density, assumed equal to 2.7941 g/cc [19]

An example calculation for the shot #1 casting is as follows. The average dry weight of casting is  $27.7512 \pm 0.0002$  lbs and the wet weight of casting is  $17.7048 \pm 0.0002$  lbs (The accuracy that the balance can measure is  $\pm 0.0002$  lbs); the density of water is  $0.99754 \pm 0.00001$  g/cc and the density of air is  $0.001161 \pm 0.000001$  g/cc ( $1\text{g/cc} = 0.036127486$  lb/inch<sup>3</sup>). The casting volume upper limit equals  $(27.7512 + 0.0002 - 17.7048 + 0.0002)/[0.036127486(0.99754 - 0.00001 - 0.001161 - 0.000001)] = 279.10669$ . The casting volume lower limit equals  $(27.7512 - 0.0002 - 17.7048 - 0.0002)/[0.036127486(0.99754 + 0.00001 - 0.001161 + 0.000001)] = 279.07835$ . The casting weight is  $279.09252 \pm 0.014169$ . If the accuracy is rounded to  $\pm 0.02$  lbs. The casting weight is  $279.09 \pm 0.02$  lbs. Likewise, the casting density upper limit equals  $(27.7512 + 0.0002)/(279.09 - 0.02) = 0.0994424$  lb; the casting density lower limit equals  $(27.7512 - 0.0002)/(279.09 + 0.02) = 0.0994267$  lbs. The casting density is  $0.0994345 \pm 0.00000787465$ . If the accuracy is rounded to  $\pm 0.00001$  lbs. The casting density is  $0.09943 \pm 0.00001$  lbs.

The facilities needed for density measurement using the Archimedes' method include [20]:

1. A scale with sensitivity to at least 0.0002 lbs. The balance has bottom weighing capability so that the casting can be submerged in the water bath
2. A calibration standard and pure silicon block to test the accuracy of the system
3. Tap or distilled water

4. A container large enough to hold the water and part
5. A means of attaching the casting to the balance while submerging the casting in the water. Here thin wires and a plate are adequate

The schematic of Archimedes' density measurement system is shown in Figure 4.1.

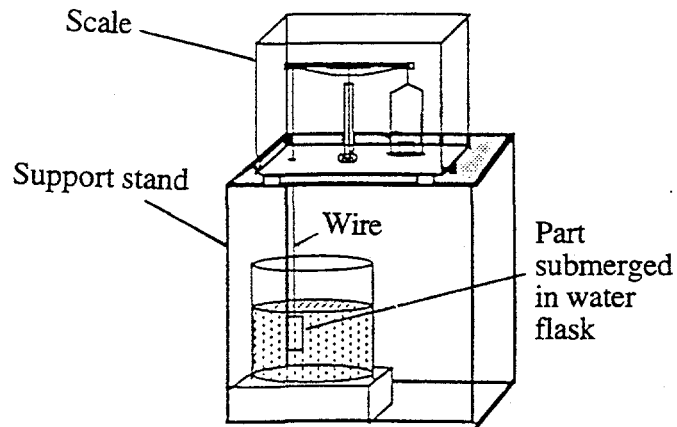


Figure 4.1 Schematic of Archimedes's measurement system[20]  
(The scale used here is Mettler MultiRange FBB30 together  
with Mettler MultiRange ID1 plus weighing terminal)

The procedures are:

1. Attach one end of the wire through the hole in the support stand to the balance and the other end to the plate
2. Measure and record the weight required to balance the wire and plate in air
3. Measure and record the weight required to balance the wire and plate in water
4. Clean the casting
5. Submerge the casting in water and attach the casting to the balance by placing the plate behind a hole in casting, the size of the hole is smaller than the plate,

and attach one end of the wire to the plate

6. Remove bubbles with a water tube
7. Weigh the casting three times

The results of Archimedes' density measurement, casting weight  $W_{t_c}$ , casting volume  $Vol_c$ , and casting density  $\rho_c$  data of the selected shots are listed in Table 4.2. The casting plus the overflow weight  $W_{t_{c+o}}$  data provided by GM are also listed in Table 4.2.

Shot	$W_{t_{c+o}}$ (lbs)	$W_{t_c}$ (lbs)	$Vol_c$ (inch <sup>3</sup> )	$\rho_c$ (lbs/inch <sup>3</sup> )
1	29.15	27.7512	279.09	0.09943
2	28.30	26.9367	272.35	0.09891
3	28.15	26.8030	270.34	0.09915
4	28.05	26.6731	269.03	0.09915
6	28.70	27.0038	270.87	0.09969
20	28.45	26.9149	270.01	0.09968
50	28.40	26.8553	269.46	0.09966
60	28.10	26.4673	266.72	0.09923
90	27.90	26.3789	266.33	0.09905
91	29.30	27.5936	275.59	0.10013
120	29.45	27.7135	276.93	0.10007
121	29.40	27.6856	276.45	0.10015
123	28.45	26.8595	269.33	0.09973
126	28.55	26.8494	268.59	0.09996
131	28.60	26.8883	269.67	0.09971
136	28.55	26.9427	270.07	0.09976
151	28.50	26.8934	269.55	0.09977
152	29.4	27.6933	276.59	0.10012
153	29.75	28.0081	279.62	0.10017
154	29.95	28.1923	281.31	0.10022
155	30.30	28.5048	284.44	0.10021
156	30.35	28.5599	285.02	0.10020

Table 4.2 Casting weight plus overflows, and trimmed casting weight, volume, and density data of selected shots

Shot 154 had the highest density among these shots. Shots 155 and 156 have the largest volume and casting weight. Their density values are next to shot 154. Shots 155 and 156 will not be included in the following plots because of the flashing.

#### 4.3 THE EFFECTS OF APPLIED PRESSURE ON THE CASTING VOLUME

The shot number, final pressure,  $P_{final}$ , maximum metal pressure from hydraulic pressure,  $P_{H, max}$ , maximum Kistler pressure,  $P_{K, max}$ , Kistler pressure at 2000 ms after intensification starts,  $P_{K, 2000ms}$ , average Kistler pressure,  $P_{K, average}$  ( $P_{K, average} = (P_{K, max} + P_{K, 2000ms})/2$ ), the mean value between the final pressure and average Kistler pressure,  $P_{mean}$  ( $P_{mean} = (P_{final} + P_{K, average})/2$ ) are listed in Table 4.3.

Shot	$P_{final}$ (psi)	$P_{H, max}$ (psi)	$P_{K, max}$ (psi)	$P_{K, 2000ms}$ (psi)	$P_{K, average}$ (psi)	$P_{mean}$ (psi)
20	9167	9251	7018	4872	5945	7556
50	9120	9236	6989	4901	5945	7532
60	4811	5635	6162	1668	3915	4363
90	4786	5456	5684	1436	3560	4173
91	14507	16767	10976	8889	9933	12220
120	13993	16639	11774	9976	10875	12434
121	14248	16782	11992	9643	10818	12533
123	9102	9269	7134	4205	5670	7386
126	9105	9320	7236	4394	5815	7460
131	9080	9520	7786	4263	6025	7552
136	9109	9685	7873	4336	6105	7607
151	9061	9120	7018	4379	5699	7380
152	14208	16760	11673	9904	10789	12498
153	16290	16545	12441	10237	11339	13814
154	16585	16607	12920	10977	11949	14267

Table 4.3 Various pressure parameters of the selected shots

To explore the effects of various pressure parameters on casting volume, the plots of casting volume versus final pressure, the casting volume versus maximum metal pressure from hydraulic pressure, the casting volume versus maximum Kistler pressure, the casting volume versus average Kistler pressure, and the casting volume versus mean pressure are shown in Figure 4.2, Figure 4.3, Figure 4.4, and Figure 4.5 and Figure 4.6, respectively.

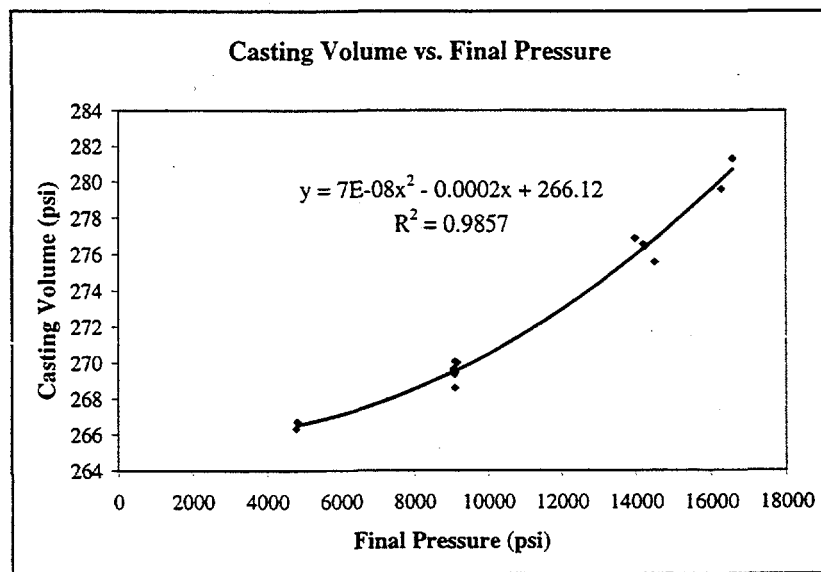


Figure 4.2 The effect of final pressure on the casting volume

The casting volume increases with increasing final pressure. However, more than one value of casting volume will correspond to a given value of final pressure.

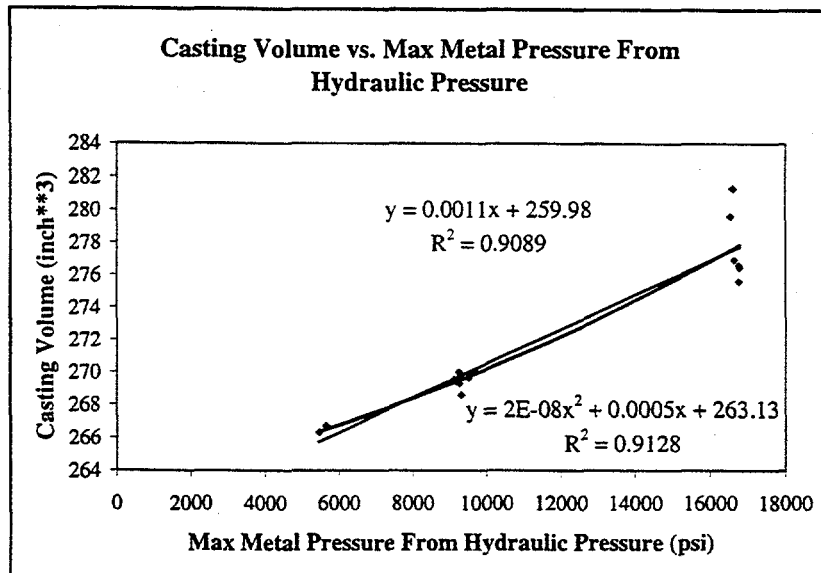


Figure 4.3 The effect of max metal pressure from hydraulic pressure on the casting volume

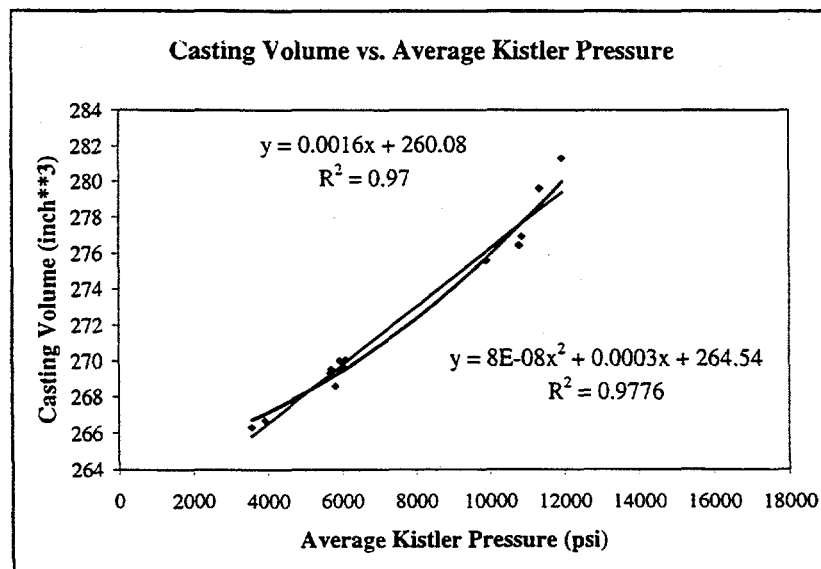


Figure 4.4 The effect of average Kistler pressure on the casting volume

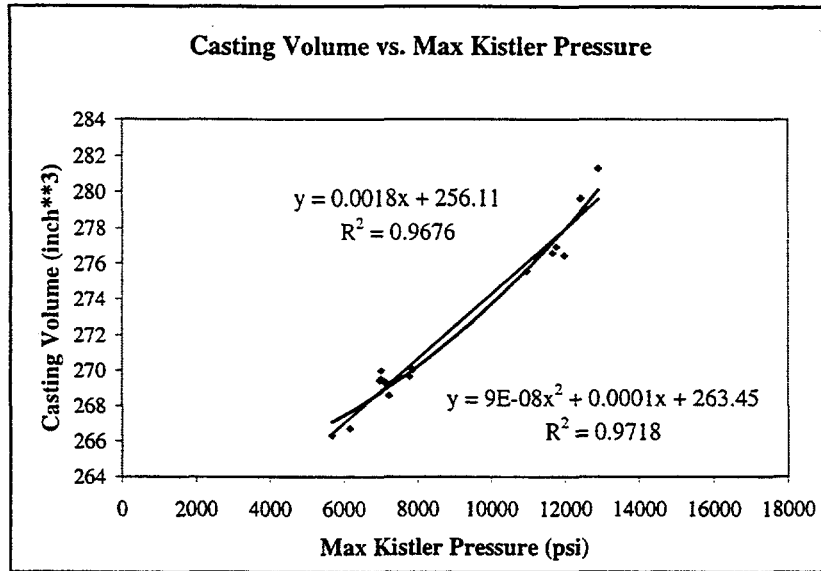


Figure 4.5 The effect of max Kistler pressure on the casting volume

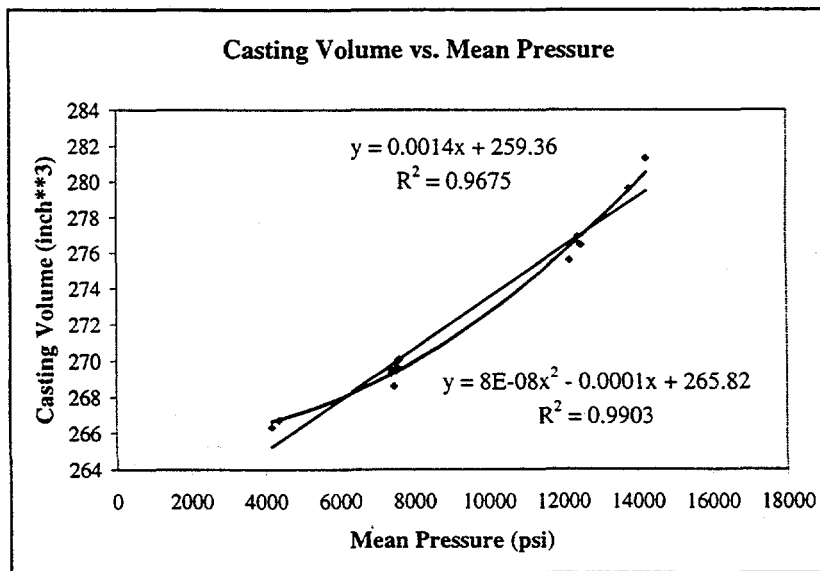


Figure 4.6 Effect of mean pressure on the casting volume

In terms of the  $R^2$  value (correlation coefficient), the mean pressure is the appropriate pressure parameter to establish the actual correlation with casting volume. The  $R^2$  values for trendlines of casting volume vs. final pressure  $y = 7E-8x^2 - 0.0002x + 266.12$ , maximum metal pressure from hydraulic pressure  $y = 2E-8x^2 + 0.0005x + 263.13$ , average Kistler pressure  $y = 8E-8x^2 + 0.0003x + 264.54$ , maximum Kistler pressure  $y = 9E-8x^2 + 0.0001x + 263.45$ , and mean pressure  $y = 8E-8x^2 - 0.0001x + 265.82$  are 0.9857, 0.9128, 0.9776, 0.9718, and 0.9903, respectively.

#### 4.4 THE EFFECTS OF APPLIED PRESSURE ON THE CASTING DENSITY

To explore the effects of various pressure parameters on casting density, the plots of casting density versus the reciprocal of final pressure, maximum metal pressure from hydraulic pressure, average Kistler pressure, maximum Kistler pressure, and mean pressure are shown in Figure 4.7, Figure 4.8, Figure 4.9, Figure 4.10, and Figure 4.11.

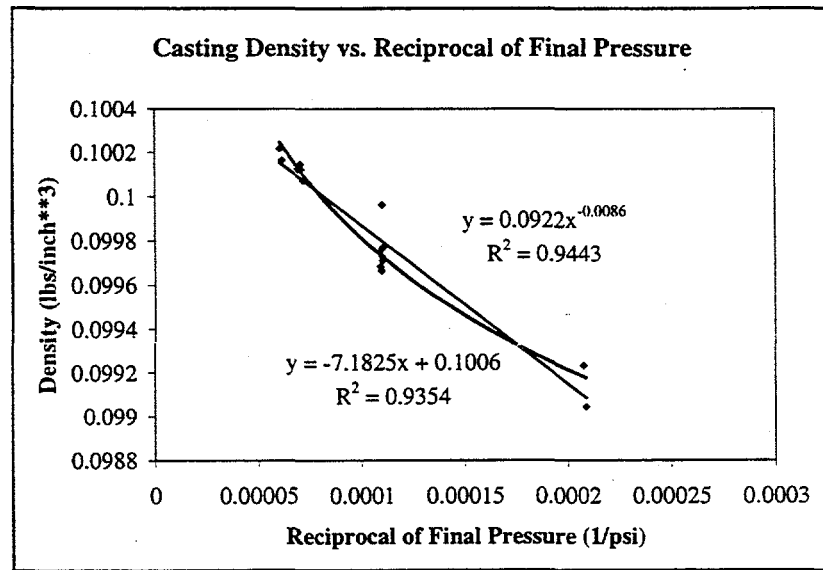


Figure 4.7 The effect of final pressure on casting density

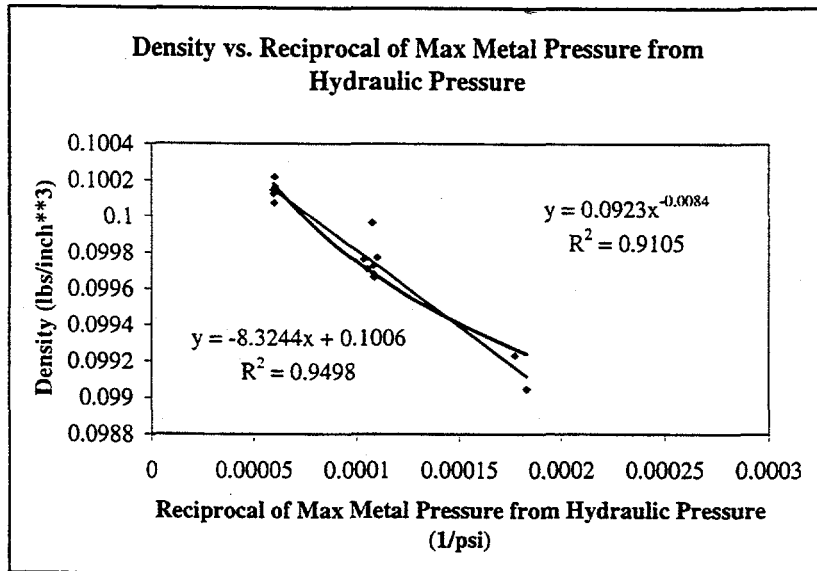


Figure 4.8 The effect of max metal pressure from hydraulic pressure on the casting density

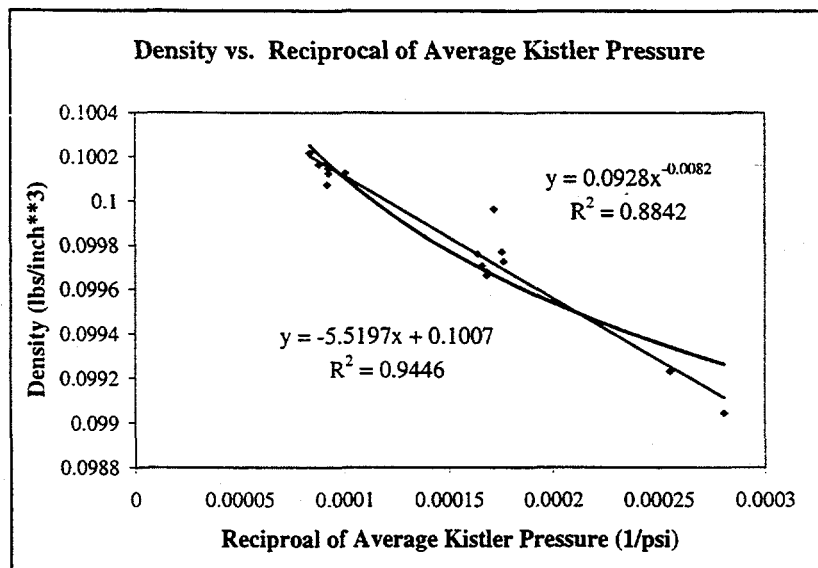


Figure 4.9 The effect of average Kistler pressure on the casting density

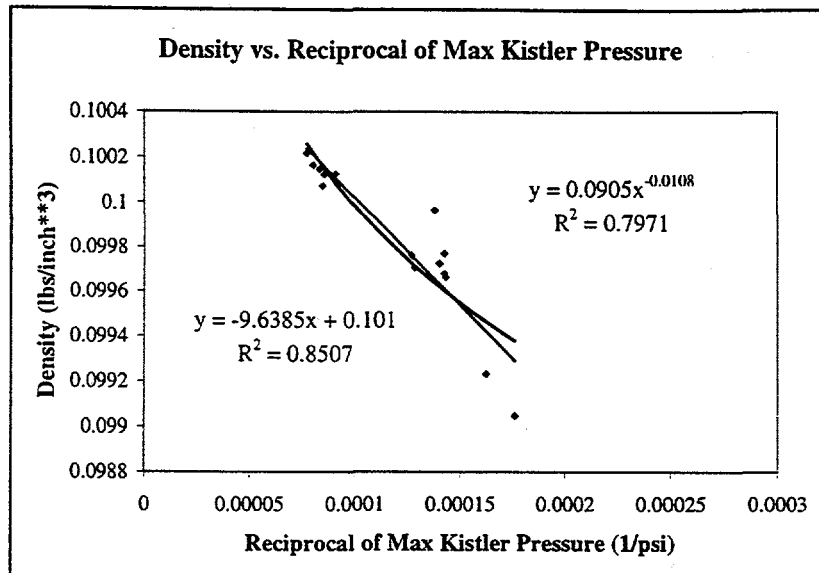


Figure 4.10 The effect of max Kistler pressure on the casting density

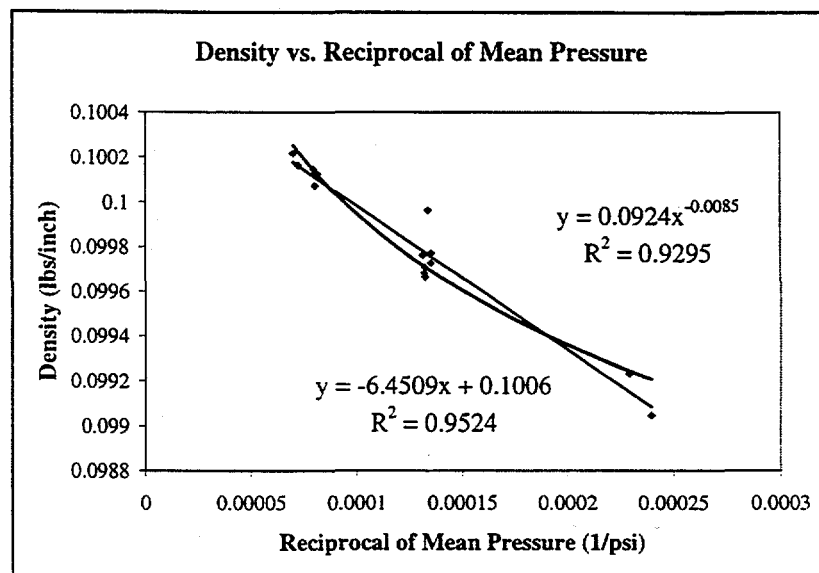


Figure 4.11 The effect of mean pressure on the casting density

From the above figures, it can be concluded that the casting density increases with increasing pressure. For a given value of reciprocal of pressure, there always exist more than one density value that correspond to it. The significant difference exists in these figure is the variation of the data points. Part of the difference in  $R^2$  values can be attributed to the gradient of the trendline. The trendline of the Figure 4.10 has the minimum gradient and has the lowest  $R^2$  value among these figures.

In terms of the  $R^2$  value (correlation coefficient), the mean pressure better correlates with casting density than other pressure parameters. The  $R^2$  values for trendline casting density vs. reciprocal of final pressure  $y = 0.0922x^{-0.0086}$ , maximum metal pressure from hydraulic pressure  $y = -8.3244x + 0.1006$ , average Kistler pressure  $y = -5.5197x + 0.1007$ , maximum Kistler pressure  $y = -9.6385x + 0.101$ , and mean pressure  $y = -6.4509x + 0.1006$  are 0.9443, 0.9498, 0.9446, 0.8507, 0.9524, respectively.

#### 4.5 THE EFFECTS OF APPLIED PRESSURE ON THE CASTING WEIGHT

Weight equals the product of volume and density. To explore the effects of various pressure parameters on casting weight, the calculated casting weight value is acquired by multiplying the calculated density gathered from the equation of the trendline of the density versus various pressure parameters and the calculated volume gotten from the equation of the trendline of the volume versus various pressure parameters. These equation can be polynomial or power as long as it has the higher  $R^2$  value. The calculated

casting weight values are compared to the actual casting weight values by using the average relative error. The actual casting weight values,  $W_{t,act}$ , calculated casting weight values, calculated casting weight using various pressure parameters,  $W_{t,cal, final}$ ,  $W_{t,cal, max H}$ ,  $W_{t,cal, aver K}$ ,  $W_{t,cal, max K}$ ,  $W_{t,cal, mean}$ , and average absolute relative error of various pressure parameters,  $E_{average, abs}$  are listed in Table 4.4.

Table 4.4 Actual casting weight, calculated casting weight, and average absolute relative error

Shot	$W_{t,act}$ (lbs)	$W_{t,cal, final}$ (lbs)	$W_{t,cal, max H}$ (lbs)	$W_{t,cal, aver K}$ (lbs)	$W_{t,cal, max K}$ (lbs)	$W_{t,cal, mean}$ (lbs)
20	26.9149	26.9428	26.8659	26.8516	26.7582	26.8948
50	26.8553	26.9365	26.8642	26.8516	26.7527	26.8914
60	26.4673	26.4575	26.4244	26.5026	26.5974	26.4562
90	26.3789	26.4551	26.3987	26.4334	26.5069	26.4272
91	27.5936	27.8284	27.7423	27.5789	27.5726	27.6743
120	27.7135	27.7274	27.7263	27.7777	27.7606	27.7170
121	27.6856	27.7771	27.7442	27.7653	27.8137	27.7369
123	26.8595	26.9340	26.8679	26.8057	26.7800	26.8708
126	26.8494	26.9345	26.8737	26.8299	26.7993	26.8813
131	26.8883	26.9311	26.8963	26.8649	26.9043	26.8942
136	26.9427	26.9350	26.9148	26.8783	26.9211	26.9019
151	26.8934	26.9287	26.8511	26.8105	26.7582	26.8701
152	27.6933	27.7692	27.7414	27.7590	27.7363	27.7299
153	28.0081	28.2055	27.7145	27.8801	27.9252	28.0077
154	28.1923	28.2720	27.7223	28.0191	28.0476	28.1091
$E_{average, abs}$ (%)		0.28	0.30	0.23	0.32	0.12

In terms of the average absolute relative error 0.12%, the mean pressure is the best pressure parameter to establish the correlation with casting density, volume and density.

The plots of actual casting weight versus final pressure, maximum metal pressure from hydraulic pressure, average Kistler pressure, maximum Kistler pressure, and mean pressure are shown in Figure 4.12, Figure 4.13, Figure 4.14, Figure 4.15, and Figure 4.16.

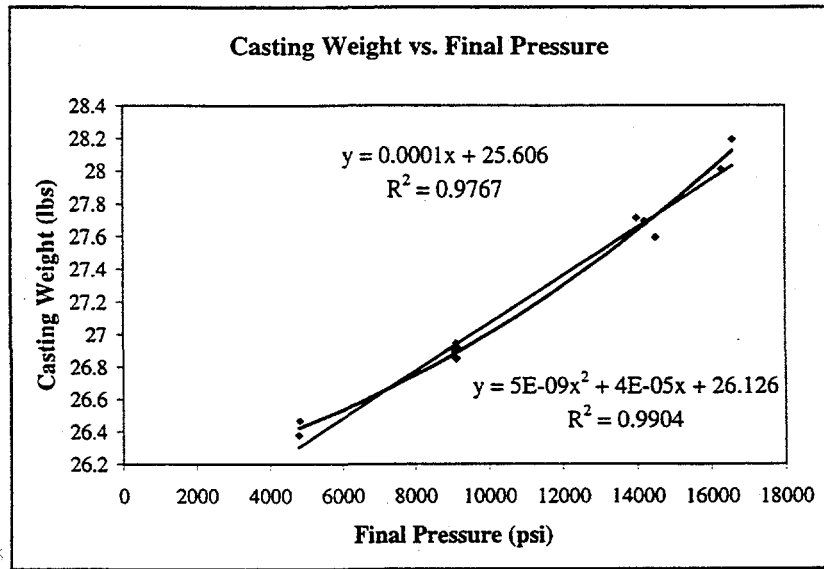


Figure 4.12 The effect of final pressure on the casting weight

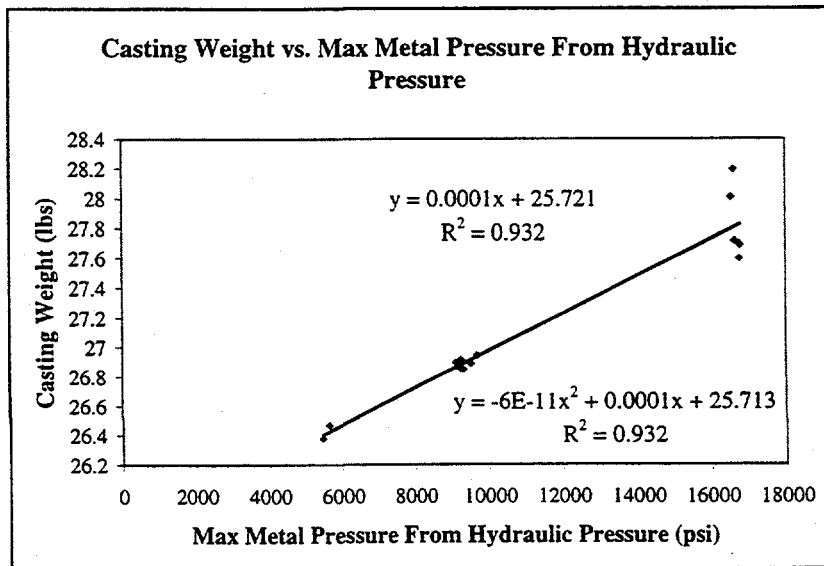


Figure 4.13 The effect of maximum metal pressure from hydraulic pressure on the casting weight

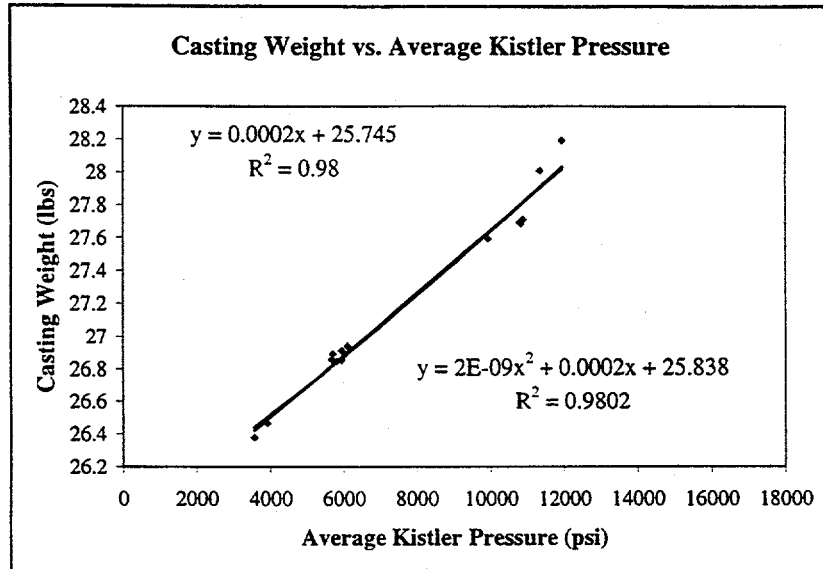


Figure 4.14 The effect of average Kistler pressure on the casting weight

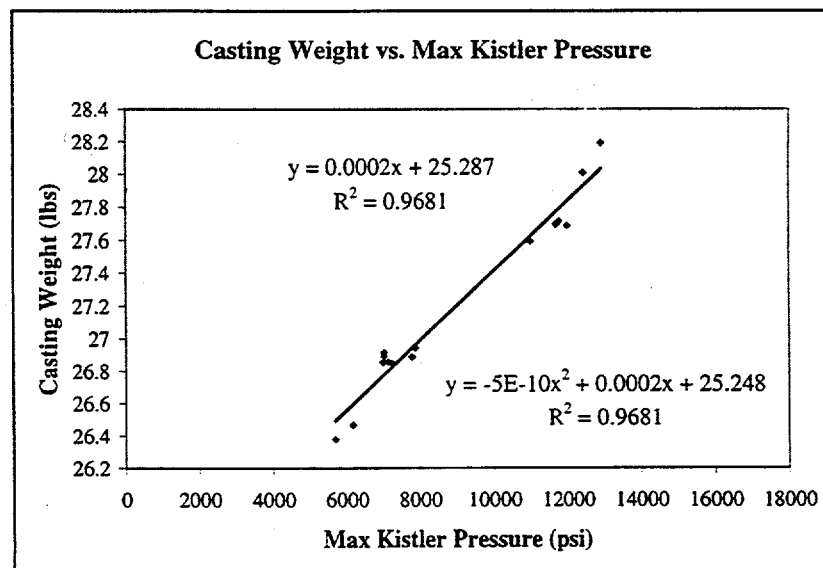


Figure 4.15 The effect of maximum Kistler pressure on the casting weight

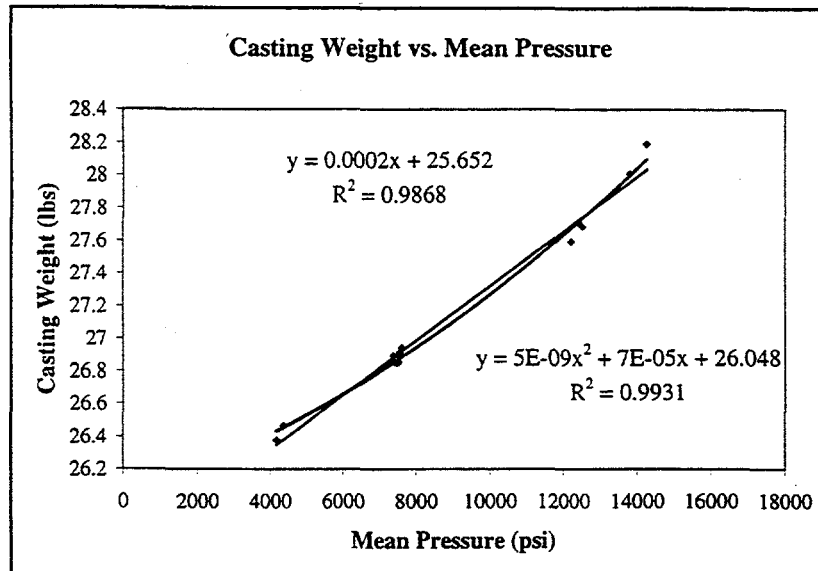


Figure 4.16 The effect of mean pressure on the casting weight

From the above figures, it can be concluded that the casting weight increases with increasing pressure. The distribution of data points in the Figure 4.16 is less ambiguous than Figure 4.12. Although the  $R^2$  value in Figure 4.12 are the second highest, there are more than one data points will correspond to a given final pressure. The distribution of data points in Figure 4.14 are no worse than Figure 4.16, but the range in which the data points fall are narrower than Figure 4.16. The range is even narrower in Figure 4.15 and the  $R^2$  value is lower than Figure 4.14. In Figure 4.13, the ambiguity is worsen around 17000 psi as compared to Figure 4.12. The  $R^2$  values for the trendlines of casting weight vs. final pressure  $y = 5E-9x^2 + 4E-5x + 26.126$ , maximum metal pressure from hydraulic pressure  $y = 0.0001x + 25.721$ , average Kistler pressure  $y = 0.0002x + 25.745$ , maximum Kistler pressure  $y = 0.0002x + 25.287$ , and mean pressure  $y = 5E-9x^2 + 7E-5x + 26.048$  are 0.9904, 0.932, 0.98, 0.9681, 0.9931, respectively. So that the mean pressure is the appropriate pressure parameter to correlate with the casting volume, density, and weight.

The runner and biscuit of shots 20, 50, 60, 90, 91, 120 and overflows of 50, 60, 90, 91, 120 were collected. The volume,  $Vol_o$ ,  $Vol_{r+b}$ , weight,  $Wt_o$ ,  $Wt_{r+b}$ , and density,  $\rho_o$ ,  $\rho_{r+b}$ , of the overflows, runner and biscuit were measured using Archimedes' density measurement method. The data are listed in Table 4.5. The casting density  $\rho_c$  and final pressure  $P_{final}$  data are also added.

shot	$P_{final}$ (psi)	$\rho_c$ (lbs/in <sup>3</sup> )	$\rho_o$ (lbs/in <sup>3</sup> )	$\rho_{r+b}$ (lbs/in <sup>3</sup> )	$Vol_o$ (in <sup>3</sup> )	$Vol_{r+b}$ (in <sup>3</sup> )	$Wt_o$ (lbs)	$Wt_{r+b}$ (lbs)
20	9167	0.09968	-	0.10043	-	94.8	-	9.5209
50	9120	0.09966	0.09368	0.10040	16.70	101.60	1.5645	10.2011
60	4811	0.09923	0.09573	0.10027	16.50	108.90	1.5795	10.9199
90	4786	0.09905	0.09347	0.10011	16.50	100.50	1.5423	10.0613
91	14507	0.10013	0.09766	0.10063	16.60	86.10	1.6211	8.6639
120	13993	0.10007	0.09697	0.10047	16.70	92.40	1.6194	9.2831

Table 4.5 Casting Weight, final pressure, weight, volume, and density of overflow, runner and biscuit of shot 20, 50, 60, 90, 91, and 120

By plotting the density of biscuit and runner, casting, and overflows versus reciprocal of final pressure, it is found that the density of runner and biscuit and density of casting increase with increasing final pressure; for a given final pressure the density of runner and biscuit is higher than the density of casting and the density of casting is higher than the density of overflows. The second finding can be attributed to the different pressures and gas content over pressure ratios in runner and biscuit, casting, and overflows during solidification.. Figure 4.17 shows the density of these three location versus the reciprocal of final pressure. Series1 are the data points for runner and biscuit; series2 are the data points for casting; and series 3 are the data points for overflows.

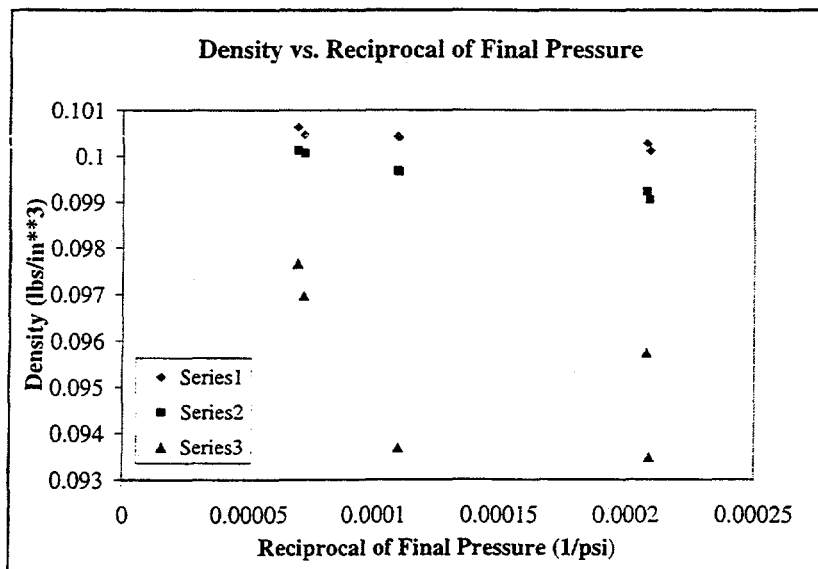


Figure 4.17 Density of runner and biscuit, casting, and overflows vs. reciprocal of final pressure

Since the final pressure is the appropriate pressure parameter to represent the overall effects of pressure applied during solidification in runner and biscuit, the mean pressures are used instead of the final pressure to represent the overall effects of pressure applied in the die cavity for the casting. By plotting the density of runner and biscuit versus the reciprocal value of the final pressure and the density of casting versus the reciprocal value of the mean pressure multiplied by 3.2 in one plot and adding one trendline for both data point sets, a straight line with  $R^2$  value 0.9774 is acquired. The density  $\rho_c$  is a function of  $v/P$  [13] as following:

$$\rho_c = \rho_t(1 - \Phi(v/P)) \quad (4)$$

$\Phi = \text{Constant}$

$v = \text{Gas content in that part}$

$P = \text{Representative pressure parameter in that part}$

The  $v/P$  ratio in the casting is about three to four times that of the runner and biscuit. A common trendline for both data point sets can be achieved by simply multiplying the  $1/P$  of the casting with the ratio of gas contents in these two parts. The plot is shown in Figure 4.18.

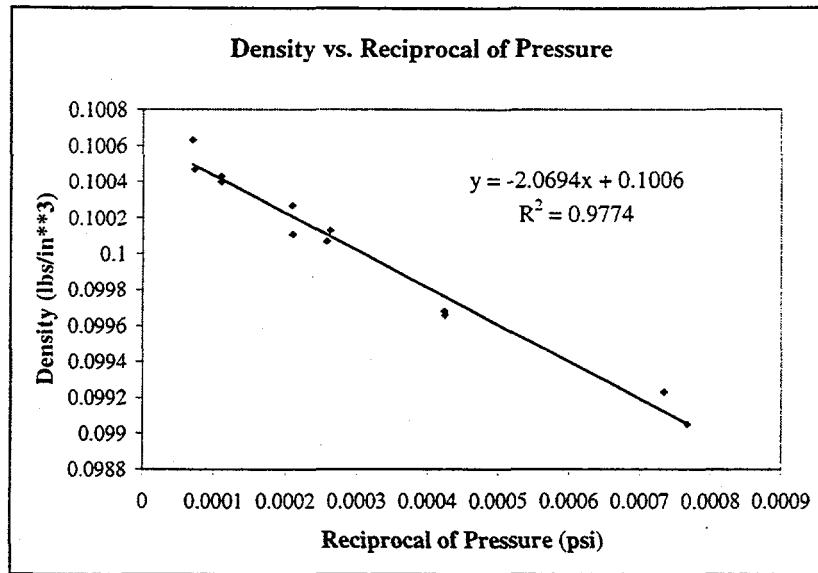


Figure 4.18 Density of runner and biscuit, casting versus reciprocal of final pressure for runner and biscuit and reciprocal of mean pressure

By comparing the equation of the trendline in Figure 4.18 to the Figure 4.11, it can be found that the constants or theoretical density values in both equations are the same; the slope of the trendline in Figure 4.18 is about 3.12 times the slope of the trendline in Figure 4.11. The number 3.12 is very close to the multiplier 3.2. This agreement confirms the assumption that the  $v/P$  in casting is about 3.2 times the  $v/P$  in runner and biscuit. It also suggests that the mean pressure is the appropriate pressure parameter for correlation with casting density.

## CHAPTER 5

### CONCLUSIONS AND RECOMMENDATIONS

Based on the data acquired from the OSU (ERC/NSM) campaign and GM CADC campaign, it can be concluded that:

1. the Kistler in cavity pressure is reliable and durable. The Kistler pressure sensor was able to sustain the one hundred and fifty-six shot campaign without degradation.
2. Pressure records from the Kistler direct pressure sensor can provide insight into the die casting process and serve as necessary complementary data to the hydraulic pressure record. The pressure records from the Kistler direct pressure sensor together with hydraulic pressure records can not only provide the information on the metal pressure range in a die cavity but also detect impact, flashing, intensification start time, gate freezing time.

3. The mean pressure between the average hydraulic pressure and the average Kistler pressure is the preferable pressure parameter to correlate with casting volume, density, and weight. So that the Kister direct pressure records serve as necessary complementary to the hydraulic pressure record.
4. The difference in density values of runner and biscuit, casting, and overflows is mainly due to the difference in pressure applied during solidification and gas content at different locations

**Recommendations:**

1. Vacuum fusion measurement should be conducted on the runner and biscuit, and casting to determine the gas content.
2. The volume and density of the remainder of the DoE/GM castings should be measured to improve the stastical significance for each pressure condition.

## BIBLIOGRAPHY

1. ASM Handbook Volume 15 Casting, Ninth Edition, Metal Handbook ASM International (1992), pp. 286-295
2. Inorganic Chemicals Department, Dow Chemical U.S.A., Product Design and Development for Magnesium Die Castings, Form No. 141-523-84, pp. 109-124
3. A. Kaye and A. Street, Die Casting Metallurgy, Butterworth Scientific (1982), page 205
4. J. Mickowski, "System for Control Critical Parameters", NADCA Transactions, (1981), Paper No. G-T81-141, pp. 1-7
5. C. Mobley and J. Brevick, "Annual Report on Die Cavity Instrumentation OSURF Project 729390", Annual Report Number 2 (1996), Ohio State University Center for Die Casting
6. Y. Mochiku, Dr. Y. Hatamura, and K. Shirahige, "Intelligent Die Casting and Seven Sensors", NADCA Transactions, (1989), Paper No. G-T89-024, pp. 1-7
7. J. Papai and C. Mobley, "Die Thermal Field And Heat Fluxes During Die Casting of 380 Aluminum Alloy in H-13 Steel Dies", NADCA Transactions, (1991) Detroit-T91-OC1, pp. 377-384
8. S. Booth and D. Allsop, "Thermal Control and Design of Dies", NADCA Transactions, (1981), Paper No. G-T81-056, pp. 1-7
9. Babington and Klepinger, "Aluminum Die Casting-The Effect of Process Variables on Their Properties", Proceedings ASTM, vol. 51, (1951) pp. 169-197
10. M. Phlipot, W. Willis, and O. Beckendorf, "The Evaluation of Selected Die Casting Process Parameters Using a Micro Processor-Based Process Monitoring System", NADCA Transactions, (1983), Paper No. G-T83-051, pp. 1-6

11. M. Tokui, A. Morita, T. Masaoka, A. Ohta, I. Suzuki, and F. Kawano, "Development and Application of Vertical Pressure Die Casting Process", NADCA Transactions, (1983), Paper No. G-T83-061, pp. 1-6
12. Y. Sugiyama, H. Iwahori, K. Yonekura, and Y. Ookouchi, "Transferred pressure and casting qualities of aluminum die casting", Transactions of AFS, Vol. 45, (1996), pp. 121-124
13. A. Gordon, G. Meszaros, J. Naizer, and C. Mobley, "Equations for Predicting the Percent Porosity in Die Castings", NADCA Transactions, (1993), Cleveland T93-024, pp. 55-62
14. Y. Yamamoto, Y. Iwata, Dr. M. Nakamira, and Y. Oukouchi, "Molten Metal Velocities and Gas Pressure in Die Cavity and Defects in Commercial Aluminum Pressure Die Castings", NADCA Transactions, (1989), Paper No. G-T89-081, pp.1-8
15. V. Venkatasamy, "Analysis of In-Cavity Thermal and Pressure Characteristics in Aluminum Alloy Die Casting", Master Thesis, Department of Industrial System and Welding Engineering, The Ohio State University, (1997)
16. V. Venkatasamy, J. Brevick, G. Pribyl and C. Mobley, "Die Cavity Sensors for Monitoring Die Casting Processes", A Manuscript to NADCA for 19<sup>th</sup> International Die Casting Congress and Exposition, (1997)
17. J. Mickowski and C. Teufert, "The control of Impact Pressure in the High Pressure in the High Pressure Die Casting Process", NADCA Transactions, (1993), Cleveland T93-122, pp. 349-354
18. N. Tsumagari, "Microstructural Features as a Measure of Process and Part Reproducibility in 390 Hypereutectic Aluminum-Silicon Alloy Die Castings", Doctoral Dissertation, Department of Materials Science and Engineering, The Ohio State University, (1995)
19. A. Kay, "Does Intensification Pressure Influence The Porosity Distribution In Aluminum Die Castings ?", Master Thesis, Department of Materials Science and Engineering, The Ohio State University, (1996)
20. A.W. Gordon, G.A. Meszaros, J.P. Naizer, P.R. Gangasani, and C. E. Mobley, "Comparison of Methods for Characterization Porosity in Die Castings", Report No. ERC/NSM-C-91-51, Engineering Research Center for Net Shape Manufacturing, The Ohio State University, August, 1991
21. Prince Machine Corporation, One Prince Center, Holland, MI 49423, Pro-Manager Version 3 User's Manual, pp. 1-30

APPENDIX A

NADCA SURVEY OF DIE CAVITY INSTRUMENTATION



North American  
Die Casting  
Association

9701 West Higgins Road  
Suite 800  
Rosemont, IL 60018-472  
708.292.3600 Telephone  
708.292.3620 Fax

NADCA® SURVEY ON DIE CAVITY INSTRUMENTATION

1. a. How many cold chamber die casting machines are in your plant? \_\_\_\_\_
- b. How many hot chamber die casting machines are in your plant? \_\_\_\_\_
2. a. How many cold chamber die casting machines is your plant currently operating? \_\_\_\_\_
- b. How many hot chamber die casting machines is your plant currently operating? \_\_\_\_\_
3. Do you have the capability of measuring the plunger position and velocity and cylinder pressure as a function of time during a shot?  Yes  No
4. Do you record plunger position and velocity and cylinder pressure?  
 Every shot  Every \_\_\_\_\_ shots  
 Only during setup or when there is a problem with the process
5. How many dies that you use are instrumented with thermocouples? \_\_\_\_\_
6. Do you record the die thermocouple response as a function of time during a shot?  
 Every shot  Every \_\_\_\_\_ shots  
 Only when there is a problem with the die or process
7. During a die use campaign, do you record die coolant temperature?  
 Continuously  Intermittently  Never
8. During a die use campaign, do you record die coolant flow rate?  
 Continuously  Intermittently  Never
9. Have you or do you make temperature or pressure measurements in or near the die cavity as part of your process monitoring or control?  Yes  No
10. Do you utilize any instrument or measurement device to monitor the extent to which the die cavity vents are open or functioning?  Yes  No
11. Do you use any method or device to measure the amount of gas removed from the die cavity during filling?  
 Yes  No
12. What instrumentation devices have you used to make die cavity or near die cavity process measurements?  
 Thermocouples  Transducers  
 Strain Gauges  Other (Please explain): \_\_\_\_\_
13. Where or how did you obtain the die cavity instrumentation devices or units? For example, were they purchased as a complete unit from a commercial supplier or constructed from components by your engineering staff?  
\_\_\_\_\_  
\_\_\_\_\_

(over)

NADCA® SURVEY ON DIE CAVITY INSTRUMENTATION (continued)

14. If the die cavity instrumentation devices or units were obtained from a source outside your die casting facility, please give us the supplier's name and phone number or, whom at your company we can call for the information.

15. Were the die cavity instrumentation devices used to continuously monitor your process or as a means of solving a die design or part production problem?

16. What are the major capabilities and limitations of the die cavity instrumentation devices that you have used?

If you wish your company to remain anonymous, please skip questions 17 and 18.

17. As a member of NADCA, would you like to participate in the NADCA Process Technology Task Group die cavity instrumentation project?  Yes  No

Please contact me about participation on the NADCA Process Technology Task Group.

18. Please provide the name of the individual completing this survey and your company's address, telephone and/or fax number:

Individual's Name: \_\_\_\_\_

Company Name: \_\_\_\_\_

Company Address: \_\_\_\_\_

Company Phone: \_\_\_\_\_

Company Fax: \_\_\_\_\_

Please return your completed survey to:

Attention: Professor Carroll Mobley  
c/o Ohio State University  
Dept. MSE  
Fontana  
116 West 19th Avenue  
Columbus, Ohio 43210  
Fax: (614) 292-1537

## APPENDIX B

### TECHNICAL SPECIFICATIONS OF BUHLER H-250SC



TECHNICAL DATA (subject to modification without notice)

Horizontal Cold-Chamber Die Casting Machine H-250SC

Locking force (strain gauge tested).....	kN	2850
Injection force, consolidation phase adjustable (dynamic)	kN	280 - 55
Plunger stroke.....	mm	380
Shot positions (standard).....	mm	0, -50, -100, -150, -200
Ejection force.....	kN	170
Ejector stroke (adjustable).....	mm	120
Dimensions of fixed die platen (H x V).....	mm	840 x 947
Dimensions of moving die platen (H x V).....	mm	840 x 840
Clearance between the tie bars.....	mm	550 x 550
Diameter of tie bars.....	mm	95
Die height min. ....	mm	200
Die height max. ....	mm	650
Stroke of moving die platen.....	mm	560
Rated installed power.....	kW	30
Machine area L x W (incl. safety gate).....	m	5,9 x 2,3
Machine height.....	m	2,5
Machine weight, ready for production.....	kg	10700
DATACESS SC control cabinet L x W x H.....	m	1,8 x 0,5 x 2,5
and DATACESS SC power cabinet L x W x H.....	m	0,8 x 0,5 x 2,0

Production data

	mm	40	45	50	55	60	70	80	90
Plunger diameter	mm	40	45	50	55	60	70	80	90
Theoretical shot volume (DIN 24480)	cm <sup>3</sup>	318	402	497	601	716	975	1273	1611
Max. shot weight for Al*	kg	0,9	1,1	1,4	1,7	2,0	2,75	3,6	4,5
Max. specific injection pressure	bar	2230	1760	1430	1180	990	730	560	440
Max. projected area**	cm <sup>2</sup>	128	162	200	241	288	390	509	648

\* The max. shot weight is calculated as follows:  
plunger stroke x plunger area x 0.75 x density

Density of	Al	Zn	Hg	Cu
g/cm <sup>3</sup>	2,5	6,25	1,63	8,0

\*\* Max. theoretical projected area at max. specific injection pressure, without consideration of core locking and dynamic part of injection process.

## APPENDIX C

### MACHINE SET-UP ANALYSIS

Measured Plunger Diameter	=	49.2 mm	=	1.937 inch
Hydraulic Cylinder Diameter (Page 2/33, Buhler Manual 1)	=	145 mm	=	5.709 inches
Hydraulic Cylinder Diameter / Measured Plunger Diameter	=		=	2.947
Recommended Gate Velocity (NADCA Guidelines)	=		=	1400 inches/sec
Measured Gate Area	=		=	0.32 inch <sup>2</sup>
Volumetric Flow Rate	=	Gate Velocity * Gate Area	=	504 inch <sup>3</sup> /sec
Measured Cavity (i.e. casting + overflow) Volume	=		=	6.1 inch <sup>3</sup>
Cavity Fill Time	=	Cavity Volume / Volumetric Flow Rate		
	=	12.1 ms		
Measured Total Casting (i.e. biscuit + runner + gate + casting + overflow) Volume	=		=	11.05 inch <sup>3</sup>
Measured Shot Sleeve Length	=		=	14.055 inches
Calculated Shot Sleeve Volume	=	$\pi/4 * (\text{Plunger Diameter})^2 * \text{Shot Sleeve Length}$		
	=	41.44 inch <sup>3</sup>		
Percent Shot Sleeve Fill	=	$100 * \text{Total Casting Volume} / \text{Shot Sleeve Volume}$		
	=	26.67 %		

$$\begin{aligned} \text{Calculated Injection Pressure} &= (d/D)^2 * \rho * V_g^2 / 2 * g * C_D^2 \\ &= 70.64 \text{ psi} \end{aligned}$$

where

$$\begin{aligned} d &= \text{Plunger Diameter, inch} \\ D &= \text{Hydraulic Cylinder Diameter, inch} \\ \rho &= \text{Alloy Density, lb/inch}^3 = 0.087 \text{ lb/inch}^3 \\ V_g &= \text{Gate Velocity, inch/sec} \\ g &= \text{Gravitational Acceleration, inch/sec}^2 = 386 \text{ inch/sec}^2 \\ C_D &= \text{Gate Coefficient of Discharge} = 0.6 \end{aligned}$$

$$\text{Intensification Pressure} = 20 * \text{Injection Pressure} = 1412.8 \text{ psi}$$

$$\text{Projected Area of Casting} = 44.95 \text{ inch}^2$$

$$\begin{aligned} \text{Locking Force} &= \text{Projected Area of Casting} * \text{Intensification Pressure} \\ &= 63505.36 \text{ psi} \end{aligned}$$

$$\begin{aligned} \text{Plunger Cross Sectional Area} &= \text{Plunger Diameter}^2 * \pi / 4 \\ &= 2.948 \text{ inch}^2 \end{aligned}$$

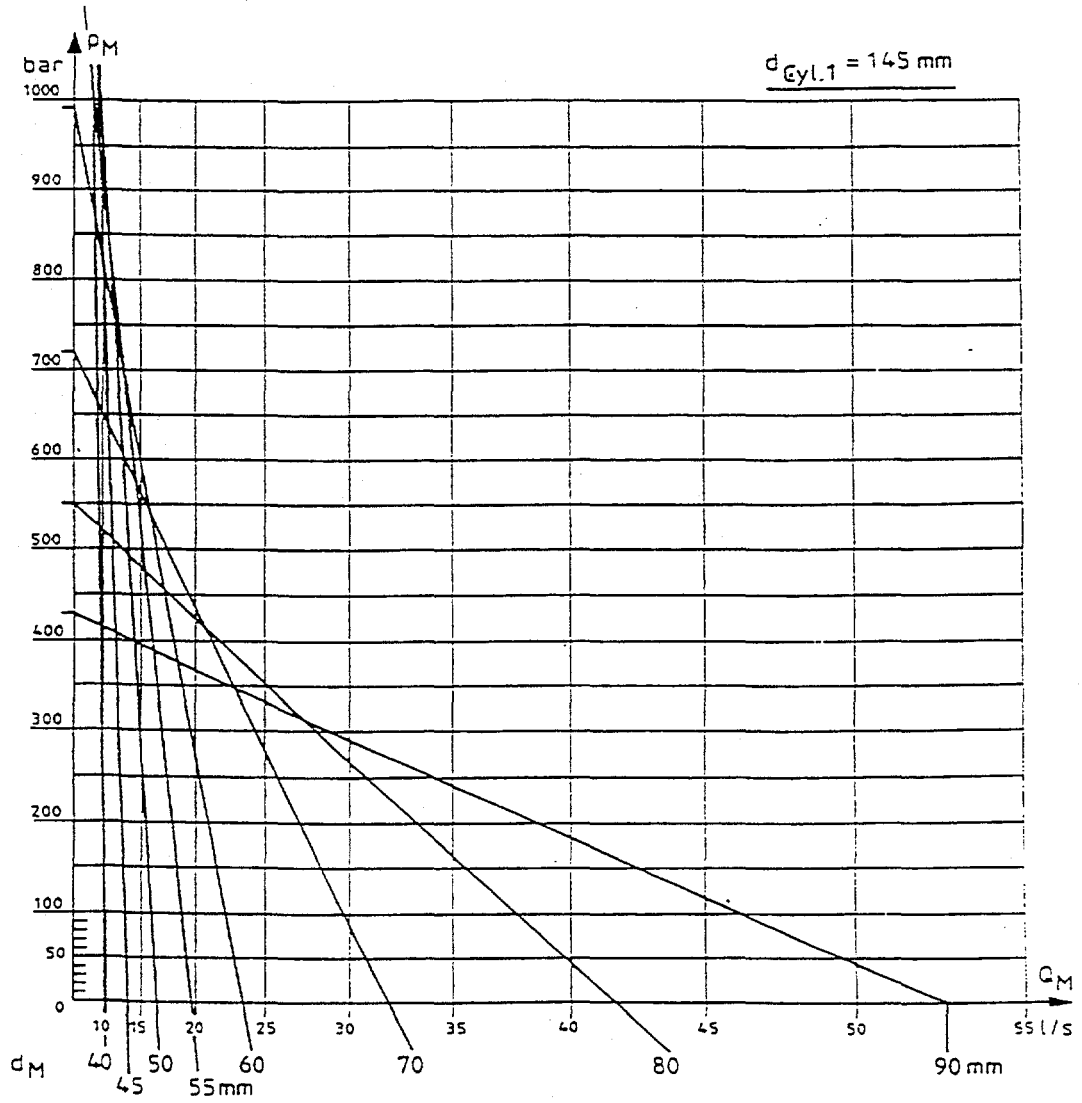
$$\begin{aligned} \text{Fast Shot Velocity} &= \text{Volumetric Flow Rate} / \text{Plunger Cross Sectional Area} \\ &= 170.96 \text{ inch/sec} \end{aligned}$$

Slow Shot Profile (Thome Model : Straight Line Acceleration)

Plunger Position, inch (m)	Plunger Velocity, inch/sec (m/sec)
0 (0)	0 (0)
9.07 (0.23)	24.98 (0.63)
10.31 (0.26)	24.98 (0.63)
11.19 (0.28)	170.96 (4.34)
13.26 (0.34)	170.96 (4.34)

APPENDIX D

PQ<sup>2</sup> ANALYSIS



APPENDIX E

DoE/ GM Data Summary

Shot	Wtc+0 (lbs)	B_L (in)	Slow Vel (in/sec)	Inter Vel (in/sec)	Fast Vel (in/sec)	Act Ft Pos (in)	Vel Rise (ms)	Pres Rise (ms)	Fill time (ms)	Fill time srt (in)	Inten Strk (in)	End Pos (in)	End Vel (in/sec)
1	29.15	1.28	9.9	25	112.4	27.36	9	17	117	27.6	0.35	40.3	62.9
2	28.3	1.68	10	24.8	103.7	27.47	10	2000	134	27.2	0.07	39.9	67.3
3	28.15	1.93	10	24.8	103.3	27.3	10	2000	137	26.95	0.12	39.65	68
4	28.05	1.98	9.9	24.9	97.3	27.48	11	2000	151	26.9	0.12	39.6	62.5
5	28.2	1.88	9.9	25	97.2	27.33	11	2000	143	27	0.1	39.7	65.6
6	28.7	1.83	10.1	25	96.4	27.35	10	21	144	27.05	0.34	39.75	57.7
7	28.65	1.98	10	24.9	97.3	27.47	17	26	152	26.9	0.36	39.6	57.6
8	28.65	1.88	9.9	24.9	96.9	27.43	16	19	149	27	0.31	39.7	54.5
9	28.65	1.93	10.2	25	96.7	27.3	12	20	145	26.95	0.34	39.65	58.3
10	28.65	1.88	10	25	97.4	27.49	12	10	150	27	0.27	39.7	55.9
11	28.55	1.88	10.1	24.9	97.2	27.29	11	23	144	27	0.35	39.7	58.6
12	28.6	1.83	9.9	25	98.6	27.31	12	14	142	27.05	0.31	39.75	56.8
13	28.6	1.98	9.9	24.9	97.1	27.44	17	14	150	26.9	0.33	39.6	61.4
14	28.6	1.88	9.9	25.1	97	27.33	11	22	144	27	0.35	39.7	59.5
15	28.6	1.83	10	24.9	97.2	27.29	12	12	142	27.05	0.31	39.75	58.3
16	28.6	1.78	10	25	98.6	27.48	12	14	145	27.1	0.33	39.8	57.9
17	28.6	1.73	9.8	24.9	96.6	27.4	11	18	143	27.15	0.35	39.85	59.3
18	28.5	1.63	9.9	24.9	97.8	27.47	12	11	141	27.25	0.3	39.95	55.4
19	28.5	1.68	10	24.9	97.9	27.29	11	17	137	27.2	0.35	39.9	57.9
20	28.45	1.83	10.1	24.9	97.1	27.46	12	19	148	27.05	0.35	39.75	54.9
21	28.4	1.78	10	24.9	98	27.31	11	24	140	27.1	0.38	39.8	57.5
22	28.4	1.93	9.8	24.9	96.9	27.45	12	20	151	26.95	0.32	39.65	56.1
23	28.45	1.78	10	25	97.9	27.48	11	13	146	27.1	0.33	39.8	56.8
24	28.5	1.68	10	25	97.3	27.45	12	73	141	27.2	0.41	39.9	63.7
25	28.45	1.68	9.8	24.9	98.1	27.33	11	23	137	27.2	0.36	39.9	57.4

Shot	Wtc+0 (lbs)	B_L (in)	Slow Vel (in/sec)	Inter Vel (in/sec)	Fast Vel (in/sec)	Act Ft Pos (in)	Vel Rise (ms)	Pres Rise (ms)	Fill time (ms)	Fill time srt (in)	Inten Strk (in)	End Pos (in)	End Vel (in/sec)
26	28.4	1.63	10	24.8	97.8	27.48	11	12	142	27.25	0.33	39.95	55.1
27	28.35	1.68	10	24.9	95.7	27.47	11	17	144	27.2	0.34	39.9	57.8
28	28.45	1.78	10.4	24.9	98.2	27.29	12	15	139	27.1	0.33	39.8	58.1
29	28.45	1.53	10	25	98.2	27.34	11	24	134	27.35	0.4	40.05	58.6
30	28.4	2.33	9.9	25	96.9	27.46	17	28	162	26.55	0.4	39.25	60.3
31	28.4	2.33	10.1	24.9	97.7	27.31	16	31	157	26.55	0.39	39.25	60
32	28.35	2.38	9.9	24.9	96.8	27.29	16	12	160	26.5	0.31	39.2	58
33	28.45	2.48	9.9	25	97.2	27.48	16	24	168	26.4	0.39	39.1	58.8
34	28.5	2.33	10	24.8	98.5	27.47	17	11	163	26.55	0.35	39.25	56.5
35	28.45	2.38	9.9	24.9	98.4	27.43	16	21	162	26.5	0.39	39.2	58.8
36	28.45	2.33	10.3	25	97.5	27.38	16	16	160	26.55	0.34	39.25	56.9
37	28.45	2.23	10.1	24.8	97.8	27.29	16	12	154	26.65	0.33	39.35	58.4
38	28.4	2.23	10	25	97.1	27.29	16	17	154	26.65	0.34	39.35	59.3
39	28.4	2.28	10.3	25	98.5	27.37	17	19	157	26.6	0.39	39.3	57.3
40	28.4	2.23	10	25	98.4	27.44	16	19	158	26.65	0.34	39.35	59.1
41	28.4	2.28	10	24.7	98.3	27.48	18	20	163	26.6	0.38	39.3	53.9
42	28.45	2.28	10	25	99.2	27.32	17	27	155	26.6	0.41	39.3	58.6
43	28.45	2.23	9.8	24.9	98.3	27.32	16	27	154	26.65	0.41	39.35	59.2
44	28.4	2.23	10.5	24.9	98.6	27.39	16	21	156	26.65	0.38	39.35	59.4
45	28.4	2.18	10	24.9	98.9	27.46	18	19	158	26.7	0.38	39.4	58.7
46	28.4	2.13	10	24.9	98.5	27.48	12	10	157	26.75	0.31	39.45	56.2
47	28.4	2.23	10	24.8	97.9	27.46	18	26	160	26.65	0.4	39.35	55.4
48	28.45	2.28	10.1	24.9	99.7	27.42	17	21	158	26.6	0.38	39.3	58.1
49	28.5	2.18	9.9	24.9	99.2	27.33	16	31	152	26.7	0.42	39.4	61.4
50	28.4	2.18	9.9	24.9	98.5	27.45	17	24	157	26.7	0.38	39.4	59.4
51	27.9	2.13	10	25	98	27.49	16	2000	156	26.75	0.1	39.45	65.2
52	27.8	2.23	10.4	25	98.2	27.42	16	2000	156	26.65	0.09	39.35	64.6
53	27.85	2.18	10.3	24.9	97.9	27.36	17	2000	153	26.7	0.11	39.4	64.9
54	27.85	2.28	9.9	24.9	97.4	27.46	16	2000	159	26.6	0.11	39.3	67.8
55	27.85	2.13	9.9	24.9	98	27.5	16	2000	156	26.75	0.1	39.45	65
56	27.95	2.13	10	24.9	99	27.35	16	2000	150	26.75	0.14	39.45	67.2

Shot	Wtc+0 (lbs)	B_L (in)	Slow Vel (in/sec)	Inter Vel (in/sec)	Fast Vel (in/sec)	Act Ft Pos (in)	Vel Rise (ms)	Pres Rise (ms)	Fill time (ms)	Fill time srt (in)	Inten Strk (in)	End Pos (in)	End Vel (in/sec)
57	27.9	2.08	10	25	98.2	27.32	12	2000	149	26.8	0.12	39.5	65.1
58	27.85	2.43	9.9	24.9	98.7	27.46	18	2000	165	26.45	0.11	39.15	65.3
59	27.85	2.43	9.9	24.8	98.2	27.48	17	2000	165	26.45	0.14	39.15	65.8
60	28.1	2.38	10	25	99.3	27.47	16	2000	162	26.5	0.19	39.2	68.6
61	28	2.23	9.9	24.8	98.1	27.46	17	2000	158	26.65	0.11	39.35	64.4
62	28.05	2.23	10.3	24.9	99.9	27.38	17	2000	154	26.65	0.19	39.35	66.3
63	28	2.33	9.9	25	99.1	27.46	17	2000	160	26.55	0.15	39.25	66.6
64	28.05	2.28	10.1	24.9	99.3	27.31	16	2000	153	26.6	0.23	39.3	67
65	27.9	2.33	10	24.9	97.7	27.46	16	2000	161	26.55	0.1	39.25	64.9
66	27.95	2.28	10.2	24.8	98.8	27.4	17	2000	158	26.6	0.15	39.3	64
67	27.85	2.43	10.3	24.9	98.8	27.38	17	2000	162	26.45	0.15	39.15	66.9
68	27.95	2.23	10.4	24.9	99.1	27.4	16	2000	155	26.65	0.14	39.35	64.2
69	28	2.28	10.2	25.1	99	27.35	16	2000	155	26.6	0.19	39.3	64.6
70	28.2	2.18	10.3	24.9	99	27.39	18	2000	154	26.7	0.17	39.4	64.4
71	28.05	2.13	10	24.8	97.9	27.48	18	2000	155	26.75	0.22	39.45	68.2
72	27.95	2.13	9.9	24.9	98	27.33	16	2000	151	26.75	0.14	39.45	61.4
73	28.05	2.23	10	24.8	98.4	27.49	17	2000	158	26.65	0.21	39.35	68.5
74	28	2.18	10.2	24.8	98.7	27.46	18	2000	157	26.7	0.21	39.4	65.8
75	28	2.13	9.9	24.9	98.1	27.3	16	2000	149	26.75	0.17	39.45	67.6
76	28.05	2.13	9.9	24.9	97.1	27.3	16	2000	151	26.75	0.15	39.45	63.7
77	27.9	2.18	10	24.8	99.3	27.3	17	2000	152	26.7	0.1	39.4	62.6
78	27.8	2.13	10	24.9	98.1	27.5	15	2000	156	26.75	0.15	39.45	63.2
79	28.1	2.08	9.9	25	100	27.36	16	2000	148	26.8	0.25	39.5	68.3
80	27.85	2.13	9.8	24.8	99	27.45	17	2000	154	26.75	0.12	39.45	63
81	28	1.98	9.9	25	98	27.33	11	2000	146	26.9	0.14	39.6	64.9
82	27.85	2.13	10.1	24.9	98.3	27.51	16	2000	156	26.75	0.11	39.45	64.1
83	28	2.08	9.9	25	97.7	27.49	17	2000	155	26.8	0.11	39.5	64.5
84	28	1.93	9.8	24.9	97.6	27.33	16	2000	144	26.95	0.21	39.65	66.4
85	28.05	1.98	10	24.9	97.9	27.48	16	2000	151	26.9	0.2	39.6	63.8
86	27.95	1.98	10	25.1	96.8	27.5	16	2000	154	26.9	0.15	39.6	62.5
87	28	2.03	10	24.9	97.9	27.31	16	2000	147	26.85	0.12	39.55	64.6

Shot	Wtc+o (lbs)	B_L (in)	Slow Vel (in/sec)	Inter Vel (in/sec)	Fast Vel (in/sec)	Act Ft Pos (in)	Vel Rise (ms)	Pres Rise (ms)	Fill time (ms)	Fill time srt (in)	Inten Sirk (in)	End Pos (in)	End Vel (in/sec)
88	27.95	1.88	9.8	25	97.3	27.47	17	2000	148	27	0.1	39.7	63.9
89	27.95	1.98	10	24.9	97.8	27.44	16	2000	149	26.9	0.11	39.6	66.5
90	27.9	1.93	10.4	24.9	96.6	27.39	16	2000	149	26.95	0.15	39.65	63.4
91	29.3	1.83	10	24.9	98.6	27.48	11	118	146	27.05	0.79	39.75	65.7
92	29.4	1.83	9.9	24.9	98.2	27.5	11	120	147	27.05	0.88	39.75	65.4
93	29.55	2.28	10	24.8	99.4	27.41	16	138	157	26.6	0.89	39.3	67.1
94	29.5	2.18	10.4	24.9	98.8	27.35	11	135	151	26.7	0.9	39.4	62.7
95	29.55	2.23	9.9	24.8	99.9	27.5	16	143	157	26.65	0.91	39.35	68
96	29.45	2.23	10	24.8	96.6	27.51	14	124	160	26.65	0.91	39.35	65.5
97	29.4	2.33	10	25	98.9	27.51	14	133	161	26.55	0.8	39.25	61.9
98	29.45	2.28	10.4	24.8	98.1	27.48	16	126	161	26.6	0.83	39.3	62.4
99	29.5	2.13	10	24.9	98	27.33	16	74	151	26.75	0.86	39.45	58.5
100	29.45	2.23	10	24.9	98.8	27.5	15	128	159	26.65	0.85	39.35	62
101	29.45	2.13	9.8	24.9	98	27.5	14	71	156	26.75	0.89	39.45	57.2
102	29.5	2.13	9.9	24.8	98.2	27.48	18	122	157	26.75	0.84	39.45	55.6
103	29.5	2.13	10	24.9	97.5	27.31	14	136	150	26.75	0.88	39.45	63.7
104	29.4	2.13	9.9	24.9	99.1	27.48	11	123	153	26.75	0.85	39.45	64.6
105	29.45	2.13	10.4	24.8	99	27.4	15	115	153	26.75	0.88	39.45	62.8
106	29.6	2.18	10	24.8	98.5	27.32	17	127	152	26.7	0.89	39.4	62.4
107	29.45	2.13	9.9	24.9	97.5	27.44	14	134	156	26.75	0.83	39.45	61
108	29.55	2.23	10	24.9	98.8	27.45	17	126	157	26.65	0.93	39.35	64.7
109	29.5	2.33	9.9	24.8	98	27.45	16	126	161	26.55	0.89	39.25	61.2
110	29.4	2.23	10.1	25	97.3	27.38	14	130	155	26.65	0.86	39.35	63.2
111	29.5	2.28	9.9	24.9	98.2	27.47	16	128	160	26.6	0.89	39.3	65.8
112	29.5	2.18	10	24.9	98.3	27.32	17	71	153	26.7	0.88	39.4	57.5
113	29.5	2.23	10	25	98.3	27.38	16	136	155	26.65	0.88	39.35	65.5
114	29.5	2.28	9.9	25	98.8	27.49	16	125	160	26.6	0.91	39.3	63.8
115	29.45	2.33	10	25	97	27.33	14	129	157	26.55	0.89	39.25	62.9
116	29.55	2.33	9.9	24.9	99	27.33	16	137	156	26.55	0.86	39.25	64.8
117	29.45	2.28	10	24.9	98.3	27.51	16	45	163	26.6	0.88	39.3	55.5
118	29.5	2.28	9.9	24.9	97.7	27.48	15	122	161	26.6	0.88	39.3	62.2

Shot	Wtc+0 (lbs)	B_L (in)	Slow Vel (in/sec)	Inter Vel (in/sec)	Fast Vel (in/sec)	Act Ft Pos (in)	Vel Rise (ms)	Pres Rise (ms)	Fill time (ms)	Fill time srt (in)	Inten Strk (in)	End Pos (in)	End Vel (in/sec)
119	29.45	2.18	10	24.9	97.9	27.33	16	49	153	26.7	0.88	39.4	56.7
120	29.45	2.23	10.5	24.8	98.1	27.45	11	130	157	26.65	0.93	39.35	65.7
121	29.4	2.18	10	24.9	97.8	27.48	16	121	157	26.7	0.85	39.4	64.4
122	28.35	2.23	9.7	24.8	96.9	27.48	19	60	161	26.65	0.4	39.35	63.5
123	28.45	2.13	10	24.9	97.3	27.44	14	23	155	26.75	0.44	39.45	59.5
124	28.45	2.13	10.1	24.8	98.3	27.31	18	15	151	26.75	0.42	39.45	57.4
125	28.5	2.08	9.9	24.8	97.5	27.34	15	14	150	26.8	0.39	39.5	59.4
126	28.55	2.23	10	24.9	97.2	27.37	16	11	157	26.65	0.36	39.35	57.3
127	28.6	2.13	10	24.9	97.5	27.34	11	7	153	26.75	0.33	39.45	55.4
128	28.6	1.88	10	25	97.6	27.33	17	9	147	27	0.36	39.7	54.2
129	28.55	2.03	10.1	24.8	98.1	27.5	17	9	155	26.85	0.4	39.55	57.7
130	28.5	2.13	10.4	24.9	98.3	27.35	15	9	152	26.75	0.39	39.45	56.6
131	28.6	1.98	10.2	24.9	98.8	27.37	15	10	148	26.9	0.38	39.6	58.8
132	28.5	1.88	10.3	25	97.7	27.41	15	6	150	27	0.31	39.7	52.3
133	28.5	1.88	10.1	25	96.3	27.46	16	8	151	27	0.35	39.7	57
134	28.5	2.08	9.8	25	97.4	27.47	20	10	156	26.8	0.44	39.5	55.7
135	28.4	2.03	10	24.9	97.6	27.35	15	8	149	26.85	0.35	39.55	59.9
136	28.55	1.83	9.9	25	98.2	27.49	17	8	147	27.05	0.4	39.75	57.4
137	28.45	2.28	9.9	24.7	97.3	27.37	18	6	161	26.6	0.36	39.3	54.1
138	28.7	2.23	10.1	24.9	96.6	27.48	16	6	166	26.65	0.34	39.35	48.4
139	28.6	2.18	9.9	24.9	98	27.46	16	8	158	26.7	0.42	39.4	56.5
140	28.55	2.13	10.1	25	98.7	27.34	16	5	155	26.75	0.35	39.45	49.6
141	28.5	2.33	10	24.8	98.6	27.41	17	84	160	26.55	0.42	39.25	63.8
142	28.45	2.28	10	24.9	97.5	27.49	17	31	162	26.6	0.4	39.3	60.3
143	28.55	2.18	10	25	99.6	27.36	16	28	152	26.7	0.39	39.4	60.8
144	28.5	2.18	10	24.9	99.3	27.44	16	22	155	26.7	0.38	39.4	61.3
145	28.45	2.28	10.1	24.9	97.6	27.49	16	78	161	26.6	0.42	39.3	67
146	28.45	2.13	9.9	24.8	97.7	27.5	16	77	156	26.75	0.44	39.45	67.1
147	28.45	2.18	10	24.8	98.2	27.33	17	16	153	26.7	0.34	39.4	59.2
148	28.45	2.18	10	24.8	98	27.47	17	21	159	26.7	0.38	39.4	57.3
149	28.5	2.23	9.8	24.8	99.4	27.47	11	14	157	26.65	0.34	39.35	58.1

Shot	Wtc+0 (lbs)	B_L (in)	Slow Vel (in/sec)	Inter Vel (in/sec)	Fast Vel (in/sec)	Act Ft Pos (in)	Vel Rise (ms)	Pres Rise (ms)	Fill time (ms)	Fill time srt (in)	Inten Strk (in)	End Pos (in)	End Vel (in/sec)
150	28.65	2.18	10	24.8	99.2	27.48	17	20	158	26.7	0.36	39.4	56.3
151	28.5	2.18	9.9	24.8	99.4	27.5	17	12	158	26.7	0.32	39.4	57.1
152	29.4	2.23	10.4	24.9	98.9	27.41	16	125	155	26.65	0.84	39.35	65.7
153	29.75	2.13	10	24.9	99.6	27.49	16	26	155	26.75	1	39.45	57.7
154	29.95	2.13	9.9	24.9	97.5	27.31	15	35	151	26.75	1.19	39.45	58.7
155	30.3	2.08	10.4	24.8	100	27.4	16	11	150	26.8	1.14	39.5	57.6
156	30.35	2.03	10	24.8	100.3	27.31	16	16	145	26.85	1.84	39.55	61.9

Shot	Pfinal, H (psi)	PK, 2000ms (psi)	PH, max (psi)	tH, max (ms)	PK, max (psi)	tK, max (ms)	PH, impact (psi)	PK, impact (psi)	Pimpact (psi)	timpact (ms)	Prt H (ms)	Prt K (ms)
1	2528	3567	9222	1802	5945	1772	-	-	-	-	74	54
2	1297	841	5274	1712	5829	1712	5242	5800	-558	1711	13	14
3	1320	1102	5424	1707	5916	1706	5289	5829	-540	1705	8	13
4	1316	1334	5457	1723	5655	1723	4720	5220	-500	1727	14	15
5	1316	1160	5555	1716	5829	1716	4895	5452	-557	1720	14	15
6	2519	3712	9236	3716	6380	1835	5067	5278	-211	1715	75	50
7	2519	4176	9225	3674	6931	1820	5107	5945	-838	1721	75	60
8	2524	4147	9291	1927	6757	1840	5110	5539	-429	1721	75	47
9	2519	4524	9262	1825	6989	1819	4961	5452	-491	1696	77	38
10	2520	4582	9247	1832	7105	1806	5048	5626	-578	1720	53	29
11	2520	4147	9262	1857	7105	1818	5008	5278	-270	1697	78	60
12	2521	4292	9266	1846	7221	1800	4990	5655	-665	1713	66	38
13	2522	4350	9251	1837	7047	1821	5019	5800	-781	1719	61	34
14	2519	4350	9233	1845	7076	1831	4939	5278	-339	1714	78	54
15	2519	4176	9233	1823	6931	1790	5026	5655	-629	1712	53	36
16	2520	4292	9233	1937	7192	1830	5231	6032	-801	1721	64	39
17	2519	4640	9255	1848	6931	1833	5074	5626	-552	1727	62	47
18	2517	4466	9335	1857	6902	1822	5030	5481	-451	1720	58	30
19	2517	4379	9247	1846	6960	1827	5037	5191	-154	1717	66	44
20	2515	4872	9251	1894	7076	1852	5045	5481	-436	1722	76	58
21	2518	4611	9229	1849	6844	1832	5158	5655	-497	1715	78	53
22	2518	4524	9236	1867	6786	1870	-	-	-	-	73	59
23	2520	4814	9313	1991	7047	1843	5282	6061	-779	1722	65	39
24	2516	4321	9222	1911	6815	1909	5074	5626	-552	1731	129	102
25	2516	4176	9236	1861	7134	1856	4994	5539	-545	1722	76	59
26	2517	4611	9244	1847	6931	1839	5077	5307	-230	1729	60	38
27	2513	4524	9218	1860	6873	1827	4935	4959	-24	1729	69	54
28	2511	5075	9222	1848	7250	1822	5249	6206	-957	1701	66	46
29	2507	5104	9262	1876	7105	1855	5045	5655	-610	1719	82	58
30	2513	4785	9262	1852	6844	1851	4972	5191	-219	1720	82	61
31	2511	4524	9200	1860	6844	1853	5026	5452	-426	1712	84	61

Shot	Pfinal, H (psi)	PK, 2000ms (psi)	PH, max (psi)	tH, max (ms)	PK, max (psi)	tK, max (ms)	PH, impact (psi)	PK, impact (psi)	Pimpact (psi)	timpact (ms)	Prt H (ms)	Prt K (ms)
32	2513	4205	9258	3036	6772	1089	4975	5046	-71	1711	58	36
33	2511	4582	9204	1853	7120	1838	4983	5467	-484	1717	76	60
34	2508	5351	9185	1829	7207	1820	5118	5597	-479	1718	55	37
35	2511	5061	9211	1852	7134	1842	4964	5351	-387	1718	74	50
36	2508	4756	9189	1808	7033	1816	5081	5554	-473	1692	67	46
37	2515	6395	9262	1828	7033	1813	5212	5873	-661	1699	58	37
38	2509	6322	9277	1867	6902	1829	5092	5583	-491	1714	71	50
39	2505	6467	9204	1835	7018	1816	5373	6163	-790	1694	74	50
40	2508	6395	9196	1846	7149	1821	5074	5858	-784	1718	70	54
41	2504	4756	9164	3722	6931	1844	5325	5916	-591	1722	75	56
42	2497	5119	9225	2003	7381	1853	5070	6018	-948	1710	92	65
43	2508	6757	9269	1891	7279	1849	4986	5742	-756	1721	89	62
44	2509	6467	9200	1817	7091	1813	5067	5945	-878	1697	70	52
45	2506	6467	9200	1841	6902	1828	4903	5003	-100	1703	70	49
46	2503	4568	9185	1814	7120	1803	5110	5742	-632	1708	49	29
47	2505	4858	9200	1862	6902	1853	5147	5655	-508	1723	82	63
48	2503	4901	9167	1834	7178	1840	5311	6076	-765	1706	74	59
49	2513	5510	9207	1857	7482	1854	4932	5583	-651	1713	86	53
50	2502	4901	9236	2125	6989	1857	4833	5148	-315	1722	79	61
51	1309	2204	5693	1722	6699	1722	5431	6569	-1138	1720	12	15
52	1320	1726	5668	1703	6105	1703	4954	5771	-817	1707	15	16
53	1312	1769	5697	1702	6308	1701	5468	6192	-724	1700	13	15
54	1317	1769	5730	1725	6192	1724	5347	5887	-540	1722	13	15
55	1313	2001	5683	1727	6453	1727	5570	6380	-810	1726	12	16
56	1322	2219	5693	1719	6540	1718	5384	6322	-938	1716	11	14
57	1318	2030	5726	1719	6496	1718	5522	6395	-873	1717	14	15
58	1319	1784	5723	1727	6177	1727	5427	6003	-576	1725	14	14
59	1321	1914	5723	1728	6105	1728	5435	5945	-510	1726	14	16
60	1320	1668	5635	1710	6177	1708	5369	6061	-692	1707	12	12
61	1313	1726	5577	1730	6148	1730	4921	5699	-778	1734	13	13
62	1313	2001	5504	1700	6177	1699	5329	6134	-805	1698	13	13

Shot	Pfinal, H (psi)	PK, 2000ms (psi)	PH, max (psi)	tH, max (ms)	PK, max (psi)	tK, max (ms)	PH, impact (psi)	PK, impact (psi)	Pimpact (psi)	timpact (ms)	Prt H (ms)	Prt K (ms)
63	1320	2074	5730	1724	6685	1723	5548	6612	-1064	1722	13	13
64	1320	1885	5653	1700	6177	1699	5355	6061	-706	1697	11	12
65	1320	1987	5715	1709	6293	1709	5460	6163	-703	1707	14	16
66	1329	1972	5624	1704	6148	1704	5242	5931	-689	1707	13	14
67	1316	1943	5693	1704	6192	1703	4950	5757	-807	1708	13	16
68	1320	2016	5610	1704	6308	1703	5158	5902	-744	1707	15	14
69	1314	1711	5617	1702	5989	1701	4735	5452	-717	1707	12	13
70	1318	1929	5628	1707	6250	1706	4913	5757	-844	1711	13	14
71	1318	2030	5653	1727	6293	1725	4928	5626	-698	1731	11	12
72	1322	1929	5580	1720	6134	1720	4913	5699	-786	1724	9	14
73	1319	1972	5602	1727	6308	1727	5085	5844	-759	1731	12	12
74	1318	1987	5683	1714	6163	1714	4855	5699	-844	1719	13	13
75	1313	1813	5650	1719	6235	1521	4771	5481	-710	1724	12	12
76	1321	1929	5642	1723	6148	1723	4961	5844	-883	1727	13	14
77	1318	1856	5580	1710	6105	1710	4830	5815	-985	1714	13	14
78	1312	1798	5464	1710	6090	1710	4903	5786	-883	1713	12	15
79	1318	2161	5653	1724	6612	1723	5595	6612	-1017	1723	12	12
80	1318	2030	5573	1729	6264	1729	5129	5960	-831	1732	15	16
81	1314	1842	5537	1726	6061	1725	5016	5713	-697	1729	13	14
82	1319	1929	5683	1713	6250	1713	4881	5757	-876	1718	13	15
83	1317	1711	5679	1729	6134	1729	4819	5757	-938	1734	14	14
84	1316	1639	5617	1729	6032	1728	4684	5438	-754	1734	12	12
85	1319	1552	5493	1712	5742	1713	4709	5409	-700	1717	12	13
86	1313	1668	5555	1717	6090	1717	4844	5670	-826	1721	14	14
87	1314	1624	5522	1720	5873	1720	4841	5525	-684	1724	12	15
88	1315	1407	5566	1733	5568	1733	4695	5177	-482	1738	13	13
89	1311	1494	5555	1716	5684	1715	4782	5220	-438	1720	12	13
90	1313	1436	5457	1708	5699	1708	4819	5394	-575	1712	12	15
91	3980	8889	16749	2596	10991	2479	5351	5757	-406	1715	505	533
92	3899	9715	16851	2488	11832	2461	4680	5625	-945	1738	540	533
93	3788	10716	16716	2489	12499	2498	5034	6250	-1216	1717	548	564

Shot	Pfinal, H (psi)	PK, 2000ms (psi)	PH, max (psi)	tH, max (ms)	PK, max (psi)	tK, max (ms)	PH, impact (psi)	PK, impact (psi)	Pimpact (psi)	timpact (ms)	Prt H (ms)	Prt K (ms)
94	3758	11165	16669	2485	12383	2481	4855	6003	-1148	1707	549	561
95	3736	10948	16720	2538	12717	2519	4629	4698	-69	1742	551	561
96	3851	10020	16811	2565	12151	2502	4695	5757	-1062	1736	554	539
97	3878	9904	16763	2496	11832	2455	4972	6453	-1481	1712	540	529
98	3906	9773	16789	2451	11644	2456	4702	5641	-939	1709	525	520
99	4105	9628	16741	2735	11760	2333	5045	5648	-603	1707	515	453
100	3860	10121	16767	2555	12093	2454	4742	6250	-1508	1715	537	533
101	4098	9585	16825	2444	11977	2433	5008	5583	-575	1727	518	474
102	3048	11412	16741	3176	11919	3123	5034	5757	-723	1727	1014	924
103	3852	10165	16829	2514	12021	2489	4815	6134	-1319	1729	547	525
104	3928	9672	16825	2550	11499	2484	5129	6032	-903	1729	530	527
105	3923	9585	16833	2550	11629	2464	4698	5278	-580	1710	536	521
106	3871	9918	16803	2467	11905	2454	4771	5844	-1073	1712	540	530
107	3844	9991	16756	2577	11992	2479	4804	5844	-1040	1730	526	529
108	3817	10310	16720	2460	12180	2475	4793	5815	-1022	1716	559	528
109	3867	9947	16741	2583	11861	2496	4760	6221	-1461	1730	536	533
110	3860	9831	16654	2564	11876	2564	4892	6076	-1184	1712	534	535
111	3848	9947	16814	2497	12050	2461	4739	6148	-1409	1716	541	521
112	4070	10614	16825	2472	12035	2432	4917	5626	-709	1719	527	462
113	3840	9976	16760	2530	11774	2473	4903	6772	-1869	1713	534	520
114	3838	10092	16727	2520	12050	2485	4895	5365	-470	1729	539	530
115	3850	9730	16814	2524	11847	2473	4786	6148	-1362	1725	534	528
116	3807	10498	16698	2495	12151	2473	4957	6337	-1380	1708	547	529
117	4151	9962	16734	2457	11919	2400	5150	5510	-360	1713	499	438
118	3876	9976	16661	2526	11832	2518	4822	6366	-1544	1734	536	517
119	4135	10049	16774	2494	11992	2395	5016	5380	-364	1720	503	440
120	3839	9976	16614	2564	11615	2564	4946	6540	-1594	1708	532	492
121	3909	9643	16782	2638	11919	2423	4804	5873	-1069	1718	535	492
122	2504	4263	9262	1873	7047	1872	4604	6250	-1646	1747	92	77
123	2497	4205	9269	1821	7134	1844	-	-	-	-	63	49
124	2499	4568	9309	1774	7627	1772	5023	5597	-574	1705	44	36

Shot	Pfinal, H (psi)	PK, 2000ms (psi)	PH, max (psi)	th, max (ms)	PK, max (psi)	tK, max (ms)	PH, impact (psi)	PK, impact (psi)	Pimpact (psi)	timpact (ms)	Prt H (ms)	Prt K (ms)
125	2498	4365	9324	1786	7250	1762	4968	5452	-484	1719	41	33
126	2498	4394	9320	1760	7250	1762	5118	6192	-1074	1075	33	24
127	2495	3843	9481	1742	7323	1747	5110	5510	-400	1706	24	19
128	2495	4612	9473	1773	7149	1773	-	-	-	-	33	28
129	2504	4278	9503	1762	7105	1766	5369	5771	-402	1715	29	25
130	2495	4118	9466	1749	7468	1752	5019	5394	-375	1703	29	25
131	2491	4263	9521	1754	7772	1752	5125	5452	-327	1707	30	25
132	2497	4452	9718	1746	7323	1751	-	-	-	-	23	25
133	2496	4249	9714	1773	7598	1773	4997	5612	-615	1735	25	22
134	2490	4133	9732	1769	7453	1766	5365	5612	-247	1728	27	27
135	2501	4640	9772	1759	7671	1761	5023	6032	-1009	1723	30	34
136	2499	4336	9685	1768	7888	1765	5016	5713	-697	1730	22	26
137	2498	4452	9925	1751	7845	1752	5016	5293	-277	1714	23	25
138	2496	4466	9885	1748	8483	1749	5205	6003	-798	1711	27	25
139	2490	4437	9900	1752	8149	1750	5008	5771	-763	1713	27	25
140	2488	4858	9852	1759	8425	1756	5037	6003	-966	1723	23	22
141	2497	4713	9149	1897	6888	1857	4841	6148	-1307	1713	130	99
142	2493	4626	9138	1856	6757	1854	5118	5409	-291	1712	79	61
143	2489	4553	9131	1843	7163	1802	4928	5873	-945	1703	77	42
144	2484	4452	9077	3714	7192	1803	5030	5351	-321	1713	70	39
145	2494	4031	9149	1897	7047	1904	4841	5757	-916	1720	127	104
146	2498	3959	9174	1920	6801	1895	5325	6511	-1186	1732	130	91
147	2489	4785	9156	1866	6714	1820	4910	5612	-702	1706	61	31
148	2497	4234	9196	2230	6728	1802	4975	5539	-564	1712	73	39
149	2487	4858	9167	1850	7482	1845	5205	6003	-798	1729	60	38
150	2490	4843	9215	2052	6975	1830	5045	5829	-784	1711	78	38
151	2486	4379	9076	1991	6902	1796	5023	5815	-792	1725	51	16
152	3898	9904	16738	2460	11673	2480	4986	6279	-1293	1709	536	522
153	4469	10237	16541	2270	12456	2280	5125	6482	-1357	1725	367	318
154	4550	10977	16603	2200	12876	2175	4968	5539	-571	1721	330	287
155	4497	5655	16505	2065	6685	2055	-	-	-	-	247	173
156	4331	9904	15998	2080	6467	2060	-	-	-	-	289	136

Set II	Wtc+o (lbs)	Slow Vel (in/sec)	Inter Vel (in/sec)	Fast Vel (in/sec)	Act Ft Pos (in)	Vel Rise (ms)	Pres Rise (ms)	Fill time (ms)	Fill time st (in)	B_L (in)	Inten Strk (in)	End Pos (in)	End Vel (in/sec)
MEAN	28.43	10	24.9	98	27.4	15	22	153	26.77	2.11	0.37	39.47	58.2
MEDIAN	28.4	10	24.9	98.2	27.43	16	21	157	26.65	2.23	0.38	39.35	58.3
MODE	28.4	10	24.9	98.5	27.48	16	24	157	26.65	2.23	0.38	39.35	58.1
STDEV	0.04	0.2	0.1	0.8	0.07	3	11	9	0.27	0.27	0.03	0.27	1.9
MAX	28.5	10.5	25	99.7	27.48	18	73	168	27.35	2.48	0.42	40.05	63.7
MIN	28.35	9.8	24.7	95.7	27.29	11	10	134	26.4	1.53	0.31	39.1	53.9
RANGE	0.15	0.7	0.3	4	0.19	7	63	34	0.95	0.95	0.11	0.95	9.8
COUNT	30	30	30	30	30	30	30	30	30	30	30	30	30
CONF LEV(95%)	0.0139	0.059	0.0278	0.2976	0.0262	0.9243	4.0423	3.1647	0.098	0.098	0.0119	0.098	0.6917
STDEV/MEAN	0.0014	0.0165	0.0031	0.0085	0.0027	0.1737	0.5158	0.0577	0.0102	0.13	0.0907	0.0069	0.0332

Set III	Wtc+o (lbs)	Slow Vel (in/sec)	Inter Vel (in/sec)	Fast Vel (in/sec)	Act Ft Pos (in)	Vel Rise (ms)	Pres Rise (ms)	Fill time (ms)	Fill time st (in)	B_L (in)	Inten Strk (in)	End Pos (in)	End Vel (in/sec)
MEAN	27.96	10	24.9	98.3	27.413	16	2000	154	26.72	2.16	0.15	39.42	65.2
MEDIAN	27.95	10	24.9	98.2	27.43	16	2000	155	26.75	2.13	0.14	39.45	64.9
MODE	28	10	24.9	98	27.46	16	2000	156	26.75	2.13	0.11	39.45	64.6
STDEV	0.09	0.2	0.1	0.8	0.07	2	0	5	0.14	0.14	0.04	0.14	1.8
MAX	28.2	10.4	25.1	100	27.51	18	2000	165	27	2.43	0.25	39.7	68.6
MIN	27.8	9.8	24.8	96.6	27.3	11	2000	144	26.45	1.88	0.09	39.15	61.4
RANGE	0.4	0.6	0.3	3.4	0.21	7	0	21	0.55	0.55	0.16	0.55	7.2
COUNT	40	40	40	40	40	40	40	40	40	40	40	40	40
CONF LEV(95%)	0.0283	0.0537	0.0245	0.2407	0.0217	0.4077	-	1.5629	0.0435	0.0435	0.0132	0.0435	0.5525
STDEV/MEAN	0.0033	0.0173	0.0032	0.0079	0.0026	0.081	0	0.0327	0.0052	0.0648	0.2878	0.0036	0.0273

Set IV	Wtc+o (lbs)	Slow Vel (in/sec)	Inter Vel (in/sec)	Fast Vel (in/sec)	Act Ft Pos (in)	Vel Rise (ms)	Pres Rise (ms)	Fill time (ms)	Fill time str (in)	B_L (in)	Inten Strk (in)	End Pos (in)	End Vel (in/sec)
MEAN	29.47	10	24.9	98.3	27.43	15	117	156	26.68	2.2	0.87	39.38	62.6
MEDIAN	29.45	10	24.9	98.2	27.45	16	126	157	26.65	2.23	0.88	39.35	62.9
MODE	29.5	10	24.9	98.8	27.48	16	126	157	26.65	2.23	0.88	39.35	65.7
STDEV	0.06	0.2	0.1	0.7	0.07	2	26	4	0.12	0.12	0.03	0.12	3.3
MAX	29.6	10.5	25	99.9	27.51	18	143	163	27.05	2.33	0.93	39.75	68
MIN	29.3	9.8	24.8	96.6	27.31	11	45	146	26.55	1.83	0.79	39.25	55.5
RANGE	0.3	0.7	0.2	3.3	0.2	7	98	17	0.5	0.5	0.14	0.5	12.5
COUNT	31	31	31	31	31	31	31	31	31	31	31	31	31
CONF LEV(95%)	0.0212	0.0599	0.0236	0.2479	0.025	0.7006	9.1538	1.4845	0.0417	0.0417	0.0116	0.0417	1.1763
STDEV/MEAN	0.002	0.017	0.0027	0.0072	0.0026	0.1344	0.2213	0.0271	0.0044	0.054	0.0377	0.003	0.0534

Set V	Wtc+o (lbs)	Slow Vel (in/sec)	Inter Vel (in/sec)	Fast Vel (in/sec)	Act Ft Pos (in)	Vel Rise (ms)	Pres Rise (ms)	Fill time (ms)	Fill time str (in)	B_L (in)	Inten Strk (in)	End Pos (in)	End Vel (in/sec)
MEAN	28.51	10	24.9	98	27.42	16	21	155	26.75	2.13	0.38	39.45	58
MEDIAN	28.5	10	24.9	97.9	27.44	16	12	155	26.73	2.16	0.38	39.43	57.4
MODE	28.5	10	24.8	97.5	27.48	16	8	155	26.7	2.18	0.4	39.4	57.4
STDEV	0.08	0.1	0.1	0.8	0.07	2	23	5	0.13	0.13	0.04	0.13	4.2
MAX	28.7	10.4	25	99.6	27.5	20	84	166	27.05	2.33	0.44	39.75	67.1
MIN	28.35	9.7	24.7	96.3	27.31	11	5	147	26.55	1.83	0.31	39.25	48.4
RANGE	0.35	0.7	0.3	3.3	0.19	9	79	19	0.5	0.5	0.13	0.5	18.7
COUNT	30	30	30	30	30	30	30	30	30	30	30	30	30
CONF LEV(95%)	0.0269	0.0505	0.0303	0.3032	0.0235	0.6668	8.0965	1.7286	0.0465	0.0465	0.0132	0.0465	1.4995
STDEV/MEAN	0.0026	0.0141	0.0034	0.0086	0.0024	0.1157	1.0689	0.0311	0.0049	0.0611	0.0969	0.0033	0.0723

	Pfinal, H (psi)	PK, 2000ms (psi)	PH, max (psi)	tH, max (ms)	PK, max (psi)	tK, max (ms)	PH, impact (psi)	PK, impact (psi)	Pimpact (psi)	timpact (ms)	Prt H (ms)	Prt K (ms)
Set II	2510	5164	9224	1971	7037	1815	4912	5432	-520	1714	74	53
MEAN	2510	4879.5	9220	1855	7033	1840	5072	5612	-527	1717	74	54
MEDIAN	2513	4524	9200	1867	6844	1853	5074	5655	-	1722	82	59
MODE	6	791	35	398	178	139	937	1081	265	10	14	13
STDEV	2520	6757	9313	3722	7482	1909	5373	6206	0	1731	129	102
MAX	2497	4176	9164	1808	6772	1089	0	0	-957	1692	49	29
MIN	23	2581	149	1914	710	820	5373	6206	957	39	80	73
RANGE	30	30	30	30	30	30	30	30	30	29	30	30
COUNT	1.9643	283.1181	12.3533	142.527	63.834	49.6114	335.307	386.6887	94.8256	3.7421	5.158	4.7213
CONF LEV(95%)	0.0022	0.1532	0.0037	0.202	0.0254	0.0764	0.1908	0.1989	-0.5095	0.0061	0.1937	0.2475
STDEV/MEAN												

	Set III	MEAN	MEDIAN	MODE	STDEV	MAX	MIN	RANGE	COUNT	CONF LEV(95%)	STDEV/MEAN
	1317	1853	1900	1929	197	2219	1407	812	40	61.1915	0.1065
	1318	1900	1929	197	2219	1407	812	40	40	23.5134	0.0135
	1318	1929	197	2219	1407	812	40	40	3.0928	0.0058	0.0398
	4	197	2219	1407	812	40	40	40	76.247	0.0398	0.0398
	1329	1853	1900	1929	197	2219	1407	812	40	61.1915	0.1065
	1309	1900	1929	197	2219	1407	812	40	40	23.5134	0.0135
	20	197	2219	1407	812	40	40	40	3.0928	0.0058	0.0398
	40	197	2219	1407	812	40	40	40	76.247	0.0398	0.0398
	1.197	1853	1900	1929	197	2219	1407	812	40	61.1915	0.1065
	0.0029	0.1065	0.0135	0.0058	0.0398	0.0398	0.0398	0.0398	0.0398	0.0398	0.0398

Set IV	Pfinal, H (psi)	PK, 2000ms (psi)	PH, max (psi)	tH, max (ms)	PK, max (psi)	tK, max (ms)	PH, impact (psi)	PK, impact (psi)	Pimpact (psi)	timpact (ms)	Prt H (ms)	Prt K (ms)
MEAN	3872	10057	16758	2548	11934	2490	4882	5895	-1012	1720	549	530
MEDIAN	3860	9976	16760	2524	11919	2473	4855	5844	-1062	1717	536	528
MODE	3860	9976	16741	2550	11832	2473	5034	5757		1712	540	533
STDEV	187	505	59	131	307	126	162	427	439	10	87	80
MAX	4151	11412	16851	3176	12717	3123	5351	6772	-69	1742	1014	924
MIN	3048	8889	16614	2444	10991	2333	4629	4698	-1869	1707	499	438
RANGE	1103	2523	237	732	1726	790	722	2074	1800	35	515	486
COUNT	31	31	31	31	31	31	31	31	31	31	31	31
CONF LEV(95%)	65.6472	177.7388	20.8666	46.2012	108.106	44.3038	57.1449	150.2532	154.391	3.5545	30.7687	28.174
STDEV/MEAN	0.0482	0.0502	0.0035	0.0515	0.0257	0.0505	0.0333	0.0724	-0.4332	0.0059	0.1591	0.1511

Set V	Pfinal, H (psi)	PK, 2000ms (psi)	PH, max (psi)	tH, max (ms)	PK, max (psi)	tK, max (ms)	PH, impact (psi)	PK, impact (psi)	Pimpact (psi)	timpact (ms)	Prt H (ms)	Prt K (ms)
MEAN	2495	4412	9425	1891	7354	1794	4541	5183	-642	1694	53	39
MEDIAN	2496	4416	9322	1774	7250	1773	5021	5663	-656	1713	37	30
MODE	2497	4452	9149	1773	7047	1752	0	0	0	1713	23	25
STDEV	5	264	281	361	473	47	1547	1781	395	124	33	24
MAX	2504	4858	9925	3714	8483	1904	5369	6511	0	1747	130	104
MIN	2484	3843	9076	1742	6714	1747	0	0	-1646	1075	22	16
RANGE	20	1015	849	1972	1769	157	5369	6511	1646	672	108	88
COUNT	30	30	30	30	30	30	30	30	30	27	30	30
CONF LEV(95%)	1.8313	94.323	100.593	129.173	169.209	16.9284	553.7079	637.3983	141.382	44.4179	11.9209	8.468
STDEV/MEAN	0.0021	0.0597	0.0298	0.1909	0.0643	0.0264	0.3407	0.3436	-0.6154	0.0733	0.6321	0.6068